

# **CORRELATING HUMAN AND FLEXIBLE DUMMY HEAD-NECK INJURY PERFORMANCE**

**Jacqueline G. Paver Ph.D.**

**Donald Friedman**

**Josh A. Jimenez**

Center for Injury Research

United States

Paper Number 13-0282

## **ABSTRACT**

The Center for Injury Research (C/IR) has developed methods to derive and correlate rollover dummy head-neck injury with NASS/CIREN data. In this paper, these methods are applied to other accident modes. Specifically, we investigated the application of the dummy rollover head-neck modifications, as well as structural injury risk, IARV, momentum exchange injury measures and criteria to frontal, offset and small overlap frontal and side impact testing.

Recently, NHTSA has implemented a comprehensive series of component regulations (FMVSS 126, FMVSS 216, FMVSS 226) [1-3] which, in combination, are intended to drastically reduce the number of crashes and occupant injury and fatalities in rollovers and other modes. However, the stiffness of the dummy neck and the disparity between IARV and momentum exchange injury measures were not addressed. We opine that injury and fatality rates are high because of poor dummy-to-human stiffness and substantially underestimated IARV injury criteria compared to consensus momentum exchange injury measures.

IIHS 40% offset and small overlap frontal and side impact tests were studied to observe the trajectory of the Hybrid III dummy head with production neck and evaluate injury measures. Then, the effect of substituting the production neck with the more flexible rollover neck was investigated. Estimates were made of the dummy head excursion, proximity of the head to vehicle structures at maximum excursion, the likelihood and severity of vehicle structure contact, and injury measures.

Results indicate that, while the flexible neck in a rollover increases head excursion by 3 inches when contacted at 7 mph, the frontal and side impact tests described here result in head contact with vehicle structures and exceed the rollover-developed AIS  $\geq 3$  momentum exchange injury criteria of the integrated bending moment (IBM) and single and double

integration product of head resultant acceleration (HRA).

## **INTRODUCTION**

This research has been addressing the rollover fatality problem for the last 12 years. The Department of Transportation (DOT) and the automobile industry have been addressing the total fatality problem since DOT's inception with the Traffic Safety Act of 1966. Some insight into the misrepresentations that delayed progress in reducing rollover fatalities and injuries has been documented. [4-13]. Although the size of the passenger vehicle fleet has increased substantially, the second author's research as a major contractor to the DOT from 1968 to 1985 had forecast much more substantial progress in reducing fatalities. One reason may be that the accident analysis of the NHTSA/Minicars Research Safety Vehicle (RSV) required passive protection airbag performance in a 30° angled impact mode. Many of today's supplemental restraint system airbags are too small to affect the trajectory or protect the head in such a test.

This introduction describes the highlights of the previously-reported [14] methodology used in addressing the rollover fatality and permanently-debilitating head-neck injury problem. The methodology section describes how the flexible rollover neck [15] research can be used to address the even larger problem of fatal and catastrophic head and neck injuries in frontal and side impacts.

## Identifying the Problem

Figure 1 illustrates the magnitude of the U.S. rollover tragedy. From the inception of the Fatal Accident Reporting System (FARS) in 1978 until 2008 [16], more than 1,350,000 occupants were killed in all of the vehicle crash modes, of which almost 318,000 lives were lost in rollover crashes alone.

Accident Year	Rollover Fatalities	Total Fatalities	Accident Year	Rollover Fatalities	Total Fatalities
1978	10,340	50,331	1994	9,472	40,716
1979	10,674	51,093	1995	9,991	41,817
1980	11,137	51,091	1996	10,096	42,065
1981	10,663	49,301	1997	10,068	42,013
1982	9,038	43,945	1998	10,334	41,501
1983	8,959	42,589	1999	10,701	41,717
1984	9,294	44,257	2000	10,530	41,945
1985	9,028	43,825	2001	10,684	42,196
1986	10,181	46,087	2002	11,309	43,005
1987	10,452	46,390	2003	11,050	42,884
1988	10,772	47,087	2004	11,210	42,836
1989	10,263	45,582	2005	11,505	43,510
1990	10,163	44,599	2006	11,417	42,708
1991	9,797	41,508	2007	10,938	41,259
1992	9,097	39,250	2008	9,628	37,261
1993	9,026	40,150	<b>Total</b>	<b>317,817</b>	<b>1,354,518</b>

Figure 1. FARS fatalities from 1978 to 2008.

## Development of Rollover Injury Risk Based on Vehicle Structural Performance

In 2008, the IIHS published data on 22,000 SUV's involved in rollover crashes with incapacitating injuries [17]. Results indicated that the injury rate was reduced by 25% for each increment of vehicle strength-to-weight ratio (SWR) from SWR 2 to 3. The IIHS also derived a relationship between window breakage in rollovers, described in terms of ejection rate, and SWR. The IIHS reported that ejection rate decreased with increasing vehicle SWR.

At approximately the same time, a compilation of JRS and other rollover tests confirmed their results. C/IR defined the following momentum exchange dummy measures:

- a momentum exchange function, called the Integrated Bending Moment (IBM), and
- single and double integration product of head resultant acceleration (HRA).

Figure 2 is a composite plot of structural injury risk and momentum exchange injury measures showing rate reduction with increasing SWR. Results show that these parameters correlated with residual crush at an IBM value of 13.5 and a HRA exceeding a criteria of 48.

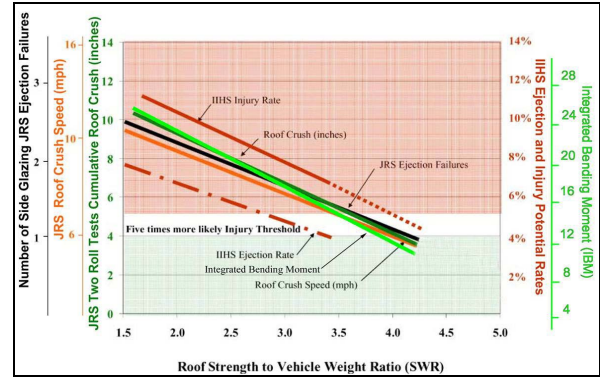


Figure 2. Composite plot of injury measures showing rate reduction with increasing vehicle SWR.

In 2008, NHTSA confirmed a NASS statistical analysis indicating that, in rollover crashes, vehicles with post-crash negative headroom (more roof crush than original headroom) were 5 times more likely to be injurious (at any level of injury) than vehicles with post-crash positive headroom [18]. Figure 3 is a plot of positive and negative post-crash headroom as a function of vehicle SWR in JRS rollover tests.

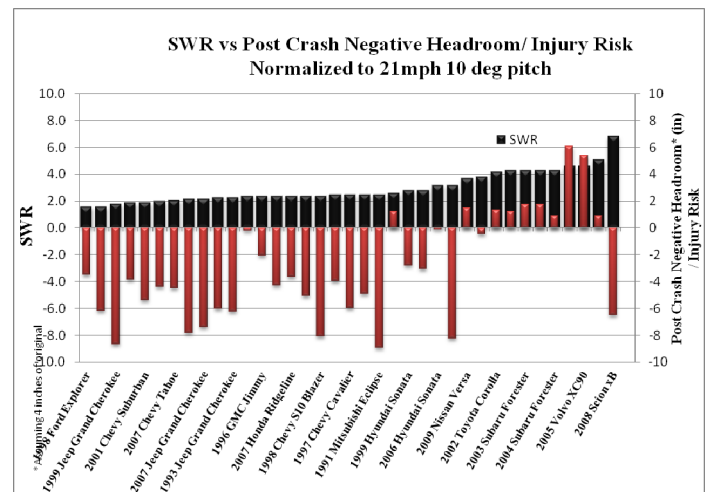


Figure 3. Post-crash positive and negative headroom in order of ascending vehicle SWR.

In 2009, a statistical analysis of NASS and CIREN files [19] evaluated the probability and odds ratio of rollover fatalities and head, spine and spinal cord injury as a function of vehicle residual crush. For residual crush in bands of 0 to 3½, 3½ to 6, 6 to 12 and 12 inches and above, the corresponding ratings in order are “good,” “acceptable” and “poor.” The “acceptable” probability is roughly 30% greater than “good” and the probability of “poor” is 2.5 times greater than “acceptable.”



The IARV injury criteria were recalibrated relative to the production neck. In tests with either neck, there was no correlation between injury risk, described by residual crush, and injury measures, described by IARV. The only consensus injury measures were roof crush and roof crush speed based on criteria developed by McElhaney [22]. Figure 7 is a map of those injury measures.

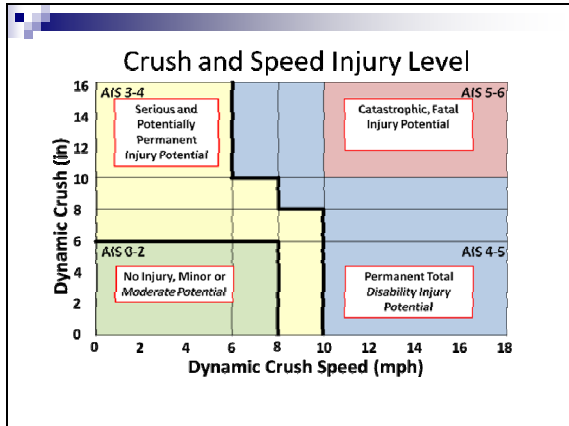


Figure 7. Consensus injury criteria map of dynamic crush injury risk criteria.

The following structural injury risk and dummy injury measure criteria were evaluated:

- the structural injury risk performance measures of the elastically-corrected residual crush and the product of roof crush and crush speed,
- the adjusted IARV lower neck Fz and My, and
- the dummy momentum exchange injury measures of dummy IBM and HRA.

Each was normalized to its AIS  $\geq 3$  reference value. For each JRS rollover test, the percentage of structural injury risk and dummy measure criteria were determined and compared. Results for the 2009 Ford F-150 are illustrated in Figure 8.

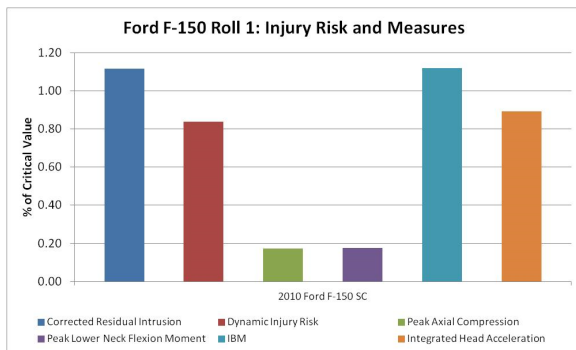


Figure 8. Injury risk, IARV and momentum exchange test results of the 2009 Ford F-150.

## METHODS

In 2000, regulatory frontal occupant crash protection testing was modified for vehicles equipped with advanced airbags. In 2010, IIHS compared the performance of vehicles equipped with advanced airbags to vehicles with 1<sup>st</sup>-generation airbags. Surprisingly, IIHS found a 15% increase in fatalities with advanced airbags [23].

The accident analysis of the NHTSA/Minicars RSV required passive protection airbag performance in a 30° angled impact mode [24]. This requirement was based on the yearly societal costs of injuries and fatalities as a function of vehicle damage areas and deltaV from the MDAI and ACIR files shown in Figure 9.

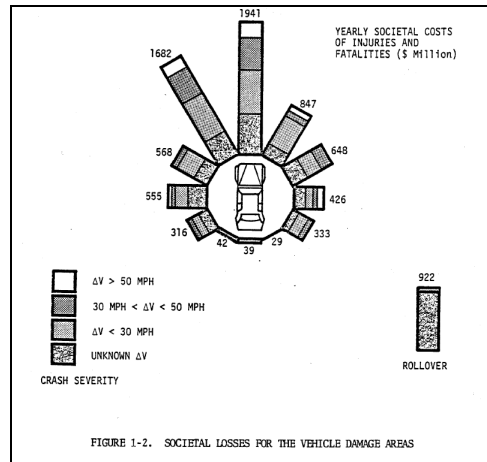


Figure 9. Societal losses as a function of deltaV and vehicle damage areas.

In motor vehicle crashes, the Principal Direction of Force (PDOF) dictates an occupant's kinematic trajectory. Supplemental restraint system airbags are not designed to cushion the head at PDOF angles greater than 9°. Most of today's supplemental restraint system airbags are too small to affect the trajectory or protect the head in such a test. Rather, the head is deflected laterally by the deploying airbag.

In this paper, the following test modes were studied.

- Frontal 30° angled barrier test PDOF~9° [25],
- IIHS 40 mph 40% offset deformable barrier test PDOF~15°,
- IIHS 40 mph 25% small overlap deformable barrier test PDOF~20°,
- Angled impact test (of Figure 7) PDOF~30° [26].

The trajectory of the Hybrid III dummy head with production neck was observed and injury measures were evaluated. Then, the effect of substituting the production neck with the more flexible rollover neck was investigated. Estimates were made of the dummy head excursion, proximity of the head to vehicle structures at maximum excursion, the likelihood and severity of vehicle structure contact, and injury measures.

## RESULTS

Figures 10 and 11 shows the dummy head near the A-pillar in the IIHS small (25%) overlap frontal tests at 40 mph.



Figure 10. IIHS 2012 Kia Soul small (25%) overlap test at 40 mph at maximum head excursion.



Figure 11. IIHS 2012 Acura TSX small (25%) overlap test at 40 mph at maximum head excursion.

Figures 12 and 13 shows videotape frames from IIHS 40% offset frontal tests of a 1996 (top) and 1999 (bottom) Hyundai Sonata into a deformable barrier at 40 mph.



Figure 12. IIHS 1996 Hyundai Sonata (40%) offset frontal test at 40 mph at maximum head excursion.



Figure 13. IIHS 1999 Hyundai Sonata (40%) offset frontal test at 40 mph at maximum head excursion.

The frames in Figures 13 and 14 show that the head was deflected by the airbag. The proximity of the head at maximum excursion was about 4 inches and 1 inch from internal 1996 and 1999 vehicle component structures, respectively.

In the IIHS small (25%) overlap tests at 40 mph, the dummy head is not as close to the A-pillar as in the frontal offset tests despite the PDOF and the deflection off the airbag because of the substantially-reduced deltaV. If a test had been run with the 30° angled impact requirement of the RSV, the head would have contacted the A-pillar because the airbag effects are less.

Figure 14 is a frame from an IIHS side impact of a 2006 Crown Victoria without airbags at 30 mph.



Figure 14. IIHS 2006 Crown Victoria side impact test (no airbags) at maximum head excursion.

Results indicate that, while the flexible neck in a rollover increases head excursion by 3 inches when contacted at 7 mph, the frontal and side impact tests described here result in head contact with vehicle structures and exceed the rollover-developed AIS  $\geq 3$  momentum exchange injury criteria of the IBM and HRA.

## DISCUSSION

Frontal airbags were mandated and implemented in passenger cars in 1995. However, NHTSA estimates less than a 20% savings of lives by airbags in frontal impacts compared to the number of lives lost. With required supplemental restraint systems and a greater than 80% belt usage, we expect a greater reduction than 20%. The fact that vehicle safety design is based on testing with the production Hybrid III neck (and its limitations) and IARV injury criteria that underestimate human injury by a factor of two explain, in part, this disparity. The next step in this research is to conduct sled tests at various PDOF angles with both the Hybrid III production and the prototype flexible rollover neck to measure and validate our estimates of head excursion, IARV, structural injury risk, and momentum exchange injury measures.

## LIMITATIONS

These studies are based on estimates of head excursion from videotapes recorded by the IIHS. The estimates of head excursion with the substitution of the prototype flexible rollover neck are judgments indicative of the authors' broad experience with frontal and side impact research and regulatory test performance. The difference in IARV and

momentum exchange injury measures were experimentally-validated and published previously.

## CONCLUSIONS

- The Hybrid III dummy production neck is not representative of the injury population.
- IARV does not represent human injury potential and underestimates it by 50% or more.
- Head-neck inclination and neck stiffness has a significant effect on injury and fatality potential in all accident modes.
- Vehicle occupant protection systems designed and rated using the production Hybrid III dummy may be the principal cause of high death and injury rates.

## ACKNOWLEDGEMENTS

The IIHS has graciously provided access to their testing results and videos and given permission to publish the video frames contained in this paper.

## REFERENCES

- [1] U.S. Department of Transportation, Final Rule FMVSS 126, 4-6-2007.
- [2] U.S. Department of Transportation, Federal Register Final Rule FMVSS 216, Vol. 74, No. 90, 5-12-2009.
- [3] U.S. Department of Transportation, Federal Register Final Rule FMVSS 226, Vol. 76, No. 12, 1-19-2011.
- [4] Federal Register, "Roof Intrusion Protection for Passenger Cars - Proposed Motor Vehicle Safety Standard 216." Docket #2-6; Notice 4, 1-6-1971
- [5] "Fisher Body Test Report, Body-Static Roof Intrusion Tests - 1970 and 1971 F, H, A, X, and B Styles." March 1971.
- [6] "The National Archives – Conversation Among President Nixon, Lide Anthony Iacocca, Henry Ford II, and John D. Ehrlichman." April 1971.
- [7] Orłowski, K.F, R T Bundorf, E A Moffatt, "Rollover Crash Tests – The Influence of Roof Strength on Injury Mechanics," Society of Automotive Engineers, Paper No. 851734, 1985.
- [8] Bahling, G.S. , R.T. Bundorf, G.S. Kasprzyk, E.A. Moffatt, K. F. Orłowski and J.E. Stocke, "Rollover and Drop Tests – The Influence of Roof Strength on Injury Mechanics Using Belted Dummies," Society of Automotive Engineers, Paper No. 902314, 1990.
- [9] Moffat, E.A., J. Padmanaban, "The Relationship Between Roof Strength and Occupant Injury in Rollover Accident Data," Report No. FaAA-SF-R-95-05-37, May 1995.
- [10] Moffat, E.A., et al., "Matched-Pair Rollover Impacts of Rollcaged and Production Roof Cars

Using the Controlled Rollover Impact System (CRIS)," SAE, 2003.

[11] R.W. Nightingale, J.H. McElhaney, D.L. Camacho, M Kleinberger, B.A. Winkelstein, B.S. Myers, "The Dynamic Responses of the Cervical Spine: Buckling, End Conditions, and Tolerance in Compressive Impacts," Society of Automotive Engineers, Paper No. 973344, 1997.

[12] J.G. Paver and D Friedman, "Is BFD a Hyperflexion Injury or Compression with Localized Bending Injury or Both?" International Crashworthiness Conference 2012, Milano, Italy. 2012. Paper No. 2012-111.

[13] B.L. Allen, et al., "A Mechanistic Classification of Closed, Indirect Fractures, and Dislocations of the Lower Cervical Spine," Philadelphia, PA, 1982.

[14] Friedman, D., Rico, D., Mattos,G.,Paver, J. PhD., "Predicting and Verifying Dynamic Occupant Protection", ESV Conference, Paper 11-0090, June 2011, Washington DC

[15] Ibid.

[16] Fatality Analysis Reporting System Database [www-fars.nhtsa.dot.gov](http://www-fars.nhtsa.dot.gov)

[17] Brumbelow, M., E.R. Teoh, D.S. Zuby and A.T. McCart, "Roof Strength and Injury Risk in Rollover Crashes," Insurance Institute for Highway Safety, March 2008.

[18] Strashny, A., "The Role of Vertical Roof Intrusion and Post-Crash Headroom in Predicting Roof Contact Injuries to the Head, Neck, or Face during FMVSS No. 216 Rollovers: An Updated Analysis", DOT HS 810 847 4, October 2007.

[19] Mandell, S., R. Kaufman, C.D. Mack and E.M. Bulger. 2010. "Mortality and Injury Patterns Associated with Roof Crush in Rollover Crashes." Accident Analysis and Prevention, 2010, 10.1016/j.aap.2010.02.013.

[20] Friedman, D., J. Paver and R. McGuan, "Design, Development and Validation of Rollover Dummy Injury Measures," International Crashworthiness Conference, Milano, Italy 2012.

[21]Paver, J., D Friedman, J Caplinger, "Rollover Crash Neck Replication and Injury Potential Assessment", International IRCOBI Conference on the Biomechanics of Injury, Bern, Switzerland: 2008.

[22] McElhaney, J., R. Snyder, J. States, M.A. Gabrielsen, "Biomechanical Analysis of Swimming Pool Neck Injuries," Society of Automotive Engineers, Inc., 1979.

[23] IIHS Status Report, "Airbags Have Evolved", Vol. 45. No. 1, Feb 6, 2010

[24] Ausherman, V.K, Khadilkar, A.V, Syson, S.R., Strother, C.E., Struble, D.E., "Technical Final Report, The Minicars Research Safety Vehicle Program", September 1981 RSV Paper.

[25] Friedman, D., "Subcompact Car Crashworthiness," Transportation Research Board, January, 1975.

[26] Insurance Institute for Highway Safety: [www.iihs.com](http://www.iihs.com)

# CHARACTERISTICS OF INJURIES IN FATALLY INJURED RESTRAINED OCCUPANTS IN FRONTAL CRASHES

**Rodney W. Rudd**

National Highway Traffic Safety Administration  
United States  
Paper Number 13-0349

## ABSTRACT

Frontal crashes have been studied extensively and have been the target of many regulatory and motor vehicle safety-enhancement efforts. While fatalities in frontal crashes, and in crashes in general, have decreased over time, there is still interest in understanding the issues that lead to these continued fatalities. This study is an extension of a prior effort that involved in-depth reviews of frontal crash fatality cases, but is conducted from an injury perspective.

Occupants who were involved in frontal crashes and restrained by a seat belt and deployed frontal air bag of late-model vehicles were selected from the National Automotive Sampling System-Crashworthiness Data System and Crash Injury Research and Engineering Network databases. The cases were individually reviewed, and key factors that contributed to the fatal nature of the crash were identified based on coded data elements and other evidence in the case. Cause of death information was further analyzed along with the coded injury causation data and occupant time-to-death.

## INTRODUCTION

Fatalities resulting from motor vehicle crashes have been on a downward trend, with the most recent year-over-year comparison representing a 1.9% decrease to 32,367 for 2011 [NHTSA, 2012]. While the decrease in the total number, as well as the rate per mile traveled, is an encouraging sign, the safety community continues to work towards reducing those numbers as much as possible. Frontal crashes make up the largest subset of fatal crashes, and have thus been the subject of much research.

The National Highway Traffic Safety Administration (NHTSA) undertook a large study of fatal frontal

crashes and published the findings in Bean et al. [2009] and Rudd et al. [2009]. This study focused on restrained occupants, and sought to identify the factors that led to their death despite being in a modern vehicle with frontal air bags. Brumelow et al. [2009] conducted a similar study looking at the frontal crash performance in the field of vehicles that had received the top rating in the Insurance Institute for Highway Safety (IIHS) offset deformable barrier frontal crash test. The NHTSA and IIHS studies both identified similar factors that were common among fatal frontal crashes, namely issues related to the extent of engagement across the front plane of the vehicle and occupant-related factors. As a result of these studies, NHTSA and IIHS both began the development of test procedures to evaluate vehicle and occupant performance in small overlap frontal and oblique crashes [IIHS, 2012; Saunders et al. 2012]

It was desired to take the work presented in Rudd et al. [2009] further by looking at the cases from an injury perspective. Injuries were considered in the review of the cases in the earlier study, but the findings did not address the nature of the injuries and their causation. The objectives of this study were to evaluate the cause of death and injury causation associated with fatalities of properly restrained occupants in frontal crashes. By focusing on the injuries and their associated causal factors, the outcome of this study can help guide efforts to improve vehicle and restraint performance as well as determine human injury research priorities.

## METHODS

The fatality cases making up this study were selected from the National Automotive Sampling System-Crashworthiness Data System (NASS-CDS) and the Crash Injury Research and Engineering Network (CIREN) data systems. Both data systems collect

vehicle- and crash-based data using the same protocols, and differ primarily in the collection of occupant-based data. Since CIREN is a trauma center-based data collection program, cases include more comprehensive occupant injury and treatment data. NASS-CDS cases were selected from case years 2000 through 2011 and CIREN cases were selected from all available cases in the system.

While this study was an extension of that presented in Bean et al. [2009] and Rudd et al. [2009], slightly different case inclusion criteria were employed to meet this study's injury-focused objectives. The occupants selected for this study must have been seated in either of the outboard front-row seating positions of a passenger vehicle of model year 2000 or newer, and must have been restrained by an appropriately-worn manual three-point belt restraint and deployed frontal air bag. Furthermore, the crash inclusion criteria were enhanced to capture additional frontal crashes using a slightly less restrictive filter. The filter in the prior study required the General Area of Damage for the most significant event (GAD1) to be the frontal plane only, while this study utilized the algorithm presented by Halloway et al. [2011]. The revised criteria captured a few additional crashes where the coded GAD1 was to the frontal portion of the left or right plane and the principal direction of force was between 320° and 0° on the left and 0° and 40° on the right.

Bean et al. [2009] assigned each occupant fatality to one or two high-level crash-classification bins in order to best characterize the most important feature of the crash experience. The five bins created were: exceedingly severe crash or anomaly, corner and/or oblique impact, narrow object impact, underride rear/side of heavy vehicle, and vulnerable occupant. For the cases that were evaluated in Bean et al. [2009] that were also included in this study, the classification(s) were carried over for this evaluation. Cases that were new to this study were evaluated by the author and assigned to the categories based on the same evaluation criteria. Some cases from the prior study, as well as a few of the additional cases identified with the expanded crash criteria, were deemed anomaly cases due to unusual crash circumstances, and were removed from this injury-focused study. Furthermore, the category for impact

to the side or rear of a heavy vehicle was expanded to include impacts to the front of a heavy vehicle as well in order to capture those crashes where the mass and geometric mismatches play a role.

Following the initial query, the cases were reviewed individually to confirm coherence with the study's objective of evaluating properly belted and air bag-restrained occupants in frontal impacts. Some of the crashes were removed from the study based on unusual crash configurations, such as being struck at the windshield level by an airborne vehicle during a rollover, or cases in which the occupant died in a post-crash fire. Cases that were identified in Bean et al. [2009] as anomaly cases were also removed.

The primary focus of this analysis was cause of death, injury sourcing, and hospital stay data, which were extracted when available, but were not coded in all cases. Injury severity was based on the Abbreviated Injury Scale (AIS; AAAM, 2005) and multi-system trauma was indicated by the Injury Severity Score (ISS). The NASS-CDS and CIREN cases were combined for this analysis, as the intent was not to conduct any nationally-representative analysis of the data.

## RESULTS

A total of 189 fatalities, from 184 vehicles in 182 crashes, were selected from the CDS and CIREN databases for analysis in this study. Fifty-eight percent (58%) of the occupants were male and 85% were in the driver's seat. There were 161 case occupants from the CDS database and 25 from CIREN, while there were three that exist in both data systems. The occupants ranged in age from 16 to 89 years of age. Figure 1 shows a breakdown of occupant age. A full listing of the cases is provided in Appendix A.

Most of the fatally injured occupants were riding in passenger cars, with about one third riding in light trucks and vans. The large majority of the case vehicles struck other vehicles (81%), while 13% struck trees or poles and 6% struck a building, bridge support, or embankment. The breakdown of the vehicle type is shown in Figure 2, and the model year breakdown is shown in Figure 3. Due to the severity and circumstances of many of these crashes, velocity

change (delta-v) was only available for less than half of the case vehicles. Of those vehicles with a coded delta-v, the lowest was 17 km/h (11 mph) and the

highest was 145 km/h (90 mph). Occupants over 65 years of age comprised the majority of occupants in crashes with delta-v below 45 km/h (28 mph).

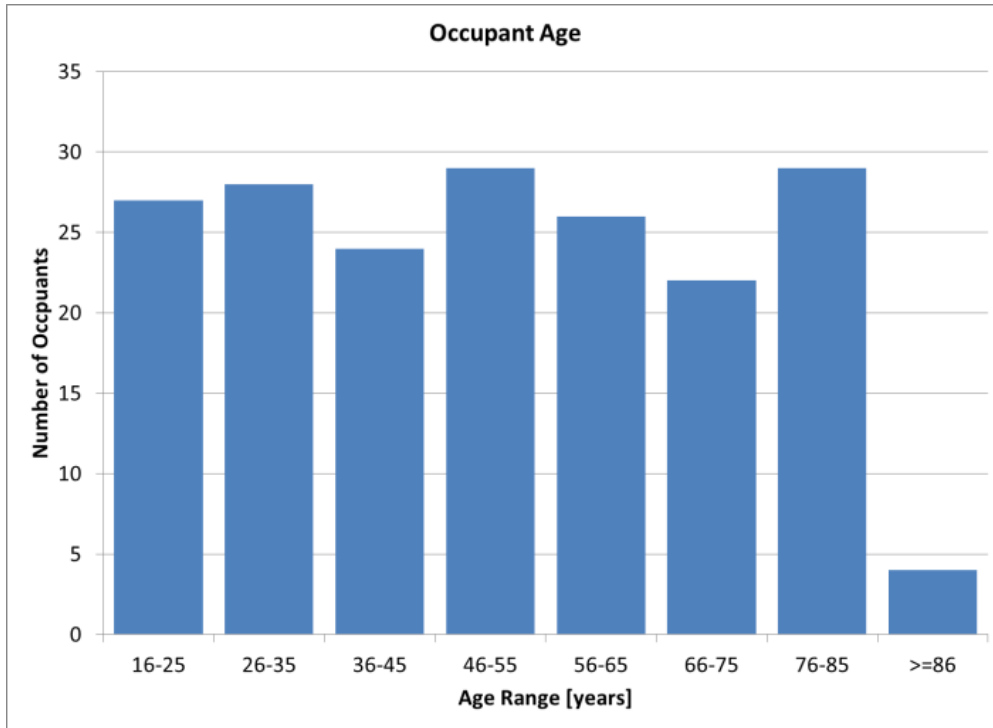


Figure 1. Breakdown of occupant age.

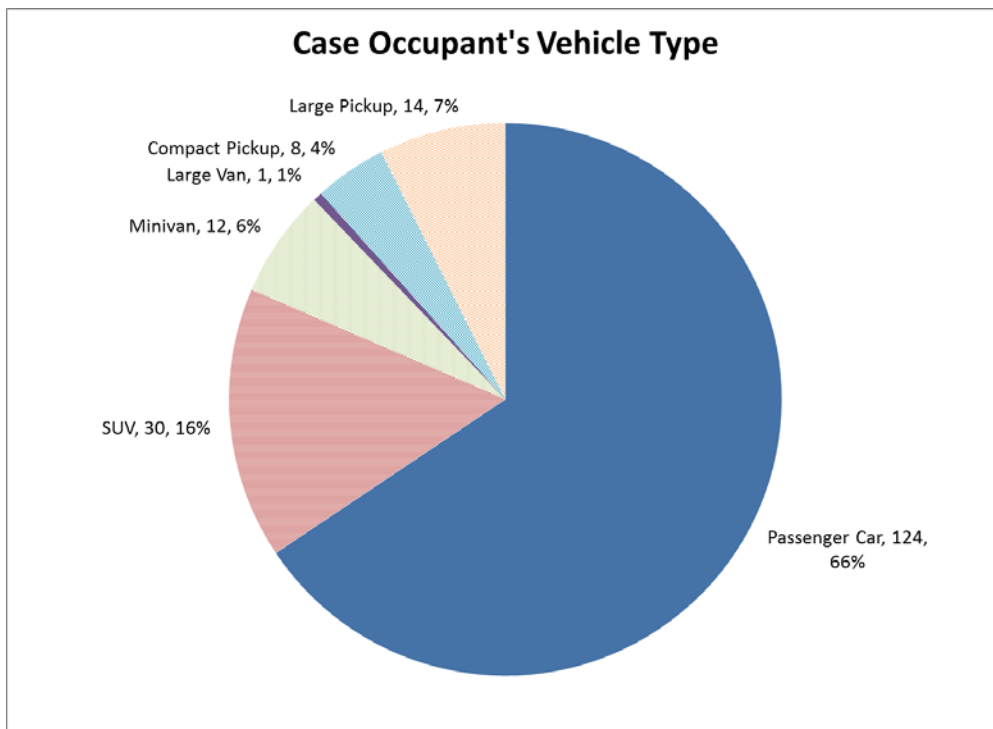


Figure 2. Vehicle type breakdown.

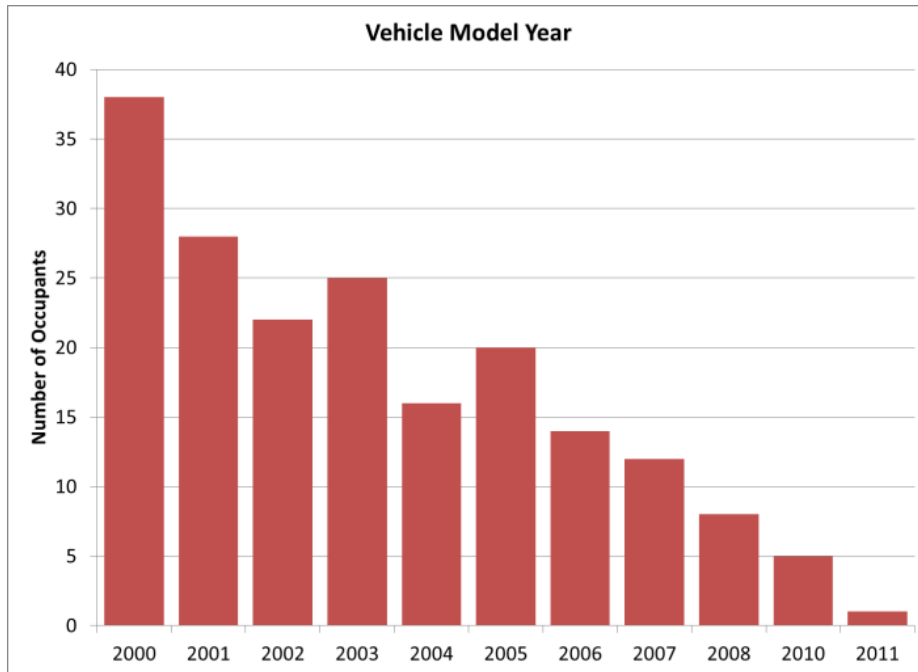


Figure 3. Vehicle model year breakdown.

Occupant outcome in the form of Injury Severity Score (ISS) and Maximum Abbreviated Injury Scale (MAIS) is shown in Figures 4 and 5. Some of the cases did not contain complete injury information because of limited ability to obtain adequate records in some fatal cases. Furthermore, the level of detail varies given that some occupants who are hospitalized will have more thorough documentation than those who may undergo only an external autopsy. The majority of the occupants in this study either died on scene or did not survive to be admitted

to a hospital. Figure 6 shows the breakdown of length of stay for different initial medical facilities. It should be noted that CDS does not consider a fatality that occurs after 30 days to be a crash fatality, but CIREN did have one case occupant who was hospitalized for 57 days. The duration of the hospital stay was shown as a function of age in Figure 7, where it is evident that younger occupants did not have as many long-duration hospital stays prior to death as older occupants.

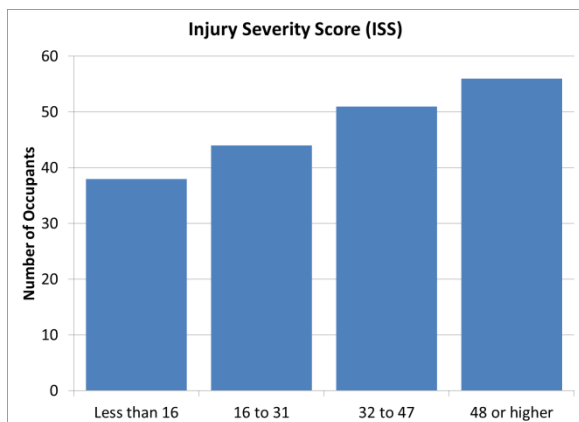


Figure 4. Injury Severity Score (ISS) breakdown.

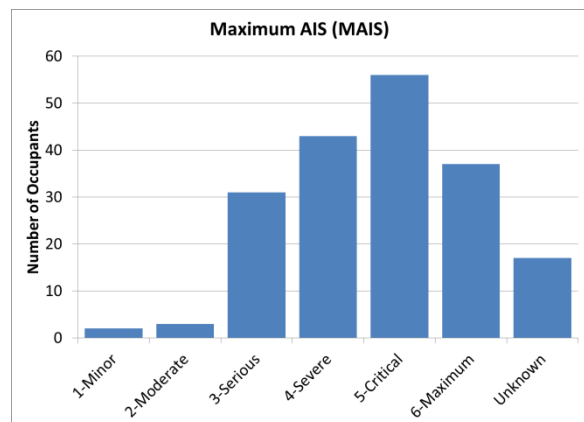


Figure 5. Maximum AIS severity breakdown.

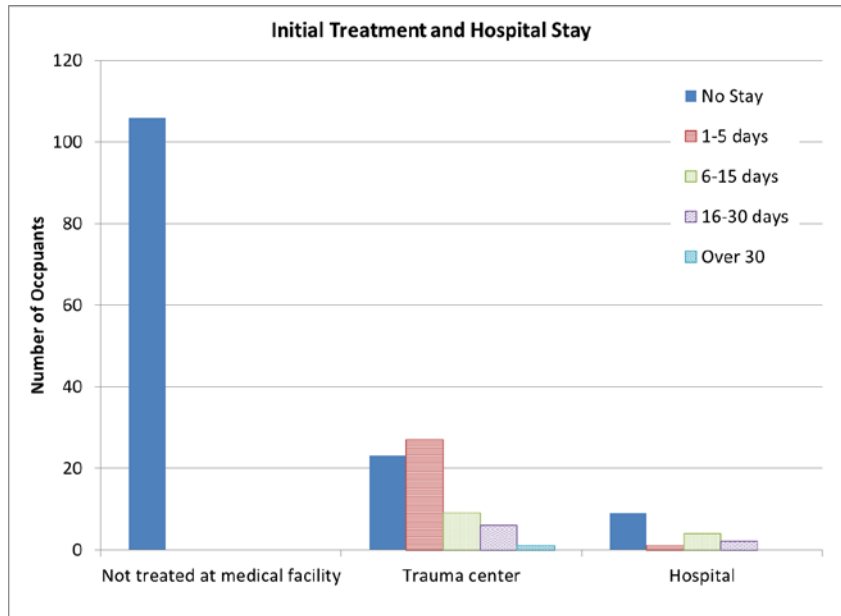


Figure 6. Initial medical facility and duration of hospital stay.

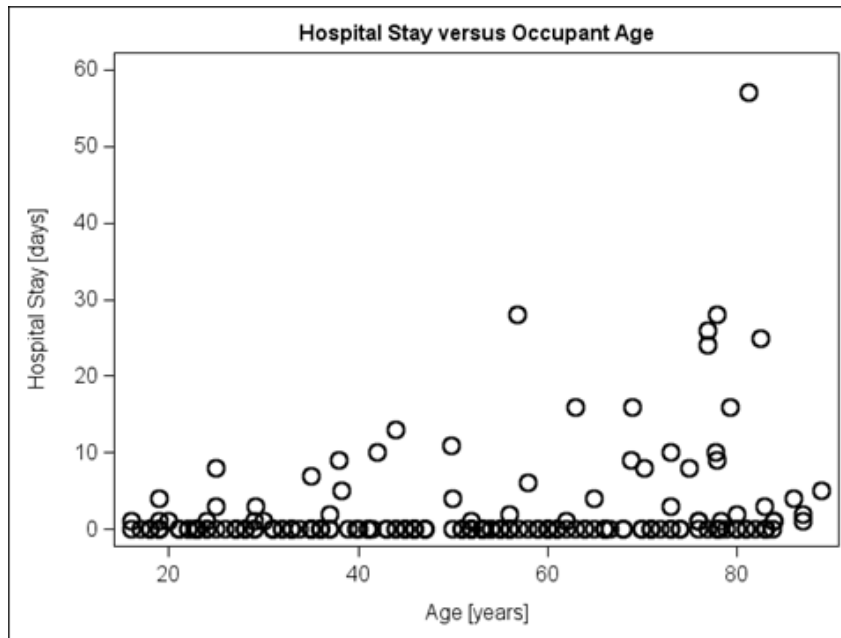


Figure 7. Hospital stay versus age.

Most of the fatalities were attributed to either a head or chest injury based on the first coded cause of death, which is shown in Figure 8. The occupants are broken down into four age ranges to show an age effect. In some cases, the victim's death was the result of complications that were not tied to a specific injury sustained in the crash, but were related to complications that arose during treatment.

The injury source associated with the first coded cause of death, for those occupants who did not die of complications, was most often the steering assembly, seat belt or part of another vehicle. The injury sources associated with the cause of death are shown for all occupants who did not die of complications in Figure 9.

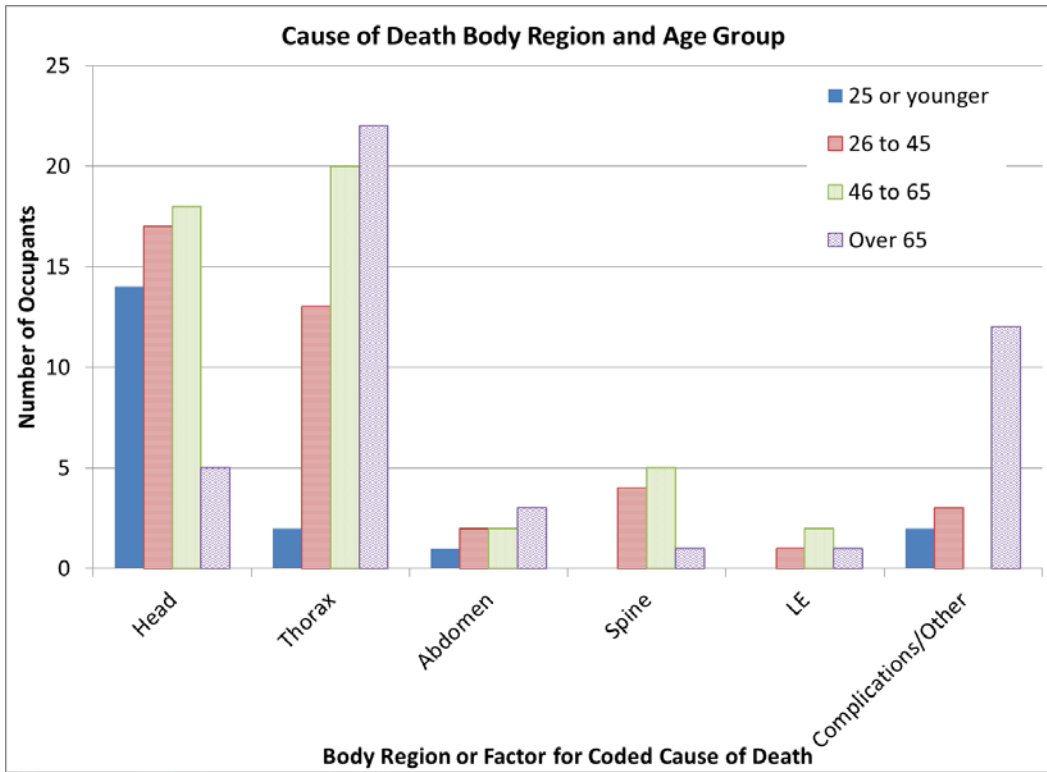


Figure 8. Occupant cause of death by body region (or complication) broken down into age ranges.

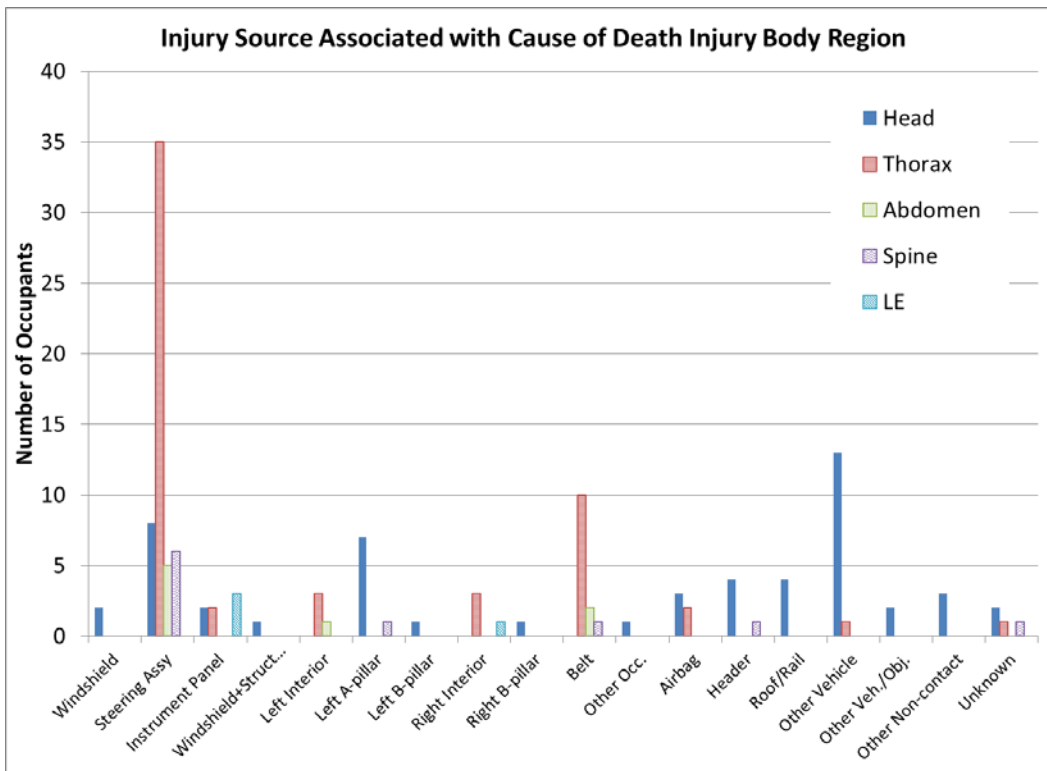


Figure 9. Coded injury source associated with first cause of death injury.

Each of the crashes was assigned to one or more categories to characterize the nature of the fatality. Table 1 shows the number of crashes in each category. Some crashes were in multiple categories if more than one relevant factor applied. Due to the size of the dataset and the small numbers in each category, combined categories were also developed

to aid in analysis. For example, since impacts to heavy vehicles typically involve mass and geometric mismatch, regardless of whether the side, front, or rear of the heavy vehicle was involved, a single heavy vehicle category was created that contained all three.

**Table 1.**  
**Fatality categorization – note that each crash may be assigned to multiple categories**

Exceedingly Severe	Corner/Oblique		Heavy Vehicle Impact/Underride			Narrow Object	Occupant Vulnerability		Other
	Corner Crash	Oblique Crash	Heavy Vehicle Front	Heavy Vehicle Side	Heavy Vehicle Rear		Occupant Age	Occupant Health	
55 (29%)	43 (23%)	31 (16%)	14 (7%)	5 (3%)	21 (11%)	14 (7%)	40 (21%)	8 (4%)	6 (3%)
	67 (35%)		40 (21%)				45 (24%)		

## DISCUSSION

The overall demographics of the study set was evenly distributed from young to old, and all of the primary passenger vehicle classes were represented. Most of the deaths occurred either on scene or on the day of the crash without an overnight stay in a hospital. While some of the cases included in this study did not include thorough injury coding, there was sufficient data to investigate the injuries that led to the occupants' deaths.

### Injury, Injury Severity Measures, and Injury Sources

The severity of the occupants' injuries, as assessed by AIS and ISS metrics, was generally severe in nature, but there were some MAIS and ISS values that were low relative to what would be expected for a fatally injured occupant. This is largely due to the number of cases where the decedent does not undergo a full autopsy or when full injury records were not received, and the full extent of injuries is not coded in the database. There are a few instances in which the initial injury severity was not very high, but the occupant died later of complications related to their injuries. In such a situation, the AIS and ISS wouldn't necessarily suggest a fatality. The cases shown in Figure 5 with only AIS 1 or 2 injuries were

instances in which a thorough assessment of the injuries was not available.

The first coded cause of death was most commonly coded to the thorax, followed by the head and then spinal cord. Of note from Figure 8 is that the oldest occupant group (over 65 years of age) died more often as a result of thoracic injuries or complications whereas the younger occupants typically died of head injuries, which is in agreement with the findings of Kent et al. [2005] for drivers in all crash modes.

The most commonly coded head injury was a brain stem laceration, and all brain stem injuries accounted for more than one third of the fatalities for which a head injury was the coded cause of death. Injuries to the cerebrum also accounted for about a third of the head-related fatalities, with the remainder being vault and basilar skull fractures as well as head crush injury. The fatal head injuries were coded to many sources inside the vehicle as shown in Figure 9, but the most common single source was the other vehicle. This primarily represents the cases involving underride of a heavy vehicle, where the structure of the other vehicle interacts with the upper portions of the case vehicle's occupant compartment. In these cases, large intrusions result, and the occupant's head interacts directly with the rear or side surface of the opposing heavy vehicle. The

steering assembly and A-pillar were also common sources, the former occurring in cases where the steering column moves up and toward the occupant as the occupant compresses the air bag while the latter occurring primarily in crashes with oblique occupant kinematics.

Thoracic injuries coded as cause of death involved mostly heart lacerations and vascular (aorta) injuries, each accounting for nearly one third of thorax-related deaths. Rib fractures also accounted for nearly one third of the thorax-related deaths, though this was likely a result of many cases not undergoing a full internal autopsy to document the injuries to the thoracic contents, which were more likely to have been the true reason for death. The thoracic injuries implicated with the death were almost always sourced to the steering assembly or seat belt.

While fewer in number than deaths linked to the head or thorax, those associated with a spinal cord injury occurred mostly in the middle-aged occupant group. All of these fatalities occurred on the day of the crash with no overnight hospital stay. The most common source of the cord injuries was the steering assembly.

Fatalities that were coded as a result of abdominal injuries occurred in eight cases, and the steering assembly was the most common source associated with the injury. These injuries were mostly severe internal organ injuries with significant bleeding. The fatalities that were associated with the injuries to the lower extremities involved a pelvic fracture in three cases and an amputation in one case. These injuries were associated with instrument panel contact or door contact, and resulted in death via excessive bleeding or complications.

### Exceedingly Severe Classification

When the cases were segregated by their exceedingly severe classification, one notable finding was that the crash severity was not as much of a factor for occupants in the oldest age group (Figure 10). Due to their fragility and frailty, older occupants comprised over 35% of the cases not considered to be exceedingly severe, but accounted for only 13% of exceedingly severe crashes. The body regions associated with the cause of death were generally similar regardless of crash severity group, though the spinal cord injuries were more prevalent in the exceedingly severe cases.

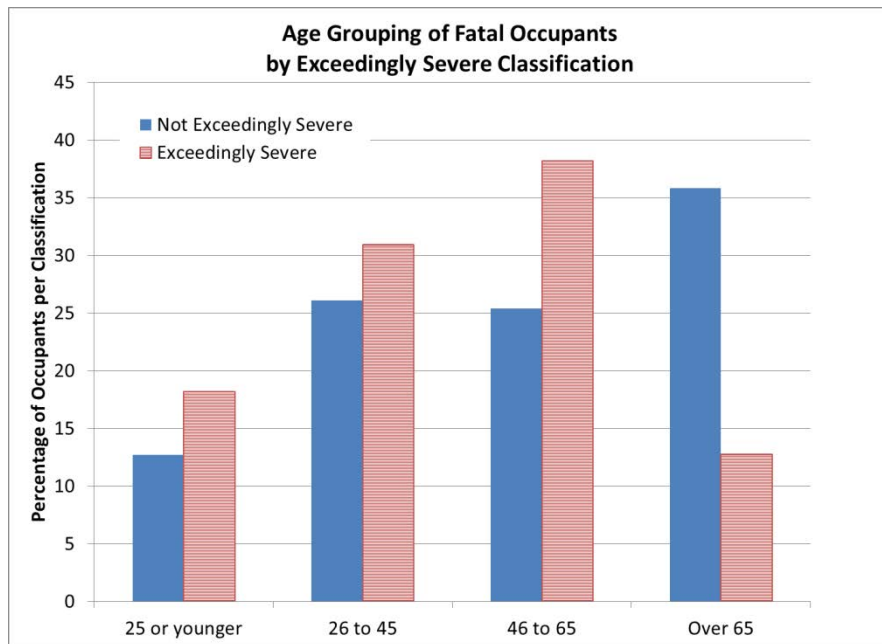


Figure 10. Frequency of occupants in exceedingly severe crashes by age groups.

As discussed in Rudd et al. [2009], crashes in the exceedingly severe category were typically those at higher speeds and involve a delta-v greater than vehicles would be exposed to in frontal crash tests required by Federal motor vehicle safety standards or the New Car Assessment Program, in which the vehicle's structure and restraints were taxed far beyond their design targets. In these crashes, it is common for the occupant compartment to deform such that any occupant restraint system could not effectively manage the occupant's ride-down of the crash. CDS occupant 2009-49-102-1-1 was the 28 year old female driver of a 2001 Jeep Grand

Cherokee, which impacted a 2008 Mercury Milan. The Jeep was traveling in the wrong direction on a high-speed divided highway prior to the crash, and the resulting impact led to a major wheelbase reduction and collapse of the occupant compartment space (Figure 11a). This collapse caused the floor under the driver's seat to move downward while the steering column likely moved rearward and upward (Figure 11b), though the unknown extent of extrication damage makes such an assessment uncertain. Regardless, the development of countermeasures for crashes of this severity poses challenges in the crashworthiness realm.



Figure 11. Left image (a) shows front right oblique view of 2009-49-102-1 and right image (b) shows case occupant's seating position.

### Corner/Oblique Classification

A number of recent studies have focused on small overlap and oblique frontal crashes and the associated challenges to the structure and restraint systems. Crashes in this study were originally classified as corner and/or oblique, but the categories were combined since the occupant kinematics and vehicle interaction have been found to be similar [Rudd et al. 2011]. Figure 12 shows the frequency of fatalities for the body region associated with the first coded cause of death by the corner/oblique classification. There is a notable increase in the proportion of head-related fatalities in the corner/oblique group. When the associated injury sources are compared, as in Figure 13, there is a trend towards more contacts towards the sides of the vehicle with the A-pillars, roof rails and side door panels accounting for a greater share of the injury sources. This finding is

coincident with other studies that have demonstrated the occupants' sub-optimal interaction with the frontal air bag due to their oblique kinematics.

CIREN case 431208557 is an oblique crash between a 2010 Toyota Prius and a 2009 Pontiac G6. The driver and right-front passenger of the Prius were both enrolled as CIREN occupants, and both succumbed to their injuries. Figure 14a shows the exterior damage and Figure 14b shows the driver's seating position. On impact, the 49 year old male driver moved forward and to the left in response to the 340° direction of force such that his head made contact with the left roof side rail (adjacent to upper A-pillar). The driver suffered a traumatic brain injury and remained deeply comatose until he died ten days after the crash upon removal from life support.

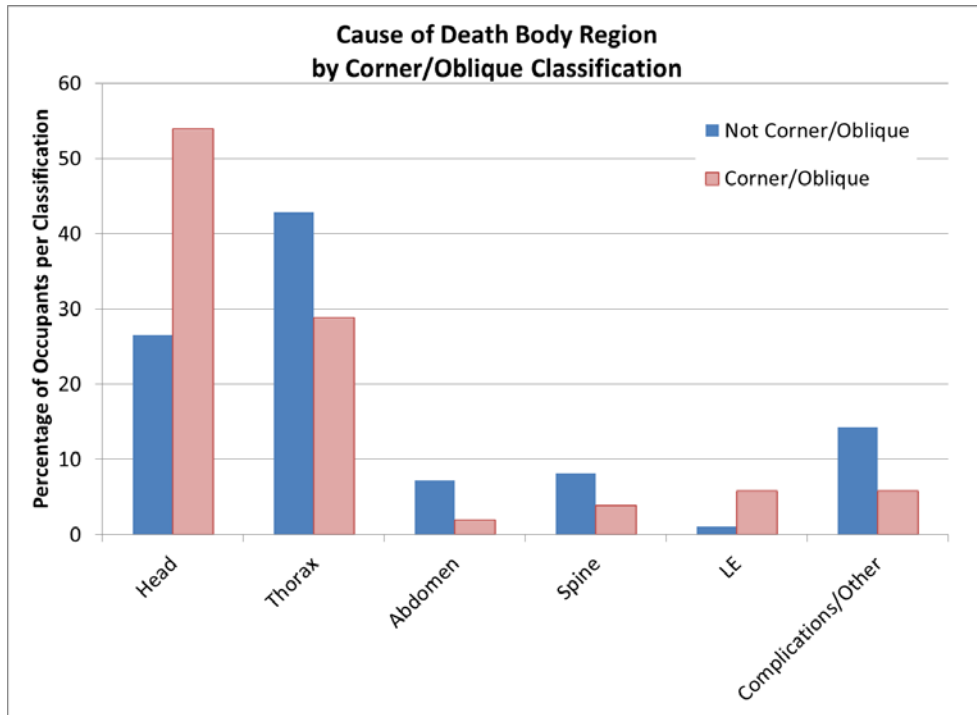


Figure 12. Occupant cause of death by body region (or complication) based on whether the crash was considered a corner or oblique impact.

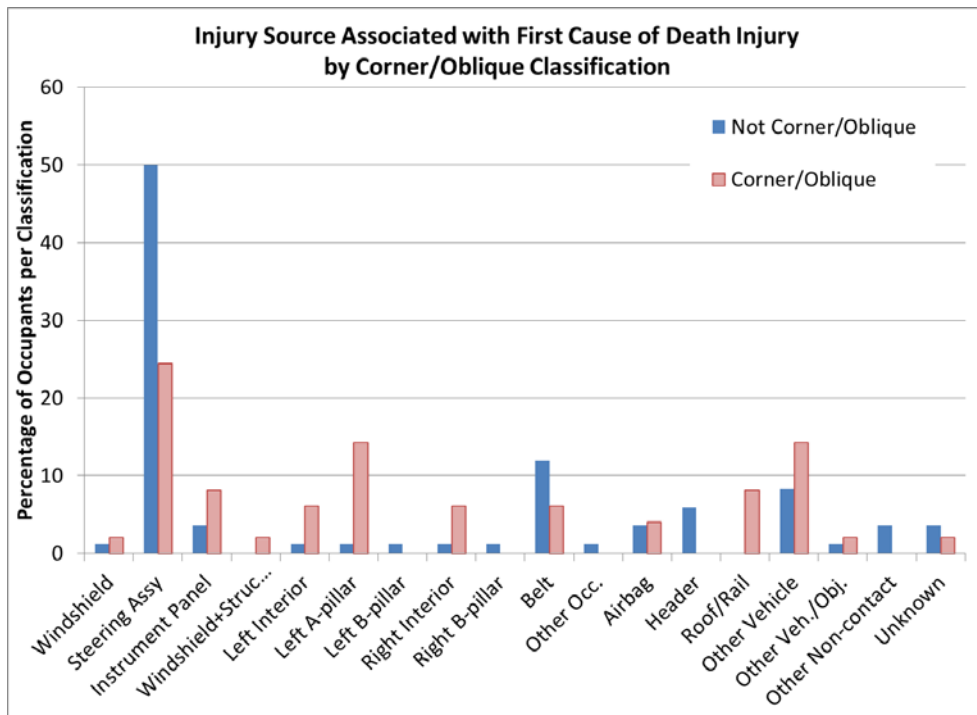


Figure 13. Sources of injury for cause of death injuries based on whether the crash was considered a corner or oblique impact.

The side curtain air bag did not deploy in this crash, but it is uncertain whether it would have provided cushioning for this particular head impact. While this was a severe crash, the occupant's slightly lateral head motion in conjunction with the intrusion of the

A-pillar was deemed to be the critical feature leading to the head injury. Aside from the head injuries, none of the driver's other injuries would likely have resulted in death.



Figure 14. Left image (a) shows front left oblique view of 431208557 and right image (b) shows case occupant's seating position.

### Vulnerable Occupant Classification

Another combined category was created for vulnerable occupants to include those with vulnerabilities associated with their age or health. Some occupants were determined to have vulnerabilities associated with their age and health, but the vast majority of the occupants in this category were there due to their age alone. The average age of the vulnerable occupants was 76 years compared to 43 for the base group. Vulnerable occupants were more likely to die of thoracic injuries or complications compared to younger occupants (Figure 15), and a greater proportion of vulnerable occupants had extended hospital stays prior to their death (Figure 16). These findings echo those found by Kent et al. [2005]

While a comparison of ISS is somewhat limited in its utility due to the number of cases without full injury data, the vulnerable occupant group did demonstrate a general trend toward a lower ISS value than the non-vulnerable occupant group in all age ranges. A

comparison of the injury sources for the occupant vulnerability groups indicates that the seat belt was responsible for the cause of death in a greater portion of the vulnerable occupant fatalities.

CIREN case 852131345 involves an 82 year old female right front passenger in a 2004 Nissan Maxima which contacted the front of a large truck. There was some underride of the occupant's vehicle relative to the truck, but it was not considered a factor for this occupant since the intrusions at her seating position were minor (Figure 17). She sustained several rib fractures, lung contusion and laceration, and fractures to the lower extremities and lumbar spine. The thoracic injuries were attributed to belt loading, and the number of fractured ribs resulted in an AIS 5 code. She survived 25 days in the hospital and died of acute respiratory distress syndrome after removal of life support. The 81 year old male driver of this vehicle survived, and was hospitalized for six days for sacral and lumbar spine fractures.

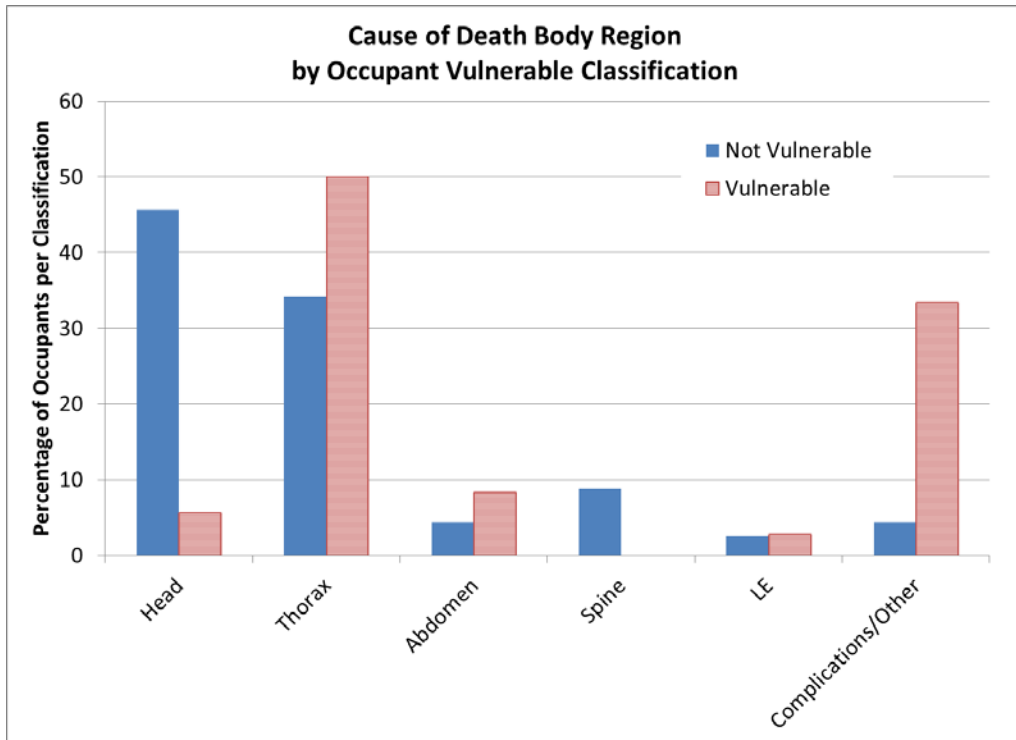


Figure 15. Occupant cause of death by body region (or complication) based on occupant vulnerability.

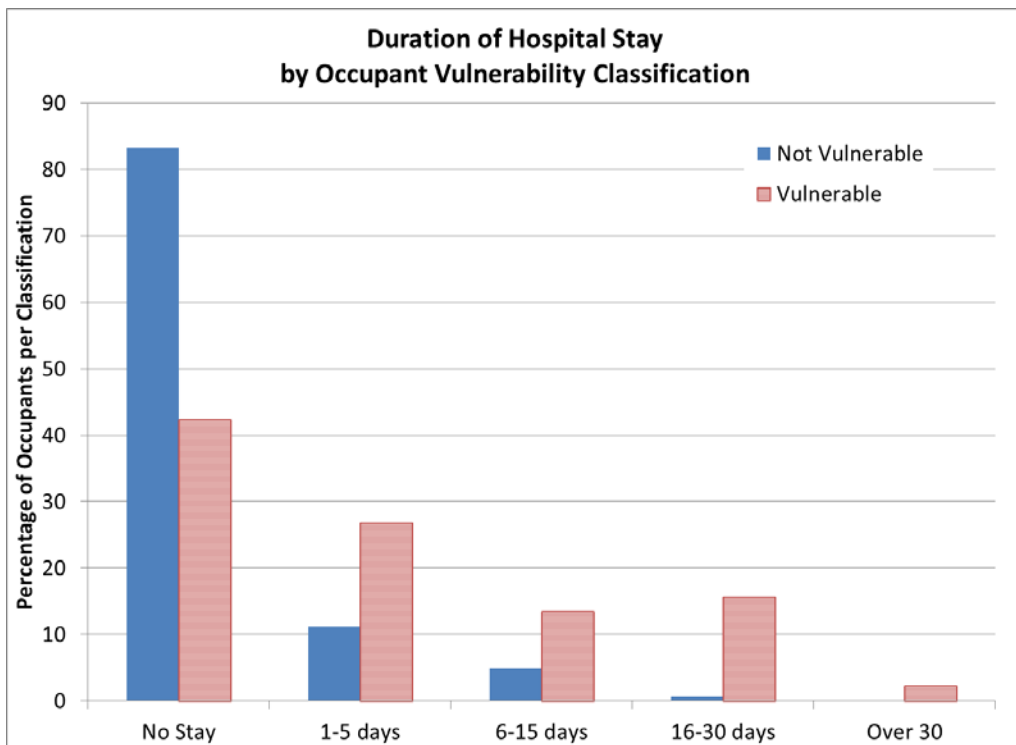


Figure 16. Duration of occupant's hospitalization before death based on occupant vulnerability.



Figure 17. Left image (a) shows front right oblique view of 852131345 and right image (b) shows case occupant's seating position.

### Limitations

This study was undertaken to gain a better understanding of the injuries that lead to the death of restrained occupants in frontal crashes. While the cases studied do represent what is happening in field crashes, this study was not intended to utilize the case weights in order to develop nationally representative findings. Furthermore, the analysis of coded data fields is based on the data provided in each of the cases, and in many cases the limited autopsy data or incomplete medical records lead to causes of death that don't accurately capture the occupant's experience. In some of these cases, inferences could be made or the cases could otherwise be reclassified to eliminate ambiguity, but that was not done in this study.

Since this study involved manual review of cases, along with subjective classification of the cases, it must be understood that a certain amount of author bias may exist in the findings. While every effort was made to consistently assign categories, arguments could be made to justify alternate categorical assignments. This limitation is exacerbated by the fact that the case data that was collected may not contain key pieces of evidence relevant to the occupants' crash experience. For example, one factor that may play a large role in occupant response is their exact seating position at impact, which is almost always impossible to know with any degree of certainty.

### CONCLUSIONS

This detailed review of injury and causation was an extension of a prior study of fatal occupants. One hundred and eighty nine fatal occupants were studied and of those 55 (29%) were deemed to be in crashes of extreme severity. Deaths attributed to head and thorax injuries each accounted for about 37% of the total, with 11% occurring as a result of complications from injury. Older occupants died more often from thoracic trauma, while younger occupants more commonly died from head injuries. The older occupants in this study were also more likely to be injured in crashes of lower severity compared to their younger counterparts and they were more likely to have an extended hospital stay prior to death. In the cases identified as corner or oblique crashes, the occupants died more often from head injuries caused by contact with outboard vehicle structures.

Future work with this dataset will consider multi-system trauma as well as the specific types of injuries, intrusions of components and their role in injury causation, and detailed restraint analysis.

### REFERENCES

AAAM (2005) "Abbreviated Injury Scale." Association for the Advancement of Automotive Medicine.

Bean, J.D., Kahane, C.J., Mynatt, M., Rudd, R.W., Rush, C.J. and Wiacek, C. (2009) "Fatalities in

Frontal Crashes Despite Seat Belts and Air Bags – Review of All CDS Cases – Model and Calendar Years 2000-2007 – 122 Fatalities.” DOT HS 811 102.

Brumbelow, M.L. and Zubby, D.S. (2009) “Impact and injury patterns in frontal crashes of vehicles with good ratings for frontal crash protection.” 21<sup>st</sup> International Technical Conference on the Enhanced Safety of Vehicles, Paper 09-0257.

Halloway, D.E., Saunders, J., Yoganandan, N. and Pintar, F. (2011) “An Operational Definition of Small Overlap Impact for Published NASS Data.” SAE Paper 2011-01-0543.

IIHS (2012) “Small Overlap Frontal Crashworthiness Evaluation Crash Test Protocol (Version I).”

NHTSA TSF Research Note “2011 Motor Vehicle Crashes: Overview” DOT HS 811 701 December 2012

Rudd, R.W., Bean, J., Cuentas, C., Kahane, C.J., Mynatt, M. and Wiacek, C. (2009) “A study of the factors affecting fatalities of air bag and belt-restrained occupants in frontal crashes.” 21<sup>st</sup> International Technical Conference on the Enhanced Safety of Vehicles, Paper 09-0555.

Saunders, J., Craig, M. and Parent, D. (2012) “Moving deformable barrier test procedure for evaluating small overlap/oblique crashes.” SAE Paper 2012-01-0577.

**APPENDIX A**

Year	PSU	Case	Veh.	Occ.	CIREN ID	Age	Gender	Seat	ISS	Model Year	Make and Model	Exceedingly Severe	Narrow Impact	Corner/Oblique	Heavy Vehicle	Vulnerable Occupant
2000	.	.	1	1	54567	33	2	11	75	2000	HOND Odyssey	✓			✓	
2000	8	226	1	1	.	42	1	11	17	2000	NISS Altima	✓		✓		
2000	11	130	1	1	.	33	2	11	75	2000	HOND Odyssey	✓				
2000	12	78	1	1	.	45	1	11	1	2000	GMC C,K,R,V-series P/U	✓				
2000	43	243	1	1	.	51	2	11	5	2000	CHRY Voyager				✓	
2000	49	254	2	1	.	41	1	11	14	2000	DODG Ram 1500 P/U				✓	
2000	76	139	3	1	.	54	1	11	75	2000	GMC Jimmy fullsize			✓		
2000	78	80	1	1	.	71	1	11	4	2000	DODG Intrepid	✓				
2001	11	178	2	1	.	45	2	11	35	2000	MERC Cougar	✓				
2001	73	33	1	2	.	46	1	13	50	2001	DODG Stratus				✓	
2001	75	113	1	1	.	53	1	11	75	2001	TOYT Avalon			✓		
2001	76	111	1	1	.	56	1	11	9	2001	NISS Sentra			✓		
2001	81	117	2	1	.	52	1	11	75	2002	TOYT Tundra			✓		
2002	.	.	1	1	551081358	22	2	11	45	2000	MITS Mirage			✓		
2002	2	114	1	1	.	68	1	11	36	2000	FORD Ranger		✓	✓		
2002	9	43	2	1	.	55	1	11	45	2001	CHEV Caprice/Impala				✓	
2002	9	131	2	1	.	33	1	11	45	2001	FORD Taurus/Taurus X			✓		
2002	12	94	2	1	.	50	1	11	21	2000	GMC Jimmy/S-15 based					
2002	12	186	2	1	.	60	1	11	43	2000	PONT J-2000	✓				
2002	12	186	2	2	.	60	2	13	75	2000	PONT J-2000	✓				
2002	42	25	1	2	57335	29	2	13	34	2002	JAG X-Type	✓				
2002	42	34	3	1	377059731	33	2	11	29	2001	DODG Intrepid			✓		
2002	42	34	3	2	377061232	61	2	13	36	2001	DODG Intrepid			✓		
2002	45	16	1	1	.	35	1	11	14	2000	CHEV S-10	✓				
2002	47	39	2	1	.	44	2	11	0	2000	FORD Taurus/Taurus X	✓				
2002	47	134	1	1	.	61	1	11	0	2002	CHEV Astrovan	✓				
2002	49	100	1	1	.	66	2	11	43	2000	CHRY Town & Country		✓			
2002	75	53	1	2	.	71	2	13	29	2000	TOYT 4-Runner					✓
2002	76	97	1	2	.	18	1	13	0	2001	CHEV Cavalier	✓				
2003	.	.	1	1	378074980	78	2	11	75	2001	MITS Galant			✓		✓
2003	.	.	1	1	857069084	29	1	11	22	2003	FORD Expedition		✓	✓		
2003	2	141	2	1	.	39	1	11	75	2000	HOND Civic/CRX	✓				
2003	9	47	1	1	.	27	1	11	75	2001	FORD F-series P/U	✓				
2003	42	61	1	2	.	47	1	13	26	2002	VW Jetta				✓	
2003	48	158	1	2	.	81	2	13	21	2002	TOYT Tacoma					✓
2003	76	134	1	1	.	46	1	11	19	2001	DODG Intrepid	✓				
2003	79	139	1	1	.	18	1	11	10	2000	CHEV G-series Van				✓	
2003	81	41	1	1	.	46	1	11	75	2003	CHEV S-10	✓				
2003	81	44	1	1	.	19	1	11	43	2003	DODG Neon			✓		

Year	PSU	Case	Veh.	Occ.	CIREN ID	Age	Gender	Seat	ISS	Model Year	Make and Model	Exceedingly Severe	Narrow Impact	Corner/Oblique	Heavy Vehicle	Vulnerable Occupant
2004	.	.	1	1	142061704	41	2	11	59	2001	JEEP Cherokee84-			✓	✓	
2004	.	.	1	1	558014121	56	2	11	29	2000	DODG Durango					✓
2004	.	.	1	1	857078140	22	1	11	75	2000	HYUN Tiburon	✓				
2004	2	62	2	1	.	81	2	11	35	2000	HOND Accord			✓		✓
2004	9	62	1	1	.	70	1	11	75	2001	TOYT Avalon		✓			
2004	41	15	2	2	.	78	2	13	21	2000	TOYT Corolla					✓
2004	42	113	1	1	.	23	1	11	43	2004	DODG Stratus				✓	
2004	43	253	1	1	.	31	1	11	14	2004	HOND Accord			✓		
2004	43	291	1	1	.	33	2	11	22	2003	DODG Caravan				✓	
2004	45	113	1	1	.	37	1	11	50	2000	HOND Civic/CRX			✓		
2004	47	83	1	2	.	76	2	13	0	2003	CHEV C/K-series Pickup		✓	✓		
2004	49	168	2	2	.	56	2	13	59	2004	MERZ S Class			✓		
2004	50	32	1	2	.	65	2	13	34	2001	SUBA Forester		✓	✓		
2004	50	147	1	1	.	80	2	11	33	2001	HOND Civic/CRX					✓
2004	73	165	1	1	.	52	1	11	59	2002	FORD Bronco II				✓	
2004	73	241	2	1	.	52	1	11	30	2004	NISS Altima			✓		
2004	76	57	1	1	.	19	2	11	29	2002	CHEV Cavalier	✓				
2004	76	157	1	1	.	68	1	11	26	2002	CHEV Cavalier	✓				
2004	79	49	1	1	.	72	2	11	14	2001	TOYT Camry					✓
2004	79	244	1	1	.	70	1	11	14	2003	CADI Deville/Fleetwood					✓
2004	82	16	1	2	.	25	2	13	33	2000	VW Jetta				✓	
2005	.	.	1	1	160121660	70	2	11	30	2003	HOND Civic/CRX					✓
2005	2	54	2	1	.	60	2	11	21	2004	DODG Neon			✓		✓
2005	4	119	1	1	.	86	1	11	10	2003	CHEV Caprice/Impala					✓
2005	9	189	1	1	.	43	1	11	75	2005	FORD Escape				✓	
2005	43	231	1	1	.	31	1	11	14	2000	JEEP Cherokee84-		✓	✓		
2005	45	116	1	2	.	87	2	13	22	2003	DODG Neon					✓
2005	45	142	1	1	.	63	2	11	22	2003	ACUR CL/TL	✓				
2005	45	196	2	1	.	69	1	11	17	2005	CHEV Caprice/Impala			✓		✓
2005	47	102	3	1	.	22	1	11	0	2001	FORD F-series P/U			✓		
2005	47	134	2	1	.	44	2	11	0	2002	PONT Firebird/Trans AM			✓		
2005	47	137	1	1	.	19	2	11	0	2001	FORD Mustang/Mustang II				✓	
2005	50	125	2	1	.	41	1	11	75	2002	PONT Grand Prix	✓				
2005	72	36	1	1	.	35	1	11	19	2004	CHEV Cavalier				✓	
2005	74	138	1	1	.	47	2	11	59	2005	TOYT Corolla	✓				
2005	75	170	1	1	.	64	2	11	29	2002	FORD Mustang/Mustang II	✓				
2005	79	139	1	1	.	74	2	11	26	2000	HOND Accord					✓
2006	.	.	1	2	852131345	82	2	13	43	2004	NISS 810/Maxima					✓
2006	4	45	1	1	.	19	2	11	38	2001	SATN LS			✓	✓	
2006	9	59	2	1	.	35	1	11	75	2006	FORD Escape			✓		
2006	11	150	1	2	.	17	2	13	35	2002	CHEV Trail Blazer				✓	

Year	PSU	Case	Veh.	Occ.	CIREN ID	Age	Gender	Seat	ISS	Model Year	Make and Model	Exceedingly Severe	Narrow Impact	Corner/Oblique	Heavy Vehicle	Vulnerable Occupant
2006	11	163	1	1	.	35	1	11	26	2006	LINC Zephyr				✓	
2006	12	161	1	1	.	30	1	11	41	2005	CHRY Town & Country			✓		
2006	41	64	1	1	.	78	2	11	33	2005	LEXS ES-250/300		✓			
2006	42	138	1	1	.	32	2	11	75	2004	KIA Sedona			✓		
2006	42	138	2	1	.	29	2	11	41	2006	CHRY 300M			✓		
2006	45	59	2	1	.	23	2	11	14	2005	FORD Focus			✓		
2006	49	137	1	1	.	19	1	11	75	2002	PONT Aztek		✓	✓		
2006	49	201	1	1	.	52	2	11	57	2006	KIA Rio	✓				
2006	50	83	1	1	.	28	1	11	34	2000	HYUN Tiburon			✓		
2006	75	22	1	2	.	27	1	13	25	2006	MIT S Eclipse		✓			
2006	75	23	2	1	.	22	1	11	0	2005	MIT S Lancer			✓		
2006	75	96	1	1	.	31	1	11	0	2000	CHRY Concorde			✓		
2006	75	98	2	1	.	25	2	11	0	2001	CHEV Malibu(97-)	✓				
2006	78	62	1	1	.	50	2	11	21	2000	DODG Ram 1500 P/U				✓	
2006	78	132	1	1	.	66	2	11	0	2003	FORD F-series P/U	✓				
2006	82	4	1	1	.	47	1	11	34	2003	CHEV C/K-series Pickup	✓				
2007	.	.	1	1	160134344	79	1	11	29	2002	BUIC Electra/Park Avenue					✓
2007	.	.	1	1	160140683	77	1	11	50	2007	LINC TownCar/Continental	✓				✓
2007	.	.	1	1	160141238	81	1	11	30	2003	MERZ E					✓
2007	.	.	1	1	385107159	83	1	11	50	2005	BUIC Electra/Park Avenue					✓
2007	.	.	2	1	385102796	53	1	11	66	2001	CHRY PT Cruiser	✓				
2007	2	139	1	1	.	79	2	11	38	2001	NISS Sentra					✓
2007	9	63	1	1	.	60	1	11	75	2006	TOYT Avalon				✓	
2007	11	39	1	1	.	64	1	11	75	2006	SUBA Legacy	✓				
2007	11	72	1	1	.	18	1	11	57	2002	HOND Accord	✓				
2007	11	135	1	1	.	80	1	11	22	2004	CHEV Malibu(97-)					✓
2007	12	180	1	1	.	56	2	11	75	2000	DODG Dakota	✓				
2007	41	160	1	1	.	54	1	11	38	2000	MAZD GLC/323/Protege			✓		
2007	42	9	1	1	.	46	1	11	38	2004	INFI FX35/45	✓				
2007	42	120	2	1	.	76	1	11	6	2003	CHRY Sebring					✓
2007	47	61	2	1	.	58	1	11	38	2005	HOND C-RV			✓		
2007	47	119	1	1	.	36	1	11	0	2001	DODG Ram 1500 P/U	✓				
2007	48	186	2	1	.	66	1	11	48	2003	TOYT Tacoma			✓		
2007	72	101	1	1	.	71	2	11	25	2001	BUIC Lesabre/Wildcat/Cen					✓
2007	72	126	1	1	.	82	1	11	19	2005	FORD Focus			✓		✓
2007	73	37	1	1	.	46	1	11	75	2000	TOYT Celica				✓	
2007	73	137	1	1	.	52	1	11	43	2005	DODG Stratus	✓				
2007	74	107	1	1	.	20	2	11	45	2000	FORD Taurus/Taurus X	✓				
2007	74	107	2	1	.	62	1	11	75	2000	BUIC Electra/Park Avenue	✓				
2007	74	107	2	2	.	62	2	13	41	2000	BUIC Electra/Park Avenue	✓				
2007	78	24	1	1	.	27	1	11	14	2000	NISS Pickup/Frontier			✓	✓	

Year	PSU	Case	Veh.	Occ.	CIREN ID	Age	Gender	Seat	ISS	Model Year	Make and Model	Exceedingly Severe	Narrow Impact	Corner/Oblique	Heavy Vehicle	Vulnerable Occupant
2008	.	.	1	2	852156114	83	2	13	35	2003	HOND Odyssey				✓	✓
2008	2	143	1	1	.	55	1	11	54	2007	HYUN Elantra	✓				
2008	4	10	2	1	.	63	1	11	17	2002	MERC Sable			✓	✓	
2008	9	53	2	1	.	37	2	11	50	2008	PONT G5			✓		
2008	9	134	1	1	.	24	1	11	75	2008	HYUN Accent				✓	
2008	9	144	1	2	.	37	1	13	75	2006	HOND Civic/CRX		✓	✓		
2008	11	103	1	1	.	51	2	11	75	2004	PONT Aztek	✓				
2008	11	211	1	1	.	21	1	11	50	2002	SATN SL	✓				
2008	12	77	1	1	.	77	2	11	75	2005	TOYT Camry	✓	✓			
2008	13	222	1	1	.	16	1	11	75	2005	CHEV Malibu(97-)	✓				
2008	43	157	2	1	.	52	1	11	13	2006	MINI COOPER				✓	
2008	43	303	1	1	.	38	2	11	14	2008	TOYT RAV-4					
2008	73	81	3	1	.	53	1	11	75	2003	FORD Mustang/Mustang II			✓		
2008	78	22	1	2	.	43	1	13	2	2004	CADI CTS				✓	
2008	78	31	1	1	.	51	1	11	0	2006	CHEV C/K-series Pickup			✓		
2008	78	31	2	1	.	36	2	11	0	2002	LEXS RX300			✓		
2008	81	65	1	2	.	83	2	13	35	2003	HOND Odyssey			✓		✓
2009	.	.	1	1	385138077	38	1	11	45	2010	HYUN GENESIS			✓		
2009	.	.	1	1	385145571	39	1	11	45	2004	NISS Titan			✓		
2009	.	.	1	1	459036835	73	2	11	45	2002	TOYT Highlander					✓
2009	2	155	1	1	.	87	1	11	34	2003	FORD Focus			✓		✓
2009	9	99	1	1	.	36	1	11	75	2007	HOND Accord				✓	
2009	11	191	1	2	.	16	2	13	45	2001	HOND Odyssey			✓	✓	
2009	41	60	1	1	.	89	1	11	10	2005	MERC Marquis/Monterey					✓
2009	43	250	3	1	.	35	1	11	43	2008	DODG Ram 1500 P/U			✓		
2009	48	32	1	1	.	57	2	11	26	2005	BUIC Rendezvous					✓
2009	48	100	1	1	.	56	2	11	0	2006	CHEV Caprice/Impala				✓	
2009	49	102	1	1	.	28	2	11	41	2001	JEEP Cherokee84-	✓				
2009	49	130	2	1	.	45	2	11	45	2001	JEEP Cherokee84-	✓				
2009	49	186	1	1	.	24	1	11	75	2005	MITL Lancer	✓				
2009	73	74	1	1	.	25	2	11	34	2008	HOND Civic/CRX	✓				
2009	73	84	2	1	.	40	2	11	43	2007	CHEV Malibu(97-)			✓		
2009	74	50	2	1	.	55	1	11	38	2002	FORD Windstar	✓				
2009	76	115	1	1	.	53	2	11	75	2003	VW Passat				✓	
2009	76	128	1	1	.	58	2	11	0	2007	HOND Fit	✓				
2009	81	58	2	2	.	56	2	13	75	2004	HOND Accord			✓		
2009	82	10	2	1	.	65	2	11	48	2007	HOND C-RV			✓		
2010	.	.	1	1	385165500	77	1	11	34	2006	FORD Ranger		✓			✓
2010	.	.	1	1	431208557	49	1	11	29	2010	TOYT Prius			✓		
2010	.	.	1	2	431208606	76	1	13	27	2010	TOYT Prius			✓		✓
2010	2	69	1	1	.	59	1	11	75	2004	CHEV Aveo				✓	

Year	PSU	Case	Veh.	Occ.	CIREN ID	Age	Gender	Seat	ISS	Model Year	Make and Model	Exceedingly Severe	Narrow Impact	Corner/Oblique	Heavy Vehicle	Vulnerable Occupant	
2010	9	144	1	1	.	74	1	11	24	2003	FORD Expedition				✓		
2010	12	64	1	1	.	83	1	11	17	2005	BUIC Century					✓	
2010	41	170	2	1	.	78	2	11	21	2007	CADI CTS					✓	
2010	41	212	1	1	.	77	1	11	29	2007	TOYT Camry					✓	
2010	45	16	2	1	.	80	1	11	0	2003	BUIC Century				✓		
2010	45	180	1	1	.	78	1	11	22	2005	LEXS LS-400					✓	
2010	49	170	1	1	.	29	1	11	75	2007	CHEV Fullsize Blazer	✓					
2010	74	131	1	1	.	28	2	11	75	2007	JEEP Liberty	✓			✓		
2010	74	167	1	1	.	24	2	11	38	2001	VW Passat			✓	✓		
2010	78	38	1	1	.	21	1	11	75	2007	HOND Accord		✓	✓			
2010	79	70	1	2	.	84	2	13	75	2002	HOND Civic/CRX					✓	
2010	81	85	1	1	.	73	1	11	43	2002	TOYT Tundra					✓	
2011	.	.	1	1	317101783	59	1	11	29	2008	NISS Altima			✓			
2011	.	.	1	1	357137502	78	1	11	43	2010	LINC TownCar/Continental			✓		✓	
2011	.	.	1	1	360206546	68	1	11	41	2006	ACUR CL/TL	✓		✓			
2011	.	.	1	2	360208690	66	1	13	29	2003	TOYT Highlander					✓	
2011	3	88	1	1	.	84	2	11	27	2008	HOND Accord			✓		✓	
2011	3	98	1	1	.	61	1	11	22	2010	HOND C-RV			✓			
2011	4	95	1	1	.	73	2	11	34	2006	HYUN Sonata	✓				✓	
2011	11	244	2	1	.	73	1	11	34	2011	FORD Fiesta				✓		
2011	45	3	1	2	.	44	1	13	26	2005	NISS Altima					✓	
2011	48	96	1	1	.	75	2	11	34	2007	NISS Altima					✓	
2011	49	139	1	1	.	35	1	11	75	2008	FORD Focus	✓		✓			
2011	73	138	1	1	.	26	2	11	14	2005	FORD Taurus/Taurus X				✓		
2011	78	19	1	1	.	23	2	11	59	2003	CHEV Suburban				✓		
2011	78	19	1	2	.	32	1	13	9	2003	CHEV Suburban				✓		
2011	81	57	3	1	.	36	1	11	50	2004	HOND Pilot			✓			
							1=Male 2=Female 11=Driver 13=Passenger										

# AN IMPROVED NORMALIZATION METHODOLOGY FOR DEVELOPING MEAN HUMAN RESPONSE CURVES

**Kevin Moorhouse**

National Highway Traffic Safety Administration  
United States  
Paper Number 13-0192

## ABSTRACT

Mean human response curves and associated biomechanical response targets are commonly developed from Post-Mortem Human Subject (PMHS) test data to guide the design of anthropomorphic test devices (ATDs) by providing “target” biomechanical responses to impact. Since differences in anthropometry and physical characteristics within a group of PMHS can result in widely varying response data, the first step in developing target biomechanical responses is typically to normalize the responses to a certain “standard” anthropometry representing the ATD to be designed or evaluated. The normalization procedure should adjust the response data to account for the variation in anthropometry and physical characteristics, and thus should collapse the group of curves closer to a single response so that a mean response can be more accurately established that represents the human response of the “standard” anthropometry selected. Several methods for normalizing PMHS test data can be found in the literature, but there is no consensus as to which is the most effective. In this study, the two most common existing normalization techniques, as well as some newly developed methodologies, were evaluated by applying them to both a side impact PMHS sled test data set, and a lateral and oblique pendulum side impact PMHS data set. The efficacy of the normalization techniques were assessed for each group of common signals by calculating the average percent coefficient of variation (%CV) for time-history curves, and an analogous measure for force-deflection curves (%CV<sub>ellipse</sub>). Both of these measures provide a quantifiable assessment of the similitude of the group of curves (i.e., the normalization technique resulting in the lowest average %CV value or %CV<sub>ellipse</sub> value most effectively collapses the curves). The normalization technique found to consistently perform the best is a newly developed extension of impulse momentum-based normalization in which the stiffness ratio was determined from effective stiffness values calculated from the test data, rather than using characteristic lengths. Utilization of an improved normalization methodology in the development of mean human

response curves should prove useful in more accurately characterizing the target human response to aid in the design of more biofidelic dummies.

## INTRODUCTION

Biomechanical response corridors developed from human subject test data are commonly used to guide the design of anthropomorphic test devices (ATDs) by providing “target” biomechanical responses to impact. The biomechanical responses typically consist of physical measures such as force, acceleration, or deflection, and could be in the time-domain or another domain (e.g., force-deflection). The ability of an ATD to match these target responses defines its biofidelity.

The target responses are most often developed by subjecting a group of Post-Mortem Human Subjects (PMHS) to an impact or crash scenario, measuring the resulting responses, and then representing each group of responses such that it characterizes the response of the selected population and can be used to evaluate the biofidelity of the corresponding ATD response. One way to accomplish this is to encompass the entire group of response curves for a given measurement using straight-line segment corridors, and then a biofidelic dummy response is expected to lie entirely within that corridor (ISO/TR9790, 1999; Lobdell et al., 1973). Another methodology is to reduce the group of responses into a single mean response curve, which itself represents the ATD design target (Cavanaugh et al., 1986; Maltese et al., 2002; Morgan et al., 1986). In addition to the mean response curve, standard deviation curves can be created around the mean to provide both a visual measure of the variation in the group of PMHS, as well as a quantitative measure of that variation for assessing the biofidelity of an ATD. Generally the standard deviation curves envelop the mean curve more tightly than the straight-line segment corridors, and there is no requirement that a biofidelic ATD response must lie completely within the standard deviation curves. Representing the target response using the mean response and standard deviation curves is more appealing than straight-line segment corridors because it provides a quantifiable framework for assessing the biofidelity of an ATD

while maintaining the shape and characteristics of the actual human response to impact.

Since there are a variety of ATDs, each representing a certain “standard” anthropometry or set of physical characteristics (i.e., 50<sup>th</sup> percentile male, 5<sup>th</sup> percentile female, etc.), it is important that the PMHS responses used to develop the design targets represent the same respective population. However, in reality there is often large variation in the physical characteristics within a group of human subjects (e.g., size, shape, inertial properties, etc.) which results in widely varying response data. Normalization is a procedure for mathematically adjusting the response data to account for the variation in physical characteristics, and is often the first step in developing target biomechanical responses. Successful normalization should collapse the group of curves closer to a single response so that a mean response can be more accurately established that represents that of the selected population.

Anthropometric variation between subjects such as differences in height and weight can obviously affect the magnitude of the response data, but differences in factors such as body mass distribution (i.e., fat-to-muscle ratio) can not only affect the magnitude but also affect the phase or timing of the response data, which is especially critical to the creation of a mean response curve. Figure 1 shows an example of two curves (blue and red) which are out of phase but similar in shape and magnitude. The resulting mean curve (black) is bimodal, much lower in magnitude, and has a shape nothing like either of the individual curves. Ideally, normalization would be able to account for the variation between the subjects which caused this out-of-phase response, thus resulting in a more representative mean response curve.

Although several methods for normalizing human subject test data can be found in the literature, the two most commonly implemented procedures are mass-based normalization as described by Eppinger (1984), and impulse momentum-based normalization as described for single mass systems (e.g., sled & drop tests) by Mertz (1984) and for two-mass systems (e.g., pendulum tests) by Viano (1989).

### Mass-based normalization (Eppinger et al, 1984)

The mass-based procedure normalizes human subject response data based solely on a mass ratio involving the subject’s total body mass and the total body mass of the “standard” subject to which the responses are to be normalized. The underlying theory was

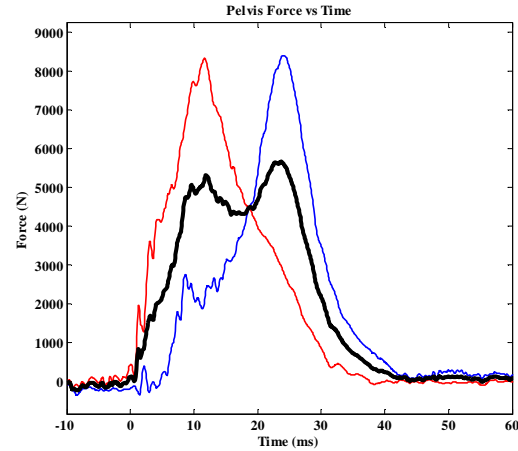


Figure 1. Mean curve resulting from two out-of-phase responses

developed based on a dimensional analysis approach to geometric scaling in which three scaling ratios containing the fundamental dimensions of mass, length, and time must be defined in order to derive scaling ratios for other engineering variables of interest. Two of these ratios were defined to assume constant density and modulus of elasticity among subjects; the third ratio is the total body mass ratio:

$$1 = \frac{\rho_{50th}}{\rho_{sub}} \quad 1 = \frac{E_{50th}}{E_{sub}} \quad \lambda = \frac{M_{50th}}{M_{sub}} \quad (1)$$

where  $\rho$  is density,  $E$  is the modulus of elasticity,  $M$  is total body mass,  $\lambda$  is the total body mass scaling ratio, and the subscripts “50<sup>th</sup>” and “sub” represent the “standard” subject and test subject, respectively. Note that since the most common “standard” subject is the 50<sup>th</sup> percentile male it will hereafter be referred to with the subscript “50<sup>th</sup>”, and  $M_{50th}$  can be easily obtained from anthropometric tables.

Normalizing factors for engineering variables of interest ( $L$  = length or deflection,  $F$  = force,  $A$  = acceleration,  $T$  = time, and  $V$  = velocity) can then be derived from the three ratios in Equation (1) in conjunction with fundamental laws of physics, as shown in Equations (2) – (6):

$$\rho = \frac{M}{L^3} \Rightarrow L_{50th} = \lambda^{1/3} L_{sub} \quad (2)$$

$$E = \frac{F}{L^2} \Rightarrow F_{50th} = \lambda^{2/3} F_{sub} \quad (3)$$

$$F = MA \Rightarrow A_{50th} = \lambda^{-1/3} A_{sub} \quad (4)$$

$$A = \frac{L}{T^2} \Rightarrow T_{50th} = \lambda^{1/3} T_{sub} \quad (5)$$

$$V = \frac{L}{T} \Rightarrow V_{50th} = V_{sub} \quad (6)$$

The strengths of mass-based normalization are that it is easy to implement, the procedure is independent of test condition (i.e., the same procedure is used for sled tests, drop tests, and pendulum tests), and the adjustment made to the response data is directly linked to the easy-to-obtain anthropometry measure of total body mass. The fact that the response data is adjusted based solely on total body mass may make it easy to implement, but it could also be considered a weakness because measures of anthropometry alone are often poor predictors of response data. The physical variation in the subjects includes not just anthropometry but also variables such as age, gender, nutrition, pathology, etc. which cannot be accounted for and predicted by anthropometry. In addition, adjusting the signals based solely on total body mass often does not work well for component-level tests such as pendulum impacts.

A limitation of this type of normalization is that the underlying theory for geometric scaling forces an assumption of full-body geometric similitude (i.e., the ratio of lengths at one body region applies to all other body regions as well) even though in reality body regions are often proportioned differently from subject-to-subject. Also, while the two fundamental material constituency assumptions of constant density and constant modulus among subjects are likely reasonable approximations, there will of course be some variation. The biggest limitation to this method is that the response data of a tall and thin osteoporotic subject with the same total body mass as an overweight and short healthy-boned subject would scale identically, implying that they would be expected to exhibit a similar response to an identical impact.

### **Impulse momentum-based normalization (Mertz, 1984; Viano, 1989)**

This procedure normalizes human subject response data based on both a mass ratio and a stiffness ratio,

and then models the impacts as a simple spring-mass system:

$$\lambda_m = \frac{m_{50th}}{m_{sub}} \quad \lambda_k = \frac{k_{50th}}{k_{sub}} \quad (7)$$

For the mass ratio, instead of a simple ratio of total body mass, an effective mass of the impacted body region is estimated from the response data using an impulse momentum analysis as shown in Equation (8):

$$\int_0^T F dt = m_{eff} v_0 \Rightarrow m_{eff} = \frac{\int_0^T F dt}{v_0} \quad (8)$$

where  $m_{eff}$  is the effective mass,  $F$  is the force during impact,  $v_0$  is the change in velocity during the impact, and  $T$  is the duration of impact. By incorporating the response data in the normalization procedure, some of the other causes for variation besides anthropometry (discussed earlier) can be somewhat accounted for. Unlike the total body mass ratio where the mass of the 50<sup>th</sup> percentile male is easily obtained from anthropometric tables, the standard effective mass of the 50<sup>th</sup> percentile male,  $m_{50th}$ , is dependent on the test condition and is thus typically unknown. Therefore the value is estimated by calculating the ratio of each subject's effective mass to their total body mass, averaging the ratio across subjects, and multiplying by the total body mass of the population to which the data is to be normalized (e.g., 76 kg for a 50<sup>th</sup> percentile male).

For the stiffness ratio, Mertz (1984) showed that by assuming a constant modulus among subjects and geometric similitude within the impacted body region, the stiffness ratio could be approximated using a ratio of characteristic lengths. For example, if the impact involves the thorax then chest depth or chest breadth might be chosen as the characteristic length used to calculate the stiffness ratio. Once a characteristic length is chosen, the corresponding length for a 50<sup>th</sup> percentile male can be obtained from anthropometric tables.

Normalizing factors for engineering variables of interest ( $t$  = time,  $a$  = acceleration,  $v$  = velocity,  $x$  = length or deflection, and  $F$  = force) can then be derived from the mass ratio and stiffness ratio in Equation (7) in conjunction with the solution to the differential equations of motion for a simple spring-mass system, as shown in Equations (9) – (13):

$$t = \pi \sqrt{\frac{m}{k}} \Rightarrow t_{50th} = \sqrt{\frac{\lambda_m}{\lambda_k}} t_{sub} \quad (9)$$

$$a = -v_o \sqrt{\frac{k}{m}} \sin\left(\sqrt{\frac{k}{m}} t\right) \\ \Rightarrow a_{50th} = \sqrt{\frac{\lambda_k}{\lambda_m}} a_{sub} \quad (10)$$

$$v = -v_o \cos\left(\sqrt{\frac{k}{m}} t\right) \Rightarrow v_{50th} = v_{sub} \quad (11)$$

$$x = v_o \sqrt{\frac{m}{k}} \sin\left(\sqrt{\frac{k}{m}} t\right) \\ \Rightarrow x_{50th} = \sqrt{\frac{\lambda_m}{\lambda_k}} x_{sub} \quad (12)$$

$$F = -v_o \sqrt{km} \sin\left(\sqrt{\frac{k}{m}} t\right) \\ \Rightarrow F_{50th} = \sqrt{\lambda_m \lambda_k} F_{sub} \quad (13)$$

Note that the normalizing factors shown in Equations (9) - (13) were derived from the equation for a single mass, single spring system so they are only valid for sled tests and drop tests where the impacting mass can be assumed infinite. For pendulum impacts, the equations of motion for a two-mass system are used to derive the normalizing factors shown in Equations (14) – (18), where  $m_p$  is the mass of the impactor.

$$t_{50th} = \sqrt{\frac{\lambda_m}{\lambda_k}} \sqrt{\frac{(m_p + m_{sub})}{(m_p + m_{50th})}} t_{sub} \quad (14)$$

$$a_{50th} = \sqrt{\frac{\lambda_k}{\lambda_m}} \sqrt{\frac{(m_p + m_{sub})}{(m_p + m_{50th})}} a_{sub} \quad (15)$$

$$v_{50th} = v_{sub} \quad (16)$$

$$x_{50th} = \sqrt{\frac{\lambda_m}{\lambda_k}} \sqrt{\frac{(m_p + m_{sub})}{(m_p + m_{50th})}} x_{sub} \quad (17)$$

$$F_{50th} = \sqrt{\lambda_m \lambda_k} \sqrt{\frac{(m_p + m_{sub})}{(m_p + m_{50th})}} F_{sub} \quad (18)$$

The primary strength of this normalization method is that it incorporates the response data so that it can potentially account for variation in response arising from subject differences other than just anthropometry. A weakness with this procedure involves using a characteristic length for the stiffness ratio, because the choice of which characteristic length to use is somewhat subjective. Also, using a characteristic length as a surrogate for stiffness requires the assumptions of constant modulus and geometric similitude within the impacted body region. However, if the effective stiffness of the subject could be estimated from the response data, similar to the effective mass, then those assumptions would not be necessary.

To date, there is no quantitative consensus as to which of the normalization techniques discussed above is most effective. Furthermore, some areas of potential improvement for both methods have been identified. Therefore, the goal of this study was to quantify the effectiveness of the two existing normalization procedures as well as some new methodologies developed in this study based on the identified potential improvements.

## METHODS

### Potential improvements to existing normalization methods

After reviewing the two most common existing normalization methods, some weaknesses and potential areas of improvement were identified, and some new methodologies were developed to address these areas. For the mass-based normalization the most prominent limitation is that body mass distribution is unaccounted for. Therefore, replacing the ratio of total body mass with a ratio involving a measure of “body type” such as the Body Mass Index (BMI) in Equation (19), or the Ponderal Index (PI) in Equation (20), was investigated as a potential improvement.

$$BMI = \frac{Mass}{Height^2} \quad (19)$$

$$PI = 10 \left( \frac{\sqrt[3]{Mass}}{Height} \right) \quad (20)$$

For the impulse momentum-based normalization it would be valuable to know the importance of the choice of characteristic length in the stiffness ratio, so various characteristic lengths and combinations of characteristic lengths (i.e., aspect ratios) were evaluated. Specifically, a characteristic length was measured along each of the three axes of the body coordinate system (e.g., chest depth, chest breadth, and chest height), directly along the line of impact, and around the circumference of the impacted area. Each of these measurements was then used as the characteristic length for the stiffness ratio as well as multiple combinations of each of these measurements.

Also, replacing the characteristic length estimate of stiffness with an actual estimate of the effective stiffness calculated from the response data was investigated as a potential improvement. As long as deflection data for the relevant body region is measured, a methodology somewhat analogous to Equation (8) for calculating an effective mass can be implemented to estimate an effective stiffness, as illustrated in Equation (21):

$$\int F dx = \frac{1}{2} k_{eff} x_{max}^2$$

$$\Rightarrow k_{eff} = \frac{2 \int F dx}{x_{max}^2} \quad (21)$$

where  $k_{eff}$  is the effective stiffness,  $F$  is the force during impact, and  $x_{max}$  is the maximum displacement during the impact. As with the effective mass in the impulse momentum-based normalization, the standard effective stiffness of the 50<sup>th</sup> percentile male,  $k_{50th}$ , is dependent on the test condition and is thus unknown. Therefore the value is estimated by calculating the ratio of each subject's effective stiffness to a characteristic length of the subject (e.g., chest breadth for a thoracic side impact), averaging the ratio across subjects, and multiplying by the characteristic length of the population to which the data is to be normalized.

### Data sets for normalization evaluation

Two data sets were chosen for the normalization evaluation – a full-body side impact sled test data set (Maltese et al., 2002) and a component-level thorax pendulum impact data set (Shaw et al., 2006).

#### *Full-body side impact sled test data set (Maltese et al., 2002)*

For the sled test data set, normalization procedures were evaluated for all test conditions that contained three or more subjects after a subject exclusion evaluation. Subjects were excluded if they failed a conservation of momentum check (Nusholtz et al., 2007) or if there was significant “leaning” which was defined as the pelvis contacting the flat wall more than 10 ms after the thorax (Irwin et al., 2005). Four test conditions with three or more subjects remained for the evaluation after subject exclusion: Rigid High-Speed Flat Wall (RHF), Padded High-Speed Flat Wall (PHF), Rigid Low-Speed Flat Wall (RLF), and Padded Low-Speed Flat Wall (PLF).

The thoracic deflection for each subject was obtained by averaging the half-deflections measured by the upper and middle thoracic chestband signals (if they both existed), or using the half-deflection from either the upper or the middle thoracic chestband signals (if only one existed). Although Maltese (2002) calculated both full- and half-deflections, half-deflections were utilized in this study as they were deemed more relevant for comparison with an ATD.

The normalization techniques were applied to several signal groups from the four sled test conditions including multiple time-histories (Thorax Loadwall, Abdomen Loadwall, Pelvis Loadwall, Upper Spine Y accel, Lower Spine Y accel, Pelvis Y accel, Thoracic Deflection) as well as the force-deflection responses for the thorax (F-D Thorax).

#### *Lateral and oblique pendulum side impact data set (Shaw et al., 2006)*

For the pendulum impact data set, normalization procedures were evaluated for both the lateral impact test condition and the oblique impact test condition, and no subjects were excluded based on the criteria discussed above.

Shaw (2006) only reported results for full-deflection of the thorax, but half-deflections were also calculated in the study and the corresponding electronic data was obtained via personal communication and used for this evaluation to be consistent with the full-body sled test data set.

The signal groups analyzed for both the lateral and oblique test conditions included the force-time histories (Force), deflection-time histories (Deflection), and force-deflection responses (F-D).

## Assessment of efficacy of normalization techniques

Each normalization technique was evaluated based on its ability to collapse each group of curves to map onto a single response, because ideal normalization should not only adjust the response data to the appropriate target population but also remove subject-to-subject variation due to differences in anthropometry and physical characteristics (e.g., age, gender, nutrition, pathology, etc.). Therefore a quantifiable assessment of the similitude of a group of curves was required.

### *Time histories*

Since the percent coefficient of variation (%CV) is often used to assess the repeatability of a set of similar ATD responses, this quantity was deemed appropriate to assess the efficacy of the normalization techniques for the time-histories:

$$\%CV = \frac{\sigma}{\mu} \times 100 \quad (22)$$

where

$\sigma$  is the standard deviation of the responses

$\mu$  is the mean of the responses

Although this measure is typically calculated for single value peak responses, in this study it was important to evaluate the similitude of the curves across time as well. Therefore the %CV was calculated at each point in time and then averaged to produce an average %CV across time. Also since the %CV metric does not perform well at low magnitudes of the response (i.e., when the mean value approaches zero), the %CV was only calculated for the time period which included the upper 80% of the mean response (i.e., for values of the mean response that are greater than 20% of the peak magnitude of the mean curve). This average %CV value provides a relative measure of how similar the curves are, where a lower average %CV indicates better grouping of the curves.

### *Force-deflection histories*

To evaluate the similitude of a group of force-deflection curves, an analogous %CV value for force-deflection space was generated. First, an ellipse was formed about each point of the mean force-deflection response with semi-major and semi-minor axes of length equal to one standard deviation each in force and deflection (Shaw, 2006). The area contained within each of these one standard deviation ellipses

was then calculated (analogous to a standard deviation), and divided by the product of the force and deflection value at each point (analogous to a mean value), thus producing a measure for force-deflection responses (%CV<sub>ellipse</sub>) which is analogous to the %CV for time histories. The %CV<sub>ellipse</sub> value at each point was averaged across the time period which included the intersection of the upper 80% of the mean force magnitude and the upper 80% of the mean deflection magnitude. As with %CV, lower values of %CV<sub>ellipse</sub> represent better grouping of the force-deflection curves, and hence more effective normalization.

## RESULTS

Although over thirty different variations of normalization techniques were evaluated, the majority of these variations involved different choices of characteristic length used to calculate the stiffness ratio in the impulse momentum-based procedure (see Methods section). However, no discernible difference in the effectiveness of the impulse-momentum normalization procedure could be identified based on the choice of characteristic length, so the results for each individual choice of characteristic length will not be shown. Also for the mass-based normalization, utilizing a ratio of BMI and/or PI instead of the total body mass ratio did not yield a noticeable difference in normalization effectiveness, so these methodologies will also not be presented.

The results from three normalization procedures will be presented in detail in this manuscript along with the non-normalized data for reference (referred to as “Non-normalized”). The first methodology, referred to as “Mass-based”, is the existing mass-based normalization procedure using a ratio of total body mass. The second methodology, referred to as “Eff Mass & Char Length”, is the standard impulse momentum-based procedure using a ratio of effective mass for the mass ratio and a ratio of characteristic lengths for the stiffness ratio. The characteristic lengths were chosen in this evaluation to be consistent with previous studies where the respective data sets were normalized using the impulse momentum-based method. Therefore, chest depth was used for the sled test data (Irwin, 2005) and chest breadth for the pendulum impact data (Shaw, 2006). The third methodology, referred to as “Eff Mass & Eff Stiff”, utilizes a ratio of effective mass for the mass ratio and a ratio of effective stiffness calculated from the response data as in Equation (21) for the stiffness ratio.

The results from the normalization evaluation are given in Table 1 for the full-body side impact sled test data set and in Table 2 for the component-level thorax pendulum impact data set. Since the average %CV and %CV<sub>ellipse</sub> were both utilized as relative measures of the effectiveness of a given normalization procedure, the percent improvement over the “Non-normalized” data are reported in Tables 1 and 2 for each of the three normalization techniques, rather than the actual numeric values of the measures. The normalization method resulting in the largest percent improvement for each signal group is highlighted in green.

For the full-body sled tests, Table 1 shows that for the eight signal groups that were analyzed in each of the four test conditions (RHF, PHF, RLF, and PLF), the “Eff Mass & Eff Stiff” normalization approach performed the best (i.e., resulted in the largest amount of improvement in curve grouping) for six of the eight RHF and RLF signal groups, seven of the eight PHF signal groups, and five of the eight PLF signal groups. For the component-level pendulum impacts, Table 2 shows that for the three signal groups that were analyzed in each of the two test conditions (Lateral and Oblique), the “Eff Mass & Eff Stiff” normalization approach performed the best in five of the six signal groups. In full, the “Eff Mass & Eff Stiff” normalization approach performed the best in 29 of 38 (~76%) of the signal groups analyzed, as compared to 7 of 38 (~18%) for the “Mass-based” approach and 2 of 38 (~5%) for the “Eff Mass & Char Length” approach.

## DISCUSSION

### *Normalization of time histories*

To illustrate an example of normalization on time-histories, the thorax loadwall time-histories for the RHF condition are shown for the “Non-normalized” condition in Figure 2, and the “Mass-based”, “Eff Mass & Char Length”, and “Eff Mass & Eff Stiff” normalization conditions in Figure 3-5, respectively.

Visual inspection of Figures 2 and 3 reveals that “Mass-based” normalization results in a small level of improvement in curve group similitude, and in fact the average %CV improves from 64.7 to 45.1 for a percent improvement of 30.3%. Inspection of Figures 2 and 4 shows that the “Eff Mass & Char Length” normalization results in an even more significant improvement in the curve grouping, with a corresponding 42.8% improvement in the %CV value. Finally, inspection of Figures 2 and 5 illustrates that the “Eff Mass & Eff Stiffness” normalization is very effective at bringing the curves

together, resulting in a 60.9% improvement in the %CV value. The trend revealed above indicates that incorporating the response data into the normalization process results in better grouping of curves and thus more effective normalization.

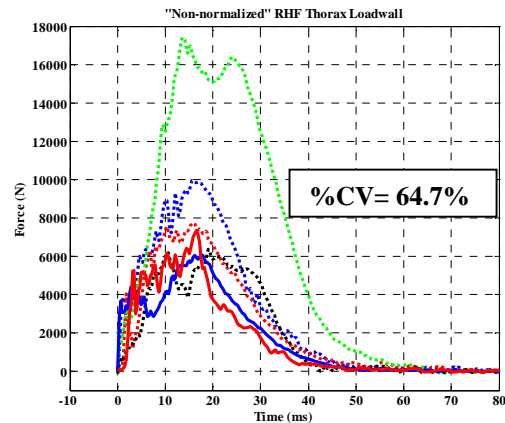


**Figure 2. “Non-normalized” RHF thorax loadwall time-histories (%CV = 64.7)**

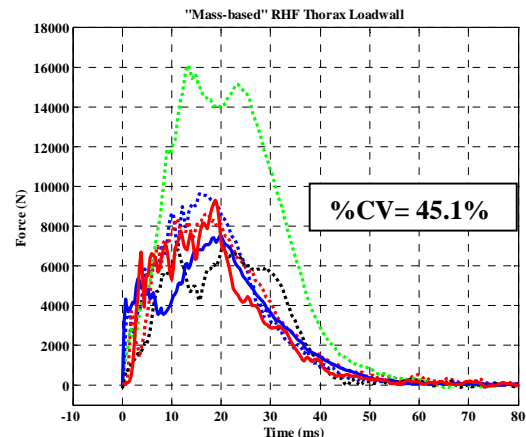


**Figure 3. “Mass-based” RHF thorax loadwall time-histories (%CV = 45.1)**

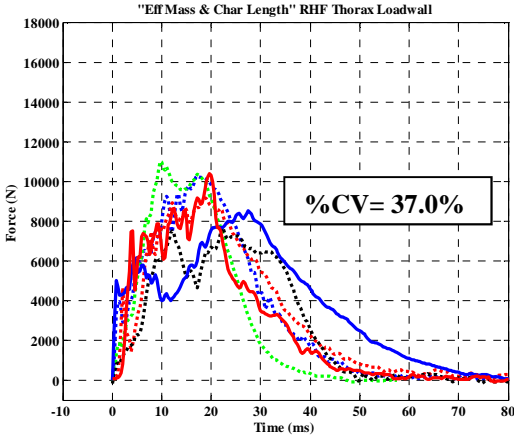


Figure 4. “Eff Mass & Char Length” RHF thorax loadwall time-histories (%CV = 37.0)

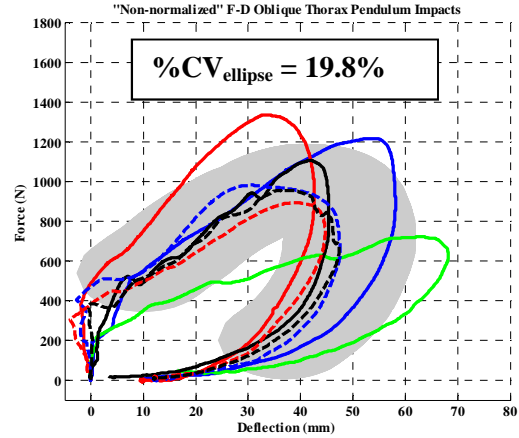


Figure 6. “Non-normalized” Oblique thorax force-deflection histories (%CV<sub>ellipse</sub> = 19.8%)

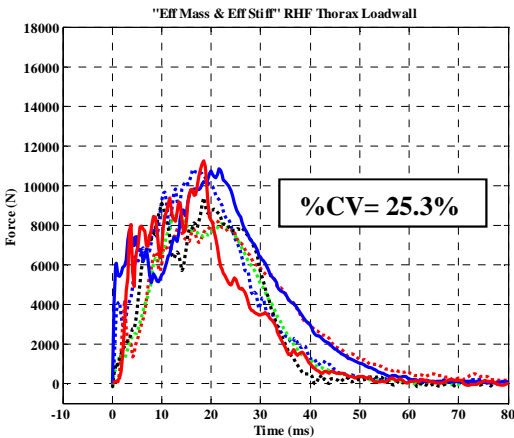


Figure 5. “Eff Mass & Eff Stiff” RHF thorax loadwall time-histories (%CV = 25.3)

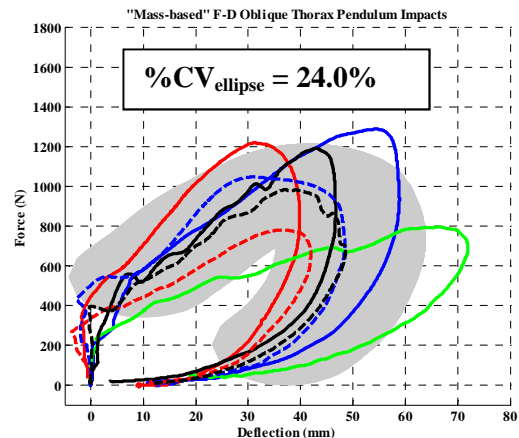


Figure 7. “Mass-based” Oblique thorax force-deflection histories (%CV<sub>ellipse</sub> = 24.0%)

*Normalization of force-deflection histories*

To illustrate an example of normalization on force-deflection histories, the force-deflection curves for the oblique thorax pendulum impacts are shown for the “Non-normalized” condition in Figure 6 and the “Mass-based”, “Eff Mass & Char Length”, and “Eff Mass & Eff Stiff” normalization conditions in Figures 7-9, respectively. The grey shaded regions represent the one standard deviation ellipses defined in the Methods section and in Shaw (2006). Note that low values of the %CV<sub>ellipse</sub> value represent better grouping of the curves and typically correspond to noticeably smaller regions of grey shading.

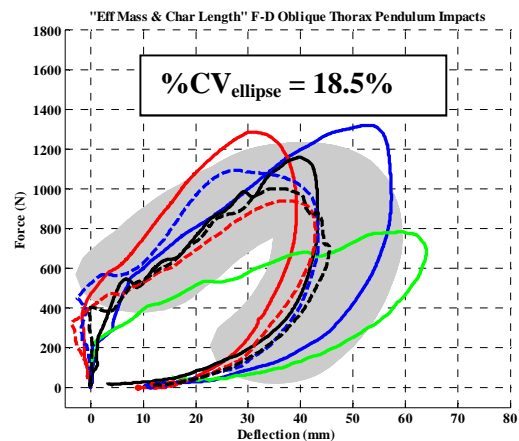
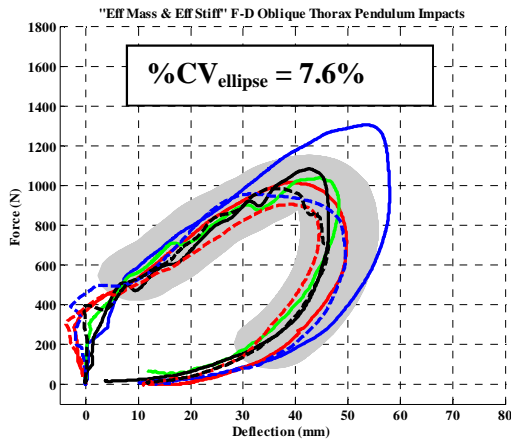


Figure 8. “Eff Mass & Char Length” Oblique thorax force-deflection histories (%CV<sub>ellipse</sub> = 18.5%)



**Figure 9. “Eff Mass & Eff Stiff” Oblique thorax force-deflection histories ( $\%CV_{\text{ellipse}} = 7.6\%$ )**

Close visual inspection of Figures 6 and 7 reveals that the grey shaded error region actually gets a little bigger with “Mass-based” normalization, and in fact the average  $\%CV_{\text{ellipse}}$  increases from 19.8 to 24.0 resulting in a negative percent improvement of -21.2%. As mentioned earlier, normalization based solely on total body mass often does not perform well in component-level tests like pendulum impacts. Inspection of Figures 6 and 8 shows that the “Eff Mass & Char Length” normalization results in a modest reduction in the grey shaded error region, with a corresponding 6.6% improvement in the  $\%CV_{\text{ellipse}}$  value. Finally, inspection of Figures 6 and 9 reveals that the “Eff Mass & Eff Stiffness” normalization causes a rather dramatic alignment of the curves and large improvement in the  $\%CV_{\text{ellipse}}$  value of 61.6%.

#### *Additional Discussion*

Several additional observations can be made from examination of Tables 1 and 2. For the component-level pendulum impacts, the “Mass-based” normalization approach actually caused the grouping of the curves to get worse than the “Non-normalized” data in all six signal groups, as evidenced by the negative percent improvements. This again supports the indication that total body mass normalization does not perform well in component-level tests.

For the upper spine, lower spine, and pelvis acceleration signals in the sled test data set, there were many instances where one or all of the normalization techniques did not improve the curve grouping relative to the non-normalized data. Furthermore, if the analysis of the normalization results is limited to only these 12 acceleration signal groups, it is much less clear which normalization

methodology performed the best. It is likely that the complexity of these signals, and the additional potential sources for variation associated with the installation of the instrumentation, greatly reduce the effectiveness of normalization for these “internal” signals. However, if the analysis of the results is limited to the other 26 signal groups (i.e., force-time, deflection-time, and force-deflection), normalization is much more effective in improving the grouping of the curves, and the “Eff Mass & Eff Stiffness” approach clearly performs the best. Specifically, it yields the greatest improvement in 21 of 26 (~81%) of these signal groups, as compared to 4 of 26 (~15%) for the “Mass-based” approach and 1 of 26 (~4%) for the “Eff Mass & Char Length” approach.

#### *Limitations*

Although the results from this study demonstrate that the normalization of impact response data using the “Eff Mass & Eff Stiff” approach is the most effective way of those examined to improve the similitude of a group of responses for the creation of a mean human response curve, some limitations in the methodology should be pointed out. First, the values for effective stiffness can only be obtained if deflection data is measured directly (e.g., chestband) or can be indirectly estimated (e.g., double integration of accelerometers). Also, the numerator of the stiffness ratio in Equation (7) for “Eff Mass & Eff Stiff” normalization is dependent on the test condition and cannot be obtained from anthropometric tables. Recall that this is also true for the numerator of the effective mass ratio. However, the effective mass and effective stiffness can still be estimated and related directly back to the 50<sup>th</sup> percentile male (or selected population), using standard anthropometric values as discussed previously.

#### **SUMMARY**

Several normalization methodologies were quantitatively evaluated by applying them to time-history data and force-deflection data from both a full-body sled test data set and a component-level pendulum impact data set. The normalization technique (of those examined) found to consistently perform the best is a newly developed extension of impulse-momentum-based normalization in which the stiffness ratio was determined from effective stiffness values calculated from the test data, rather than using characteristic lengths. Utilization of this normalization methodology in the development of mean human response curves may prove useful in more accurately characterizing the target human response to aid in the design of more biofidelic dummies.

**Table 1. Normalization results for the full-body side impact sled test data set**

	Signal	Mass-Based (% improvement)	Eff Mass & Char Length (% improvement)	Eff Mass & Eff Stiff (% improvement)
<b>RHF</b>	Thorax Loadwall	30.3 %	42.8 %	60.9 %
	Abdomen Loadwall	13.1 %	25.9 %	28.1 %
	Pelvis Loadwall	12.7 %	5.8 %	41.2 %
	Upper Spine Y accel	13.8 %	5.1 %	18.9 %
	Lower Spine Y accel	11.1 %	-23.2 %	10.2 %
	Pelvis Y accel	-2.1 %	-6.4 %	14.0 %
	Thoracic Deflection	13.2 %	-60.6 %	-21.2 %
	F-D Thorax	40.6 %	9.5 %	70.7 %
<b>PHF</b>	Thorax Loadwall	40.3%	42.2 %	57.0 %
	Abdomen Loadwall	3.6%	35.1 %	54.8 %
	Pelvis Loadwall	55.0%	48.3 %	67.7 %
	Upper Spine Y accel	5.4%	8.1 %	7.6 %
	Lower Spine Y accel	9.4%	13.9 %	17.1 %
	Pelvis Y accel	7.6%	8.8 %	9.4 %
	Thoracic Deflection	36.3%	22.4 %	40.3 %
	F-D Thorax	60.3 %	56.2 %	70.1 %
<b>RLF</b>	Thorax Loadwall	9.5 %	19.8 %	23.4 %
	Abdomen Loadwall	3.0 %	30.3 %	36.0 %
	Pelvis Loadwall	2.1 %	10.1 %	27.6 %
	Upper Spine Y accel	-8.7 %	-54.7 %	-25.4 %
	Lower Spine Y accel	-0.7 %	-2.8 %	0.2 %
	Pelvis Y accel	5.6 %	2.9 %	0.6 %
	Thoracic Deflection	-17.4 %	-51.9 %	-4.4 %
	F-D Thorax	-1.3%	-5.7 %	24.1 %
<b>PLF</b>	Thorax Loadwall	40.4 %	5.6 %	18.2 %
	Abdomen Loadwall	28.1 %	43.8 %	46.7 %
	Pelvis Loadwall	3.7 %	-37.7 %	30.8 %
	Upper Spine Y accel	-8.6 %	-8.6 %	-7.9 %
	Lower Spine Y accel	6.6 %	7.0 %	8.4 %
	Pelvis Y accel	16.3 %	-25.8 %	25.8 %
	Thoracic Deflection	28.7 %	21.4 %	26.9 %
	F-D Thorax	55.1 %	0.9 %	20.3 %

**Table 2. Normalization results for the component-level thorax pendulum impact data set**

	Signal	Mass-Based (% improvement)	Eff Mass & Char Length (% improvement)	Eff Mass & Eff Stiff (% improvement)
<b>Lateral</b>	Force	-16.5 %	9.0 %	-20.3 %
	Deflection	-2.8 %	14.4 %	25.5 %
	F-D	-25.0 %	21.0 %	25.0 %
<b>Oblique</b>	Force	-7.8 %	5.9 %	34.8 %
	Deflection	-14.0 %	5.4 %	41.0 %
	F-D	-21.2 %	6.6 %	61.6 %

## REFERENCES

- CAVANAUGH, J. M., NYQUIST, G. W., T., GOLDBERG, S. J., and KING, A. I. (1986). Lower abdominal tolerance and response. Proc. 30th Stapp Car Crash Conference, pp. 41-63.
- EPPINGER, R. H., MARCUS, J. H., and MORGAN, R. M. (1989). Development of dummy and injury index for NHTSA's thoracic side impact protection research program. SAE 840885. Society of Automotive Engineers, Warrendale, PA.
- IRWIN, A. L., SUTTERFIELD, A., HSU, T. P., MERTZ, H. J., ROUHANA, S. W., and SCHERER, R. (2005). Side impact response corridors for the rigid flat-wall and offset-wall side impact tests of NHTSA using the ISO method of corridor development. Proc. 49th Stapp Car Crash Conference, pp 423-456.
- ISO/TR9790. (1999). Road vehicles-lateral impact response requirements to assess the biofidelity of the dummy. Technical Report No. 9790, International Standards Organization, American National Standards Institute, New York, NY.
- LOBDELL, T.E., KROELL, C. K., SCHNEIDER, D. C., and HERING, W. E. (1973). Impact response of the human thorax. Proc. Symposium on Human Impact Response, Plenum Press, New York, NY, pp. 201-245.
- MALTESE, M. R., EPPINGER, R. H., RHULE, H. H, DONNELLY, B. R., PINTAR, F. A., and YOGANANDAN, N. (2002). Response corridors of human surrogates in lateral impacts. Proc. 46th Stapp Car Crash Conference, SAE 2002-22-0017, pp 321-351.
- MERTZ, H. J., (1984). A procedure for normalizing impact response data. SAE 840884. Society of Automotive Engineers, Warrendale, PA.
- MORGAN, R. M., MARCUS, J. H., T., and EPPINGER, R. H. (1986). Side impact – the biofidelity of NHTSA's proposed ATD and efficacy of TTI. Proc. 30th Stapp Car Crash Conference, pp. 27-40.
- NUSHOLTZ, G. S., HSU, T. P., BYERS, L. C. (2007). A proposed side impact ATD bio-fidelity evaluation scheme using cross-correlation approach. Proc. 20th International Technical Conference on the Enhanced Safety of Vehicles (ESV), Paper Number 07-0399.
- SHAW, J. M., HERRIOT, R. G., MCFADDEN, J. D., DONNELLY, B. R., and J. H BOLTE, IV (2006). Oblique and Lateral Impact Response of the PMHS Thorax. Proc. 50th Stapp Car Crash Conference, pp 147-167.
- VIANO, D. C., (1989). Biomechanical responses and injuries in blunt lateral impact. SAE 892432. Society of Automotive Engineers, Warrendale, PA.

# SENSITIVITY AND LOAD PATH ANALYSIS FOR THE H-III IN FRONTAL IMPACT

**Hee Seok Kim**  
**Seok Joon Hong**  
**Kun Chul Yeom**  
**Seong Soo Cho**

Research & Development Division of Hyundai Motor Group  
Korea

**Michiel Unger**  
TNO Automotive Safety Solutions (TASS)  
Germany

Paper Number 13-0252

## ABSTRACT

The main objective of the paper is to develop an analysis method of the mechanisms that controls the behavior of the H-III neck, thorax, and lower extremity injuries in a USNCAP and Euro-NCAP frontal impact. The analysis method will be utilized within the engineering design of safety systems to obtain optimal injury values. For this research were conducted in 5 steps.

Step1. Load path analysis based on numerical simulations, crash tests and 6 sled tests of various conditions with extended instrumentation (ex. Angular rate sensors, Rib-Eye). The numerical models were validated with the sled test data, to allow analysis of the load path mechanisms.

Step2. Sensitivity analysis of the safety system and dummy sub-systems with validated models. The sub-system simulation study was conducted in detail for finding out physics of the load paths mechanism and the sensitivity of the injury value characteristics.

Step3. It was going to a systematic approach to injury mechanism through the kinematics. Then, relations between kinematic and physical load paths were characterized.

Step4. Details analyze the effects on each part for various pulse and safety restraint components. Then it will be showed effectiveness guidelines of various safety restraint components.

Step5. 4 sled test for confirmation.

Finally, the study resulted in identification of the mechanisms that mainly affect neck, thorax and lower extremities injury values. Based on the mechanism analysis, design guidelines could be help to safety system design of the target performance.

## INTRODUCTION

Recently as the requirements of frontal crash became more strict, especially, the neck and thorax injuries of H-III 5th in passenger side became more challenging than the others. Moreover, the NHTSA's introduction of the new NCAP 5-star rating system [1] starting with 2011 MY vehicles put even higher demands to the safety system development than before. According to this rule, especially, the

improvement of the neck injury is very important to achieve a 5-star rating for passenger. But it is difficult to know what is the best improvement method, what is exact the injury mechanism. Because dummy movement depends on many complex variables and limited conditions can be tested. Also the field significance of the neck injury mechanism is appropriately reflected relative to the more prominent roles of the head and thorax [2]. So it is necessary to the analysis the main effect factors and contribution related to dummy injuries by advanced tests and simulations.

On tibia injury, in 1996, the European Community released new 40% offset crash – it is consist of crashing car on a ODB (Offset Deformable Barrier) at 56 km/h - relating to frontal impact vehicle crash. It has increased the importance of low extremities injury such as tibia injury.[3] Furthermore, IIHS of US, EuroNCAP, KNCAP, CNCAP and even Asian NCAP, introduced 64kph 40% offset crash at the same time. So, importance of reducing low extremities injury grown with respect to the other system requirements.[4] One of the main reasons for increasing importance of low extremities injury is the most frequent and costly consequences of those injuries for the survivors of crashes. Therefore, the insurance claims for vehicle occupants whose most serious injury was a fracture of a weight-bearing bone cost \$2.06 billion every year [5-6]. In addition to direct medical costs, lower extremity injuries were associated with high incidences of long-term problems that sometimes require additional treatment and interfere with patients' ability to return to work [6]. So, it is very important that reducing low extremities injuries and developing effective protection system for low extremities injuries.

This paper described about the dummy injury mechanisms for neck, chest and low extremities and their kinematics by using various CAE tools and test methods. These results should be useful to understand the H-III 5<sup>th</sup> and H-III 50<sup>th</sup> injuries guide the safety restraints development and interior vehicle package.

To figure out injury mechanism, 6 sled tests were conducted for mid-sized vehicles with 7 cameras and enhanced measurements. These tests were used to

obtain data for dummy injury mechanism analysis and also to obtain data set for MADYMO/LS-DYNA model validation. The test simulated 64kph offset and 56kph full frontal impact each 3 times. All the tests were conducted with a 50%tile male driver and a 5%tile female passenger. Furthermore the dummies were installed with enhanced measurement sensors which were 6ch lower neck load cell, 6 belt load cell, 2 belt spool sensors, rib eyes, head/chest/pelvis/foot 3 axis angular sensor each part , 2 angular sensors in the tibia, and foot load cells. (see figure 1)

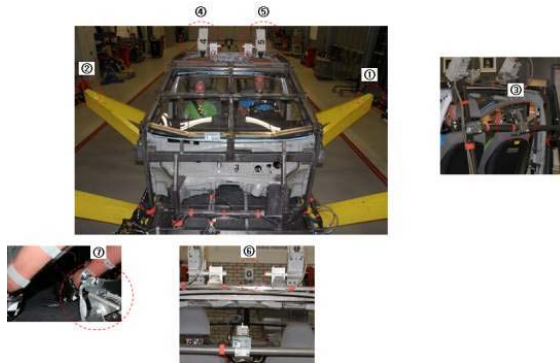


Figure 1. Sled test setup.

## LOAD PATH ANALYSIS

### Load Path of Head and Neck

Basically, neck injury mainly occurred from various moments by flexion and extension bending and compression force. Furthermore, the Nij criteria which are a function of upper neck forces and moment, play a dominant role in the crash performance star rating under the US NCAP. Therefore, we need to analyze this injury mechanism.

The Nij in US NCAP is defined as equation (1) and Table 1.

$$N_{ij} = \left[ \frac{F_z}{F_{zc}} \right] + \left[ \frac{M_{ocy}}{M_{yc}} \right], M_{ocy} = M_y - (F_x \times l) \quad (1)$$

Table 1.  
Summary of Neck injury criteria value

		Sign	50%tile	5%tile
F <sub>zc</sub>	Tension(N)	(+)	6806	4287
	Compression(N)	(-)	6160	3880
M <sub>yc</sub>	Flexion(Nm)	(+)	310	155
	Extension(Nm)	(-)	135	67

The dummy neck and upper neck sensor are composed as figure 2 and sign conventions are followed by J211 standard.

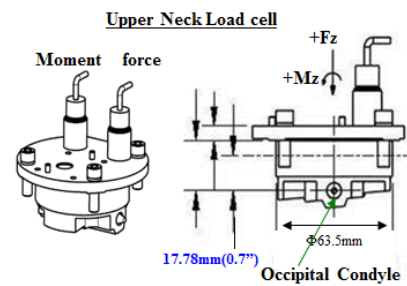


Figure2. Dummy neck and upper neck load cell structure.

The Head/Neck dynamics is mainly affected by airbag and seat belt. However the effects of inertia force cannot be passed over. Therefore the force source of head/neck can be described as figure 3.

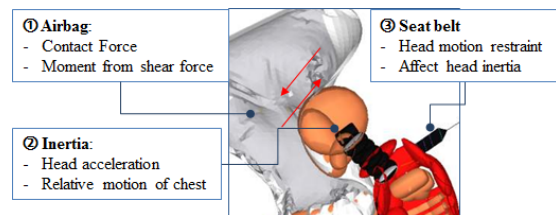


Figure 3. Load path diagram for the head.

Generally, the neck injury pattern in an NCAP test can be divided into 3 phases as figure 4. Phase 1 is seat belt only affected phases, which is occurring before the head contacts the airbag. Phase 2 is affected airbag and belt phase, which is occurring during the principal head loading phase by the airbag. Phase 3 is the rebound phase. So external forces, such as airbag pressure and belt force are gradually tapered off.

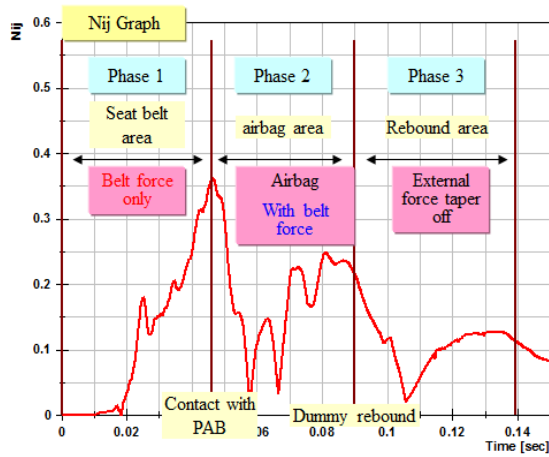


Figure 4. Typical Nij trajectory for 5%tile neck.

$M_{ocy}$  graph is very similar to head angle trajectory. But it has some difference tendency (see figure 5). Because, when head contacts the airbag, an added momentum results from the contact force in x direction. Furthermore it also has a nonlinear characteristic property for nodding block which is composed of rubber.

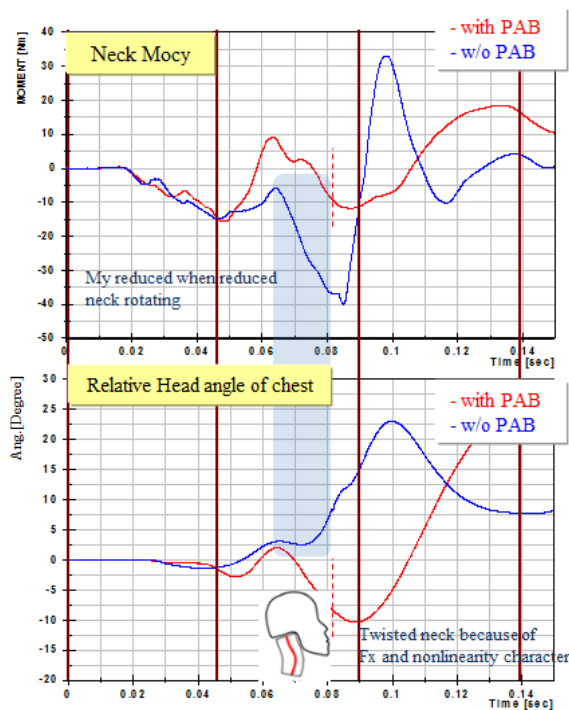


Figure 5. Neck  $M_{ocy}$  and relative head angle of chest.

In phase 1, when chest is caught by the seat belt, the head is moved relative forward due to head inertia. At that time, in the neck is occurring a tension force (positive z direction) and an extension moment by this relative head motion of the chest. The tension force (or compression force) of neck is depends on relative head-acceleration of the chest and relative head angle.

In phase 2, there is an additional main interaction area between head and airbag with respect to phase 1. According to airbag shape and pressure distribution a force balance exist among airbag load, head inertia and neck load. In which the neck loads arise from differences in the relative motion of the head with the chest. How three types of airbag design affect the neck loads is explained in figure 7b.

In case of type 2 the airbag generates forces that balance the neck loads such that the head is pushed to follow the thorax motion in the most natural way. In the other two cases the forces do not balances well and the neck gets loaded and will deform. Normally, when chin caught by the airbag or face contacted by asymmetry airbag, it will be visible in the neck load.

In phase 3, it is head and chest rebound phase. Therefore sign of neck moment ( $M_y$ ) is changed from negative to positive. Sometimes, the head has a hard contact with the headrest, B-pillar or other hard part, so that it causes a high Nij. But, this paper will not deal that kind of special conditions.

In most cases the chest is rebounding earlier as the head. When chest is rebounded, the upper neck is still moving forward with the head as airbag keeps venting. This will results in flexion of the neck. After that, head rebounding will be started. (see the figure 6)

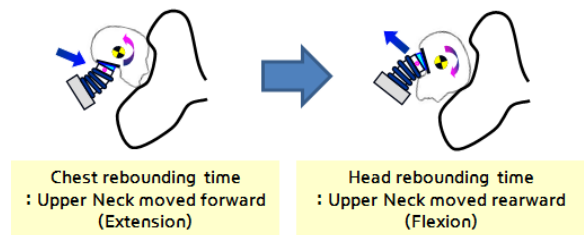


Figure 6. Dummy head movement on phase 3.

The  $F_z$  force depends on the vehicles pulse severity. If vehicles pulse severity is high, chest of dummy will be rebounded strongly. In that case, there will be tension force occurred on the neck. On the other hands, if the head rebounds earlier before the chest can be the compression force on the neck.

Finally, the neck injury mechanism was summarized for each phase in Figure 7(a), Figure 7(b) and Figure 7(c).

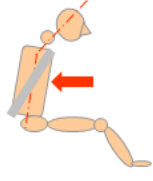
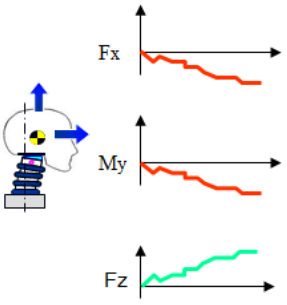
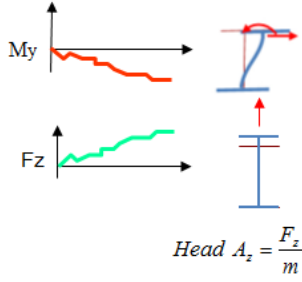
External Force	Translation motion (A)	Rotating motion (B)	Results injury
		None	

Figure 7(a). Neck Injury mechanism on phase 1.

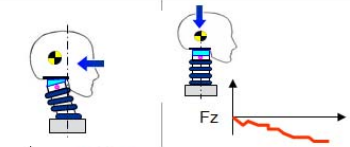
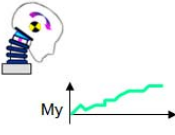
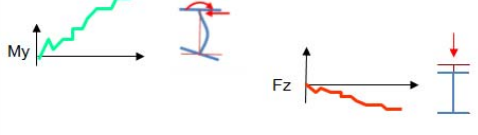
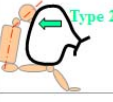
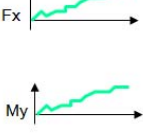
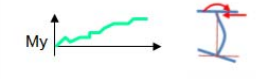
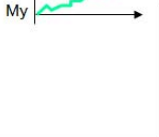
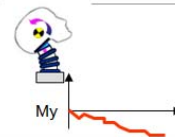
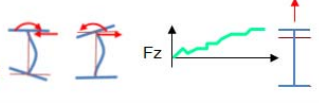
External Force	Translation motion (A)	Rotating motion (B)	Results Injury
			
		None	
			<p><math>A &gt; B = \text{Flexion}</math> <math>A &lt; B = \text{Extension}</math></p> 

Figure 7(b). Neck Injury mechanism on phase 2 by airbag loading.

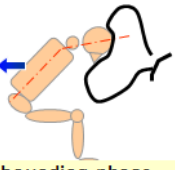
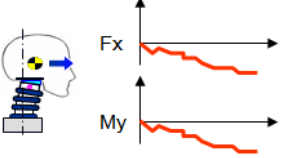
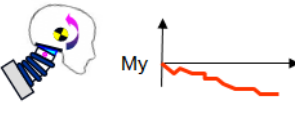
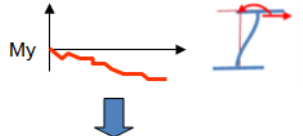
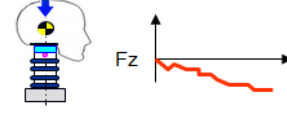
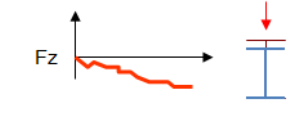
External Force	Translation motion (A)	Rotating motion (B)	Results injury
 <p>Rebounding phase → forces are gradually tapered off</p>		<p>Chest rebounding time</p> 	
	<p>When pulse severity is high</p> 	<p>Head rebounding time</p> 	
	<p>When pulse severity is low</p> 		

Figure 7(c). Neck Injury mechanism on phase 3.

### Load Path of the Chest

Chest injuries are represented by the 3ms peak acceleration and deflection. The chest deflection of

the H-III dummy is measured on just one point at the middle of thorax. The thorax injury mechanism is very simple and clear. Because thorax has no joint itself except connecting point between neck and pelvis.(see Figure 8) Therefore, it will be carry out more detail analysis at the sensitivity analysis section.

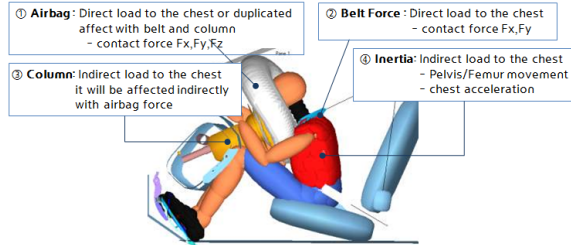


Figure 8. Load path diagram of thorax.

### Load Path of Low Extremities

Tibia injury mechanisms are very complicated to understand, quantify and summarize. First of all, when you want to understand the Tibia injury mechanism in detail, the sign convention of the Tibia needs to be clear. Basically, it is followed by J1733 standard. (see Figure 9)

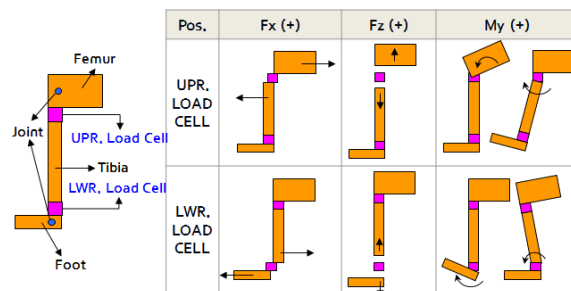


Figure 9. Sign convention of the Tibia.

Tibia has two joints, one is the knee between femur and upper tibia and the other is the ankle between lower tibia and foot. The sign of tibia sensor signals depend on where the external force is applied (below or above the sensor). So, we made a simple tibia model used LS-DYNA. (see Figure 10) Then we could find out exact sign convention depends on the external load position.

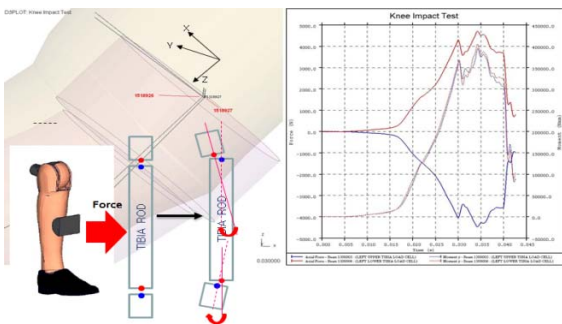


Figure 10. Simple tibia model for checking sign convention depends on external force position.

In case of a force applied by the femur, for example, upper tibia  $F_x$  and lower  $M_y$  have the same sign, in case of force to upper tibia part(below sensor), there is upper  $F_x$  and lower  $M_y$  injury occurred with opposite signs. It means that upper  $F_x$  and lower  $M_y$  occurred simultaneously. Lower  $F_x$  and upper  $M_y$  either. According to our sled test results, basically upper  $F_x$  and lower  $M_y$  had a similar injury pattern. However, when it had an external force, the  $F_x$  magnitude increased.(see Figure 11)

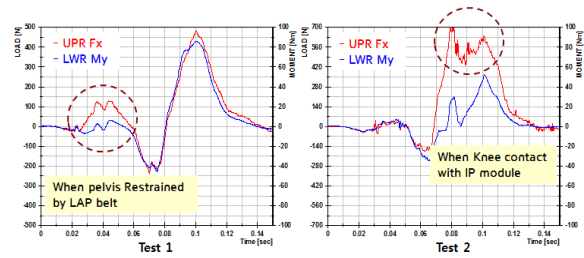


Figure 11. Upper  $F_x$  and Lower  $M_y$  graph pattern.

During the crash the tibia loading has three phases which are forward, rotation and rebound phase. A summary of the tibia injury mechanism can be found in Figure 12(a),(b),(c) based on the test results analysis.

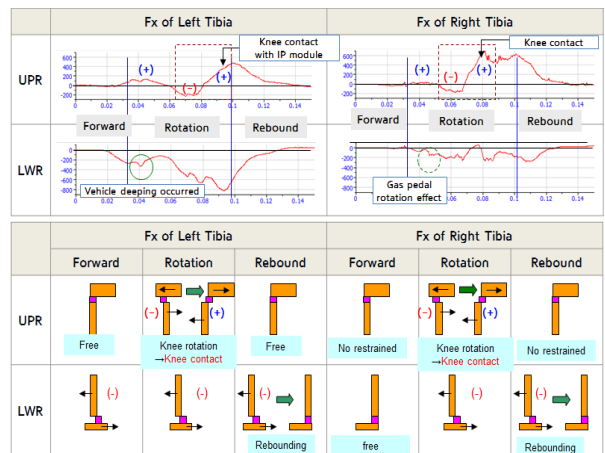


Figure 12(a). Tibia  $F_x$  injury occurred trajectory.

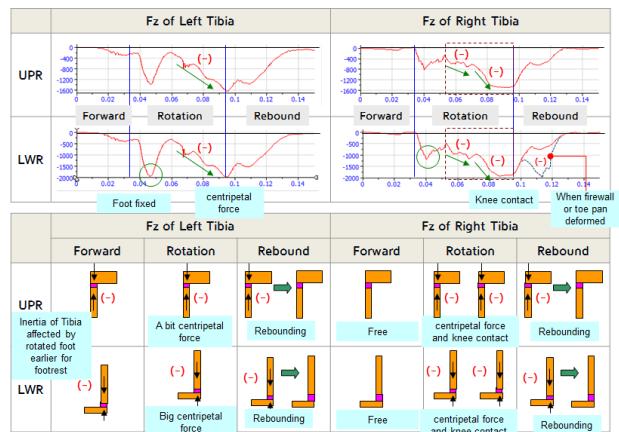


Figure 12(b). Tibia  $F_z$  injury occurred trajectory.

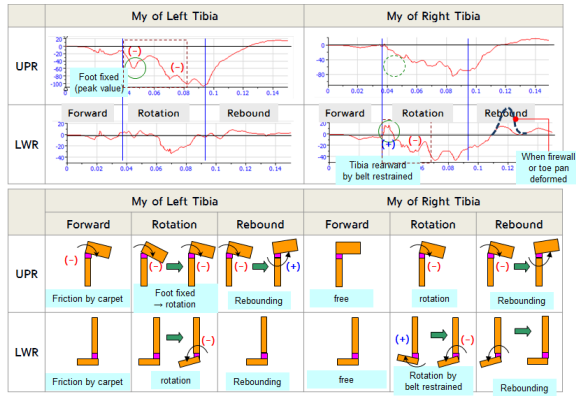


Figure 12(c). Tibia  $M_y$  injury occurred trajectory

### SENSITIVITY ANALYSIS

This section objective is sensitivity analysis of the dummy response for variation in the principal load paths. Therefore, it was followed below process;

- Use correlated model as reference
- Define principal levels and parameters of the load paths
- Define modelling method to evaluate the variations
- Perform DoE or parameter variation studies
- Analyse the results

The following software were used: MADYMO 7.4.1, Hyper study, and LS-DYNA for this analysis.

#### Sensitivity Analysis of the Neck

This study was conducted based on passenger side with H-III 5<sup>th</sup> female dummy. Basically, the pick neck loads occurred before the head is fully loaded by the airbag. However in some cases the during airbag ride down increased extension moment can be occurred. This moment could be caused by shear force and normal contact force between dummy head and airbag. Therefore, it was conducted a DoE by CAE analysis in two difference conditions (with and without airbag) as Table 2(a), (b).

Table 2(a). Variables for full scale dummy analysis at Phase 1

No	Loading condition	Level	Remark
1	Pretension Force	2	2.0/3.0 kN
2	Pretension damping	3	0,40,80
3	Seat Stiffness	3	16%,100%,183%
4	Buckle torsion angle	2	5.7°,17°

Table 2(b). Variables for component scale analysis at Phase 2

No	Loading condition	Level	Remark
1	Body Pulse	2	56kph,64kph
2	Airbag pressure	2	10% increased
3	Airbag venting	3	Enlargement
4	head contact height	3	0, 20, 40mm
5	head rotation	2	0.95 and 1.0

According to the results, the first peak neck load was caused by belt pretension force that pushed the dummy into the seat. It means that it could be reduced most effectively by increasing seat stiffness. Secondary a less aggressive (slower) pretensioner or more stalk rotation could reduce neck loads of the Phase-1. (see Figure 13 (a))



Figure 13(a). Sensitivity analysis results at Phase-1.

In Phase-2, the thorax deceleration by the belt caused the initial extension moments on the neck. The airbag interaction results in a the flexion moments on the neck and it makes the neck most sensitive to the airbag stiffness. Furthermore, the effects of the head position, and travel path were secondary to the airbag stiffness. (see figure 13(b))

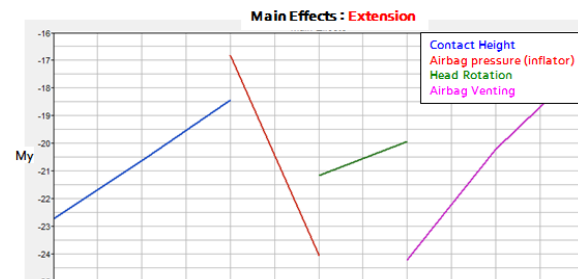


Figure 13(b). Sensitivity analysis results at Phase-2.

#### Sensitivity Analysis of the Chest

This study was conducted based on driver side of H-III 50<sup>th</sup> male dummy. This analysis was conducted at a thorax component level with a static status of the thorax. (see Figure 14) Also this research was conducted into two separate parts; one with belt load only and one with airbag and belt loading.

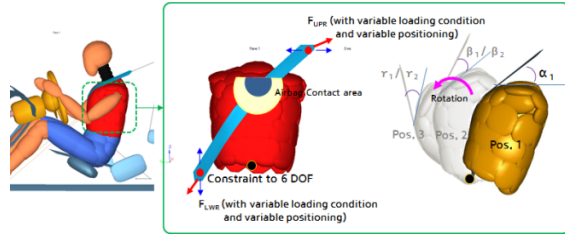


Figure 14. Variables and conditions for chest sub-system analysis

In case of belt force analysis were conducted for three positions according to the three phases; initial stage (phase 1), during airbag ride down (phase 2) and rebounding (phase 3). (see Table 3(a),(b) and Figure 15) But airbag and belt loading area was conducted at phase 2 only. Because airbag does not affect at phase 1 and minimally in phase 3.

**Table 3(a)**  
Variable matrix of belt loading at each condition

No	Airbag Condition	Variables	Remark
1	Airbag Force per Contact increment/ellipsoid	0-150 N	6 level
2	Contact Area Size	5/10	2 level
3	Contact Plane Angle	0,xx	2 level

**Table 3(b)**  
Variable matrix of airbag loading with belt

No	Belt Condition	Variables			Remark
		Case1 (Initial Position)	Case2 (Pos. 70ms)	Case3 (Pos. 100ms)	
1	Upper Belt Loading – $F_{UPR}$	2.5 kN, 3.0 kN	←	←	2 level
2	Lower Belt Loading – $F_{LWR}$	2.5 kN, 3.0 kN	←	←	2 level
3	Upper Angle (D-ring Z position) – $\alpha$	Ref. +40mm	$\beta_1 / \beta_2$	$\gamma_1 / \gamma_2$	2 level
4	Lower Angle (Buckle $\gamma$ -rotation)	0, 23°	←	←	2 Level
4	UPR Belt Position – D-ring Y (Belt Fitting)	0, 50mm (Inboard)	←	←	2 level
5	LWR Belt Position – Buckle Z (Belt Fitting)	0, 30mm (higher)	←	←	2 level

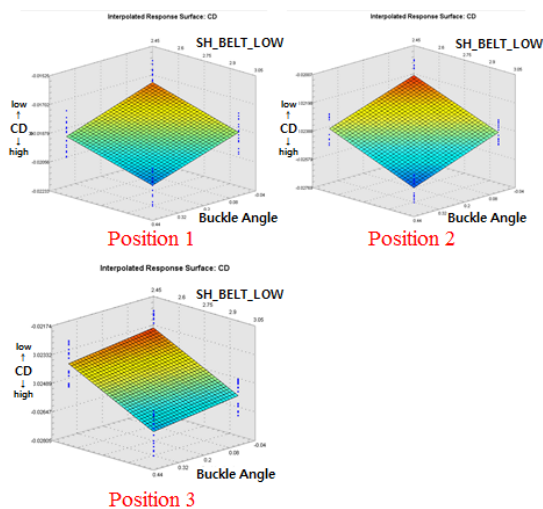


Figure 15. Sensitivity analysis results for belt loading of the chest.

In phase 1 and position 1, the chest deflection was mainly affected by the buckle torsion angle and the upper belt force. These variables continued to affect at position 2 and 3 in Phase 1. But the biggest effect was the lower shoulder belt force followed by the buckle angle and upper shoulder belt force. According to the research, the force component in the compression direction was increased during the ride down as the belt angle changes with respect to the thorax. This means that even though the same belt force at the chest, chest deflection was more increased when chest was in more ride down position.

In phase 2 studies, understandably, the added airbag loading increased the chest deflection. Reducing the load of the airbag on the chest will also reduce the chest deflection. Furthermore the simulation indicates that the chest was more sensitive to the load on the top as a load spread over a wider chest area.(see Figure 16)

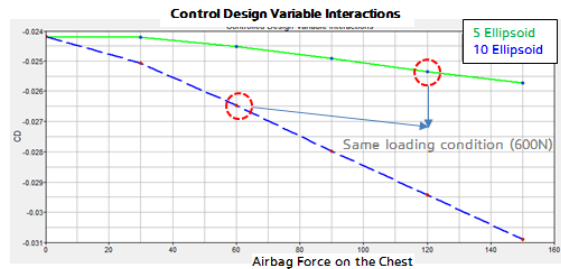


Figure 16. Sensitivity analysis results at airbag loading with belt force.

### Sensitivity Analysis of the Tibia

In tibia sensitive study, the full dummy model of LS-DYNA was used to verify effectiveness of the inertia load. Therefore, we were comparing to injury value pattern between basic model and changed condition model at each conditions. (see Figure 17)

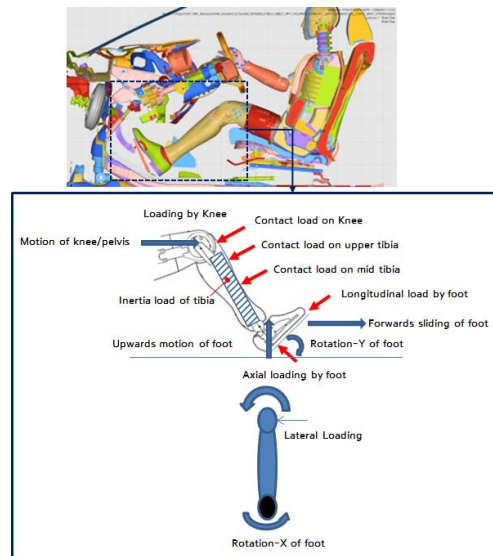


Figure 17. Various loading condition of the tibia.

According to this study, tibia loads were strongly to changes in the tibia mass. This is indicating that tibia loads are caused mainly by tibia deceleration and not by loads coming from upper body. Therefore the controlling of the tibia will improve the tibia loads. Basically, tibia acceleration is controlled mainly by pelvis and foot motion. Also the tibia contact with lower IP generates a load that creates a balance force for the tibia inertia load which is reducing  $M_y$  in the tibias. It means that tibia kinematics is controlled by IP, femur and foot. Typically contact force with IP should be low such that they cannot affect much the pelvis motion. So the IP design will not affect much the overall tibia kinematics, but it can be bring more the load balance over the tibia. On the lower side, the foot motion is affected by acceleration pedal, pedal arm, foot stopper, toe board padding, and floor carpet. As soon as the foot starts to rotate the compression force will generate a shear component and moments increases. So, a reduction of  $M_x$  moment in the tibia is feasible with stronger and wider acceleration pedal to increases foot support. Lower  $F_x$  (results in upper  $M_y$ ) is influenced by foot stopper, pedal rotation and foot impact with pedal arm or fire wall.

In case of using a wider acceleration pedal (see figure 18), the compression force due to pedal contact increased due to the fact that the heel did not slip off, tibia  $M_x$  were reduced as mentioned above. But tibia index injury is reduced due to the fact that tibia index is more sensitive for the moment than the forces on the tibia. (see Figure 19(a),(b))

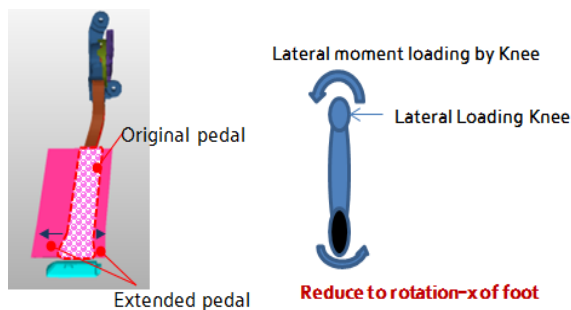


Figure 18. Loading condition of Tibia for reduce X rotation of foot.

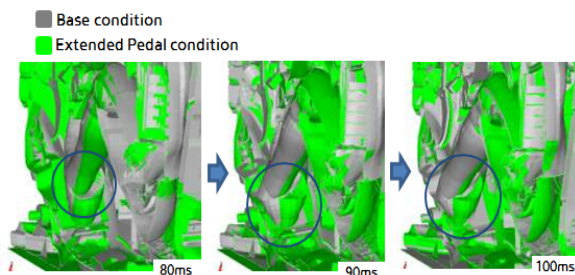


Figure 19(a). Compare to foot movement.

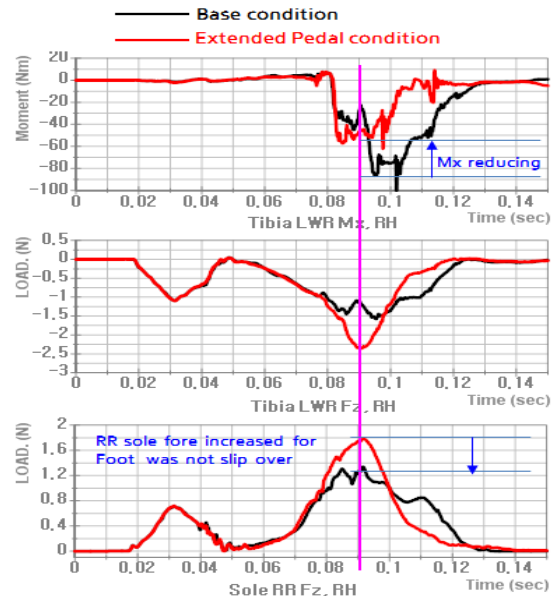


Figure 19(b). Compare graph for different pedal condition

The design objective is to push toes up and allow the foot to travel as much as possible forwards during the higher acceleration phases. Furthermore, padding on the fire wall will avoid a hard contact of foot on the fire wall. In addition, the IP design should allow the resulting tibia motion without interference of any stiff parts.

## DISCUSSION AND LIMITATIONS

First, this research was conducted on sled tests and CAE analysis for a target of mid-size passenger car. Although the dummy models have been extensively validated for the standard sensor outputs, the new advanced sensor technology (Rib-Eye and etc.) was used in the project for improving the validation.

Some mechanisms showed to be very sensitive for minimal changes in the system, such as the right foot kinematics. As results the tibia moments and loads were not very reproducible in detail. However the overall mechanism remains similar such that the overall levels of the injury values for the tibias were still comparable.

Second, the results were based only on the analyzed two load cases (50th Driver Euro-NCAP and 5th Passenger USNCAP). The evaluation of other load cases might be needed to have overall balanced system that results in optimal protection that fulfills all the requirements.

## CONCLUSION

**Improvement Strategy for Neck Injury** In phase 1, a combination of a high power anchor pretension force and soft seat characteristics can result in a relative high neck injury value. This can be improved with a less aggressive pretensioner and a stiffer seat cushion such that the dummy thorax is

less accelerated.

In Phase 2, the design objective in this phase is to control the head motion with the airbag such that the relative motion to the thorax is minimal. At start of the ride down the thorax deceleration by the belt and the airbag deployment dynamics were causing extension moments ( $-M_y$ ) on the neck. It means that this could be improved by having a more stabilized airbag at start of the initial contact. A softer airbag will decrease the positive contact force ( $+F_x$ ) and increase the relative motion of the head with chest such that an increase in  $-M_y$  occurred. The airbag design will influence the moment of the airbag on the head. Especially the use of tethers could influence the initial moment transfer and also stabilize the airbag position. In addition, the airbag generates compression forces on the neck due to the head rotation and airbag volume above the head. These forces could relate to the airbag pressure. Therefore active venting during the crash could help to fine tune the pressure balance of the airbag, and it also could be reduced the overall neck injury values when the peak values occurred after the initial phase.

#### **Improvement Strategy for Chest Injury**

The sensitivity study indicates that the reducing the lower belts load with increased dummy rotation should decrease the chest deflection. Reduced travel of the pelvis could be influence to reduce the lower shoulder belt force. Therefore, additional anchor pretensioner will be reducing the pelvis motion and increasing relative rotation of the thorax. In addition, airbag load path to the thorax should be minimal. Also airbag should load the chest preferably above the area of chest sensor as the chest deflection appears to be more sensitive in that area. Furthermore the use of shorter tethers will help to reduce the airbag pressure on the specific chest area. Steering wheel collapsing is crucial to obtain more space to absorb the crash energy and to reduce the airbag load on the chest.

#### **Improvement Strategy for Tibia Injury**

Tibia loads were related to the tibia mass. This was indicating that tibia loads were caused mainly by tibia deceleration and not by loads coming from upper body. Therefore, controlling the acceleration of the tibia in lower levels will improve the tibia injury. Tibia acceleration controlled mainly by pelvis restraint and foot motion. Upper tibia or knee acceleration can be controlled by pelvis restraint. Increased contact load of knee will increase pelvis deceleration and tibia loads. Tibia loads by lower IP contact should be needed for minimize  $M_y$  moment and keep a load balance in tibias. Also the tibia loads could be improved by controlling the foot motion. The implementation of that will require design changes to pedal construction and padding of the fire wall. Reduction of  $M_x$  moment in the tibia is feasible with wider acceleration pedal and stronger pedal. Lower  $F_x$  (results in upper  $M_y$ ) is influenced by foot stopper, pedal rotation and foot impact with pedal arm or fire wall. For example, a guidance plate could improve tibia loads by smoother moving of the foot beyond the pedal arm. In addition, padding on the

fire wall will avoid a hard contact of foot on fire wall.

Finally, in this paper, we had been described about injury mechanisms of neck, thorax and lower extremities in detail. This research will help you to understand the injury occurring mechanism of the dummy in frontal crash. Also it will be used Injury predictability guide lines for each restraint system and vehicle conditions.

#### **REFERENCE**

- [1] NHTSA NCAP Program Final Decision Notice, Federal Register, Vol. 73, No. 134, 40016-40050, July 11, 2008.
- [2] Wu, J., Shi, Y., Beaudet, B., and Nusholtz, G., "Hybrid III Head/Neck Analysis Highlighting Nij in NCAP," SAE Int. J. Passeng. Cars - Mech. Syst. 5(1):120-135, 2012, doi:10.4271/2012-01-0102.
- [3] Mugnai, A. and Burke, G., "Simulation of an Offset Crash for Tibia Index Evaluation", SAE Technical Paper 2000-01-0882, 2000.
- [4] Kim, H.S., Jung, J.Y. " Study on tibia injury analysis and protection for each cases during the offset impact", HMC Conference CB-2012-075, 2012.
- [5] State Farm Insurance. 1999. Private communication. Na-tional estimate based on distribution of claim costs. Inju-ries in Auto Accidents: An Analysis of Auto Insurance Claims. Insurance Research Council, 1999.
- [6] Zuby, D., Nolan, J., and Sherwood, C., "Effect of Hybrid III Leg Geometry on Upper Tibia Bending Moments," SAE Technical Paper 2001-01-0169, 2001

# ANALYSIS OF ABDOMINAL INJURIES IN OBESE AND NONOBESE RESTRAINED OCCUPANTS

**Hitoshi Ida**

**Masashi Aoki**

**Michihisa Asaoka**

Toyoda Gosei Co., Ltd.

**Koji Mizuno**

Nagoya University

**Masahito Hitosugi**

Dokkyo Medical University

Japan

Paper Number 13-0236

## ABSTRACT

This study clarified the effect of body physique to abdominal injury distribution in terms of frontal passengers at frontal collision using NASS/CDS database with medical knowledge and engineering analysis.

Present research based on the real-world accident data showed that distribution and severity of abdominal injuries of the restrained front seat occupants in frontal collisions was reflected by the body physique. Obese occupants tend to suffer from the injuries of middle-lower abdomen owing to the seatbelt compression. From the reconstruction of the occupants' kinematics, severity of abdominal injuries largely depended on the pelvic displacement in both obese and nonobese occupants. Therefore, to decrease the severity of abdominal injuries, knee airbag is one of considered proper devices as restraint systems for controlling pelvic displacement.

The result of frontal collision simulation with human model THUMS with various body physiques clearly shows that the mechanism and the effects of reduction of abdominal injuries.

## INTRODUCTION

The restrained front seat passengers sometimes suffer from abdominal injuries in frontal collisions. However, there have been a few studies dealing with the abdominal injuries by seatbelt [1-3]. Furthermore, obesity has become a serious worldwide problem

involving 500 million persons. Owing to the protrusion of the abdomen, obese occupants considered as more suffer from severe abdominal injuries in frontal collisions.

To clarify the difference of pattern and severity of abdominal injuries between obese and nonobese occupants, retrospective analysis using real-world accident data was performed. Then, the kinematics of occupants of the obese and nonobese occupants was reconstructed with finite element model.

## METHOD

National Automotive Sampling System /Crashworthiness Data System (NASS/CDS) database was used to investigate the abdominal injuries of the front passengers in frontal collisions. In the analysis, 5280 front passengers in passenger vehicles and commercial vehicles were extracted from 1995 to 2011.

Note that the dataset of NASS/CDS has about ten thousand in traffic accident deaths and injuries every year, and which occupies about 0.3% of 3.2 million people in 1999[4].

In this study, frontal collision is defined from eleven o'clock to one o'clock in impact direction, front side of vehicle was damaged. To evaluate the trend in adult, the occupants with height of more than 140cm was examined.

Furthermore, to understand the mechanism of abdominal injuries of restrained front passengers, kinematics of the occupants at the collision was

reconstructed using the modified THUMS, version 3.

## ANALYSIS OF ABDOMINAL INJURY IN FRONTAL COLLISION

### Injury Part and Injury Severity

To clarify abdominal injuries ratio of total injuries in frontal collision, injuries of 5280 front passengers were analyzed with injury body regions and injury severity (AIS). To conduct accurate analysis, 4365 injuries with AIS of 2 or more were selected.

First, distributions of injuries by the region and severity are shown in Figure 1. The abdomen (401) is less common than the lower limb (889), head (804), chest (783) and upper limb (658). However, severe injuries, AIS of 4 or more, are occurred at only three body regions: the head, chest and abdomen. In these injuries, injured body regions which led to death were the chest (92), head (91), abdomen (24). Therefore, to lessen the fatalities, abdominal injuries in frontal collision should also be prevented.

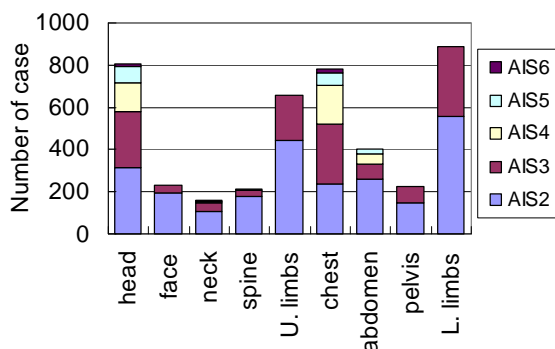


Figure 1. Distribution of injuries by AIS.

### Abdominal Injury and Effect of Restraint System

To clarify the effects of occupant restraint system, injuries of front passengers in frontal collision with seatbelt or without seatbelt were analyzed. Number of unbelted occupants was 1185, belted occupants was 3596, and unknown was 499 among 5280 front passengers.

To determine the injury frequency for each body region, the number of injury occurrence of AIS of 2 or more for each body region was divided by the number of belted or unbelted occupants, respectively. The effectiveness of seatbelt was confirmed: AIS of 2 or more injury was smaller for belted occupants than

the unbelted occupants for all body regions. Especially reduction rate of the head was 79%, face was 84%, neck was 71%, pelvis was 76%, and lower limbs were 65%. Significant effect of wearing seatbelt was observed in the head, neck part and lower body (Figure 2). On the other hand, the reduction rate of abdominal injuries with belt restraint in the abdomen is 53%, smaller value than as shown in the head or neck.

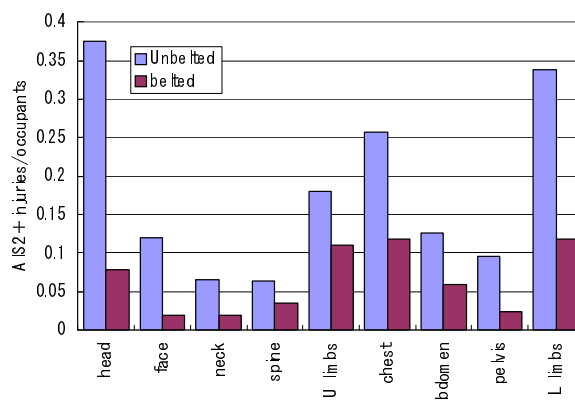


Figure 2. Incidence of AIS 2+ injuries by seatbelt.

This trend is more noticeable for the persons with AIS of 3 or more. Injury reduction rate by seatbelt was at the head 81%, face 86%, neck 83%, pelvis 81%, lower limbs 73%, however, the value is smaller, 43%, at the abdomen. The seatbelt effectiveness for preventing abdomen injuries was limited (Figure 3). These results suggest that the prevention of the abdominal injury by seatbelt or airbag in frontal collisions is more difficult than that of other body regions.

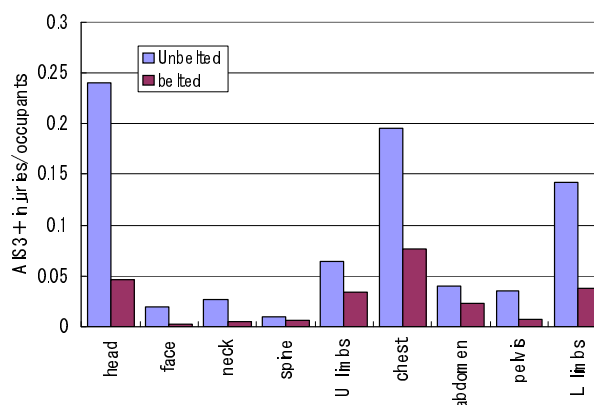


Figure 3. Incidence of AIS 3+ injuries by seatbelt.

For the front seat occupants at frontal collisions, we

divided them for three groups: the cause of death was due to the head injuries (head group), chest injuries (chest group) or abdominal injuries (abdomen group).

Then, distribution of the survival time in each group was examined. The rates of the persons died within one hour of the collision were 37% in the head and 40% in the chest group, however, smaller as 24% in the abdomen group (Figures 4 – 6).

When comparing the AIS in each group, mean abdomen AIS in abdomen group (3.8) was smaller than mean chest AIS in chest group (4.4) or mean head AIS in head group (4.3).

If adequately treated, fatality may be more reduced for the abdominal injuries than the head or chest injuries. Consequently, clarifying the abdominal injury site and its causing mechanism is important in order to reduce the number of fatal and serious injuries in frontal collisions.

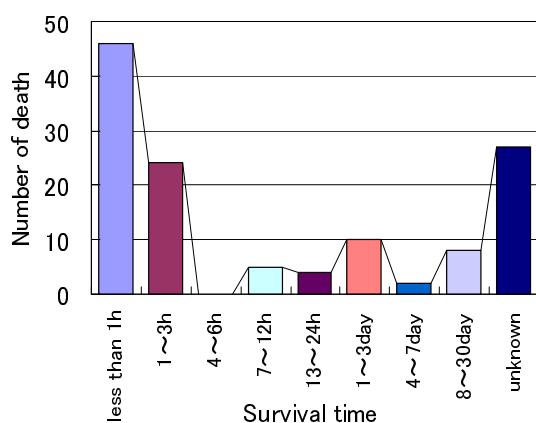


Figure 4. Distribution of survival time (head group).

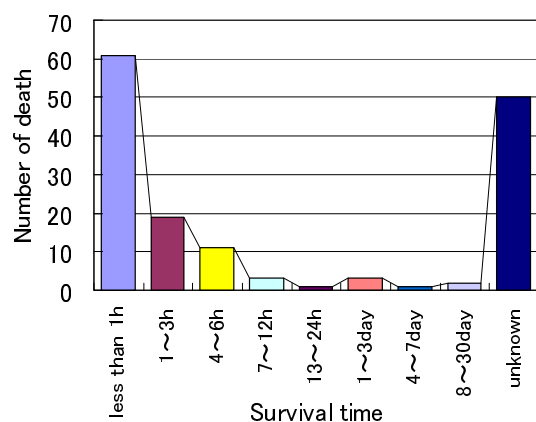


Figure 5. Distribution of survival time (chest group).

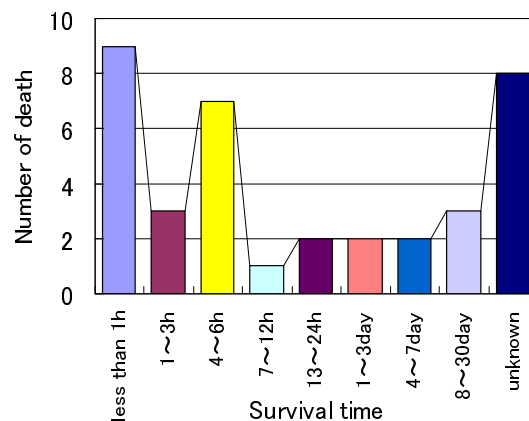


Figure 6. Distribution of survival time (abdomen group).

### Abdominal Injury Factor of Occupant with Seatbelt

Concerning the injury source of 213 abdominal injuries with seatbelt, the compression by seatbelt accounts for more than 60% (Figure 7).

As other sources of injury than seatbelt, there are cases of door trim or center console, which suggests that the front passenger was thrown out in an oblique or side direction. However, in order to analyze mechanisms of injuries in frontal collisions, we focused on the seatbelt injuries which accounts for more than 60%.

The 131 abdominal injuries caused by lap belt were classified by injured organs as follows: the liver 29 (21%); spleen 40 (29%); intestine (small intestine, large intestine and mesenterium) 43 (31%). Accordingly, the three organs of liver, spleen and intestine accounted for 82% (Figure 8).

The abdominal injuries due to lap belt also involved kidneys (8%) and diaphragm (6%). Because kidneys are located in the retroperitoneum and diaphragm could be damaged by chest compression, these injuries were excluded for analysis. Finally, the liver, spleen, intestine by lap belt were examined.

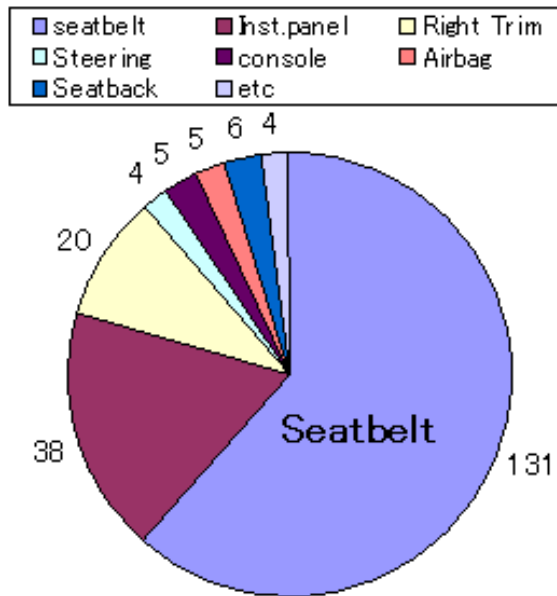


Figure 7. The source of abdominal injuries with AIS 2+ caused by seatbelt.

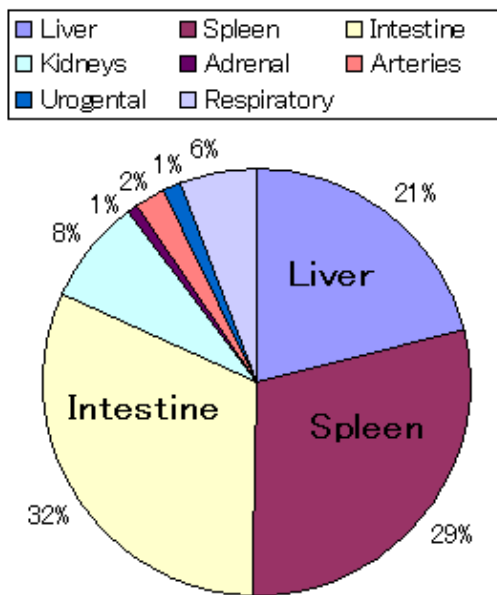


Figure 8. Distribution of involved organs in the abdominal injuries with AIS 2+ caused by seatbelt.

### Body Physique and Abdominal Injury with Seatbelt

To clarify the relationship between obesity and abdominal injuries, 112 cases (except one case of unknown body weight) of abdominal injuries by lap belt were analyzed. Body mass index (BMI) was calculated with body weight divided by square of

height. For the 111 cases, occupants were divided as obese (BMI  $\geq 25$ , 51 cases) or nonobese (BMI  $< 25$ , 60 cases).

Table 1. Abdominal injuries with AIS2+ caused by seatbelt

	BMI $< 25$	BMI $\geq 25$
Liver	20 (33%)	9 (18%)
Spleen	26 (44%)	13 (25%)
Intestine	14 (23%)	29 (57%)
Total	60	50
Ave,height(cm)	164.5	162.0
Ave,weight(kg)	57.6	80.2
Ave.EBS (kph)	45.1	51.5
Ave.BMI	21.3	30.6

Distributions of injured region, background of the occupants in both obese and nonobese groups are shown in Table 1.

In the view point of position of the organs, the liver and spleen is located in the upper abdomen, and the intestine is located mainly in the middle-lower abdomen (Figure 9).

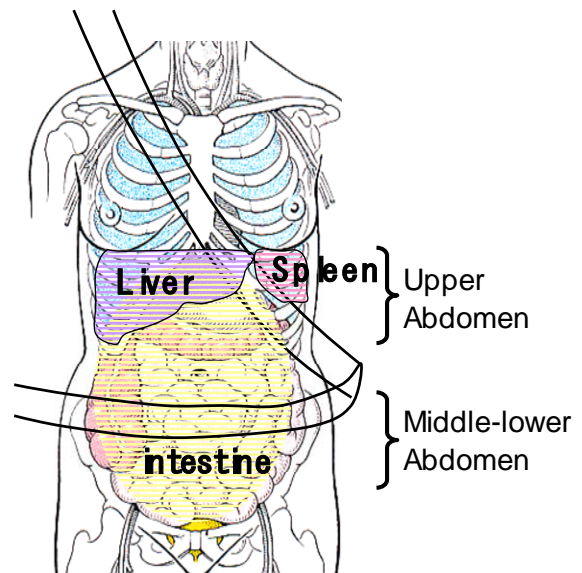


Figure 9. Abdominal organs [5].

Then, we further divided the occupants with injuries in the upper abdomen or in the middle-lower abdomen. Most of obese occupants suffer from

middle-lower abdominal injuries (57%), whereas, nonobese mostly (77%) suffer from upper abdominal injuries (Figures 10 and 11).

The differences of proportion were statistically significant (Chi-square test,  $P < 0.0003$ ).

Owing to the protrusion of the middle-lower abdomen with obesity, the distribution of abdominal injuries was changed.

For the obese occupants, as seatbelt is easily penetrate into the abdomen, it is desirable to put the lap belt on the lower abdominal iliac in obese occupants.

Although, the number of injuries of the upper abdomen was decreased in obese occupants deteriorated rather in the mean AIS. Especially for the spleen, the mean AIS was 2.85.

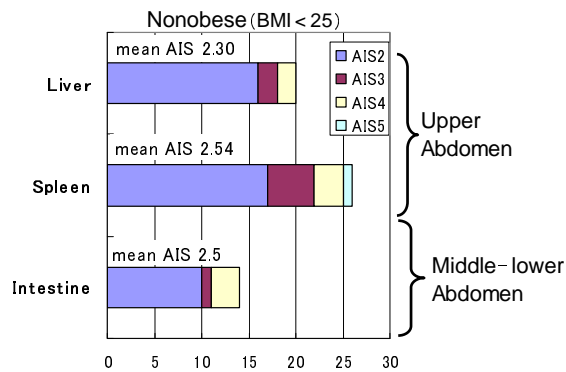


Figure 10. Distribution of injured organ and the mean AIS for the abdominal injuries with AIS 2+ (nonobese restrained occupants).

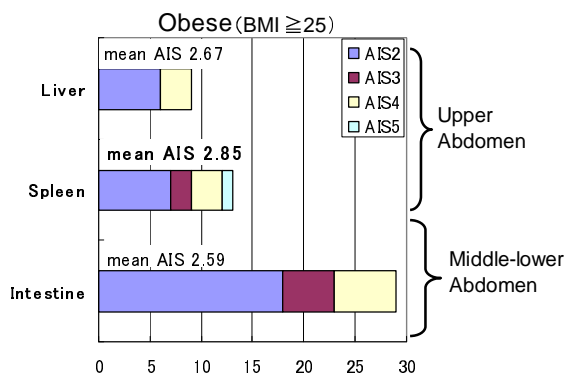


Figure 11. Distribution of injured organ and the mean AIS for the abdominal injuries with AIS 2+ (obese restrained occupants).

## VERIFICATION USING HUMAN MODEL

To verify the trend of the abdominal injuries of obese occupants, obese human finite element (FE) model was made based on THUMS, version 3. The base THUMS was AM50th percentile of 175 cm height and 78 kg weight (equivalent of BMI 25). In addition to the AM50th occupant, the FE simulation of obese occupant was carried out. As reference data, the obese occupant with 168 cm height and 111 kg weight was quoted from CIREN presentations [6]. Based on the thickness of subcutaneous fat shown in abdominal CT image, body surface of original THUMS was scaled up to BMI of 34 with 105 kg weight using weight ratio in Table 2. FE simulation represented a sled test of frontal collision at impact velocity of 56 km/h (35 mph) because the average EBS (Equivalent Barrier Speed) exceeded 50 km/h in abdominal injuries of obese occupants in accident data. The simulation was conducted for AM50th and obese occupants seated in the front passenger with restraint system of airbag and seatbelt to evaluate the injury risk of abdomen for the normal lap belt position (Figures 12 and 13).

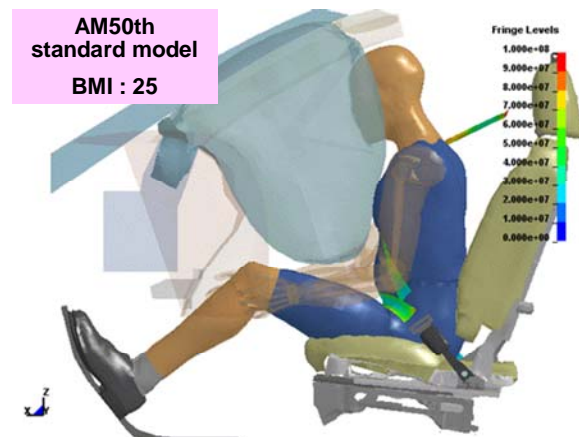


Figure 12. 35 mph sled FE simulation (AM50th standard model: BMI 25).

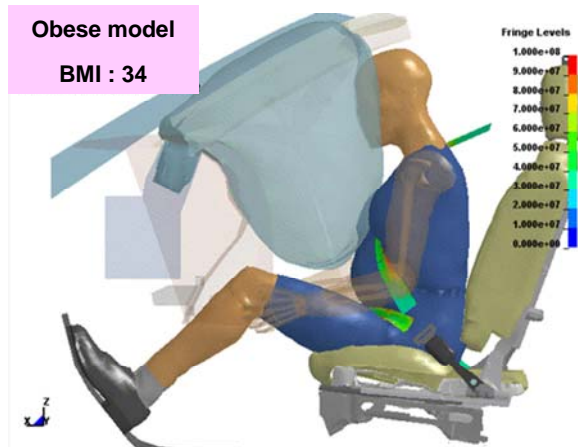


Figure 13. 35 mph sled FE simulation (obese model: BMI 34).

Table 2 presents the ratio of the obese model to AM50th standard model for the body weight and seatbelt contact force. The body weight ratio was 1.35. For the contact force between the shoulder belt and the upper abdomen, the ratio of the obese model to AM50th was 1.19. For the contact force between the lap belt and the middle-lower abdomen, this ratio was 1.42. Therefore, the load to the abdomen caused by the lap belt was larger in obese occupants. This result was coinciding with the accident data that the intestine injuries were observed frequently to the obese occupants (Figure 11).

**Table 2.**

**The ratio of the obese model to AM50th standard model**

	Standard (BMI 25)	Obese (BMI 34)
Weight (kg)	78	105
Weight ratio	1.00	1.35
Shoulder belt force ratio	1.00	1.19
Lap belt force ratio	1.00	1.42

Figures 14 and 15 show the stress of the seatbelt for the AM50th standard model and obese model. The shoulder belt path of the obese occupant model can shift in the lateral direction from the medium location because of the protruding abdomen. As a result, the shifted shoulder belt can compress the spleen. This can be a reason why the AIS of the spleen injuries were larger for the obese occupants.



Figure 14. Seatbelt stress at sled FE simulation (AM50th standard model: BMI 25).

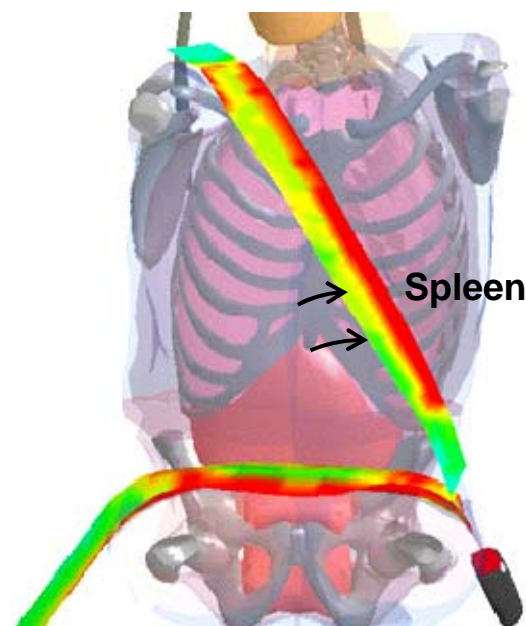


Figure 15. Seatbelt stress at sled FE simulation (obese model: BMI 34).

It is known that the knee airbag (KAB) can reduce the lap belt force in addition that it can reduce the knee injury risks. In this study, the possibility of knee airbag to reduce the abdominal injury risks of obese occupants by the reduction of the lap belt contact force, was examined. Figure 16 and 17 show the shoulder belt and lap belt force for the AM50th

occupant and obese occupant, respectively. There was no significant change in the shoulder belt contact force by equipping the knee airbag. However, lap belt contact force of the obese model can be reduced significantly, and its level was comparable with the AM50th standard model. It was shown that the knee airbag could be effective to reduce the injury risk of the lower abdomen.

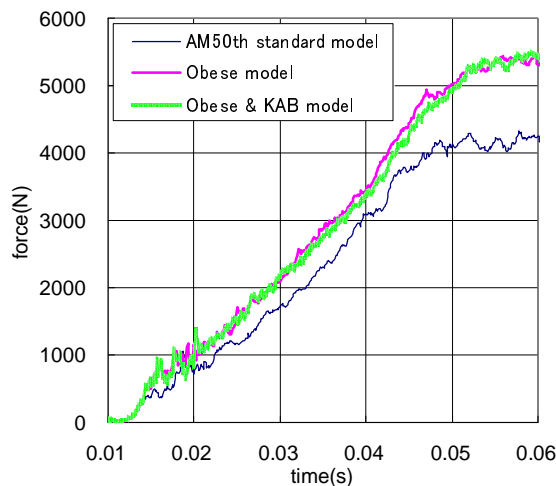


Figure 16. Shoulder belt contact forces.

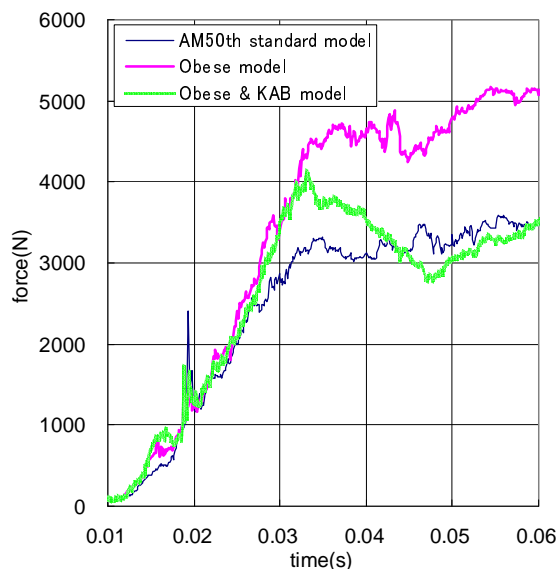


Figure 17. Lap belt contact forces.

## CONCLUSIONS

Injuries of front passengers in frontal collisions were analyzed using NASS/CDS database. The following results were obtained with medical and engineering viewpoints:

1. Abdominal injuries are the third part of severe injury following the head and chest. More than 60% of abdominal injuries of restrained front seat occupants are caused by seatbelt. Among them, the liver, spleen and intestine accounted 82% of visceral injuries of the abdomen by seatbelt.
2. Abdominal injuries by lap belt depend heavily on body physique. Nonobese occupants more suffer from injuries at the upper abdomen and obese more suffer from middle-lower abdomen.
3. Obese human FE model (BMI 34) was developed for sled simulation at 56 km/h. The contact force of lap belt with the middle-lower abdomen was significant larger in obese occupants.
4. According to the FE simulation, it was shown that the knee airbag was effective to reduce lap belt contact force with middle-lower abdomen of obese FE model. The knee airbag has a potential to reduce abdominal injuries to the obese occupants.

## REFERENCES

- [1] Richard Kent, et al., "Biomechanical Response of Pediatric Abdomen, Part 1: Development of an Experimental Model and Quantification of Structural Response", STAPP CAR CRASH JOURNAL, Vol.50, (2006)
- [2] Craig D. Foster, et al., "High-Speed Seatbelt Pretensioner Loading of the Abdomen", STAPP CAR CRASH JOURNAL, Vol.50, (2006)
- [3] Jerome Uriot, et al., "Investigations on the Belt-to-Pelvis Interaction in Case of Submarining", STAPP CAR CRASH JOURNAL, Vol.50, (2006)
- [4] National Highway Traffic Safety Administration, National Center for Statistics and Analysis, "Traffic Safety Facts 1999: Overview" (Washington, DC) ([http://www.nhtsa.dot.gov/people/ncsa/pdf/Overview\\_99.pdf](http://www.nhtsa.dot.gov/people/ncsa/pdf/Overview_99.pdf)).
- [5] Tachenatlas Der Anatomie, 4th edition, Bunkodo Co., Ltd. (2002)
- [6] Jeffrey Augenstein, et al., "Elderly Occupants – Clinical Outcomes", National Highway Traffic Safety Administration, Crash Injury Research (CIREN) presentations, (2001) ([http://www.nhtsa.gov/Research/Crash+Injury+Research+\(CIREN\)/Research/](http://www.nhtsa.gov/Research/Crash+Injury+Research+(CIREN)/Research/))

# OCCUPANT BEHAVIOR DURING A ONE-LANE CHANGE MANEUVER RESULTING FROM AUTONOMOUS EMERGENCY STEERING

**Salvatore Battaglia**

**Kajetan Kietlinski**

**Michiel Unger**

TASS Germany GmbH

Germany

**Robin van der Made**

**Roy Bours**

TASS International

The Netherlands

Paper Number 13-0383

## ABSTRACT

The safety of vehicle occupants has evolved recently due to the market implementations of new sensing technologies that enables predicting and identifying hazardous road traffic situations and thus actively prevent or mitigate collisions. The obvious benefits of the active safety systems has also been recognized and acknowledged by the regulatory and consumer bodies responsible for transportation, and as a result, the new standards, regulations and public rewards are being introduced. The active safety systems can prevent or mitigate collisions by controlling the motion of the vehicles through autonomous actuation of either: braking, steering or both simultaneously. The autonomous control of the vehicle inevitably affects the motion of the travelling occupants with respect to the vehicle interior. Depending on the severity of the maneuver, the occupant motion may lead to non-optimal postures for the in-crash phase if the collision is unavoidable or may impair the capability of a driver to resume the control of a car after the autonomous evasive maneuver. These considerations create the direct need for developing the active systems together with passive systems with the ultimate objective to best protect the occupants. This paper presents a simulation methodology for developing new automotive safety systems in an integrative manner that ensures optimal exploitation of benefits of active and passive systems. It also presents the simulation results of the study into the occupant behavior during the emergency evasive maneuver. The investigation was performed using the combination of newly available simulation techniques for modelling the Advanced Driver Assistance Systems (PreScan software) and for modelling the real human behavior under low-g conditions (MADYMO software). The results obtained showed the severity of the out-of-position occupant postures created by the autonomous evasive

system. It was also observed that the lateral acceleration, being the effect of the maneuver, may cause the driver to impact the b-pillar, and thus potentially impair the further driving capabilities. The study was performed based on the numerical simulations and some of the model components were not fully validated. Further investigations will follow and will be focused on additional validation of the method and its components and finally on quantitative assessment of the revealed problems. The presented methodology and its application for investigating the occupant behavior under low-g loading shows the relevance of developing the new safety systems in an integrative manner. The simulation methods and techniques will play significant role in the integrated safety systems development processes, allowing to test the conditions of high complexity in order to represent the real life scenarios and thus ensuring better occupant protection.

## INTRODUCTION

Despite the recent rapid technology advancements in the field of automotive safety, road accidents are still one of the main causes of severe injuries and premature deaths in contemporary societies. Introduction of driver assistance systems (ADA systems or ADAS) generates new opportunities to mitigate the damage caused by traffic accidents or, in many cases, prevents them from happening. ADA systems such as autonomous emergency braking (AEBS) or lane keeping assist (LKA) and lane change assist (LCA) support the driver in hazardous traffic situations by controlling longitudinal (by braking) and lateral (by steer torque) motion of the vehicle in case of collision risk. These systems, though relatively new to the market, have proved their significance for vehicle safety and are recognized already by legislative authorities and

consumer bodies. The European Commission is introducing legislation for AEB and lane departure warning systems (LDW) in commercial vehicles [1]. The consumer testing protocols are currently being prepared for AEB systems, dedicated for city and interurban traffic and LDW, and will be introduced to the standard Euro NCAP protocol as of 2014. Several initiatives are working on developing standards describing system requirements and standard test programs. Some examples are the Crash Avoidance Metrics Partnership initiative (CAMP) and NHTSA confirmation test requirements. In Europe the EC funded projects such as PREVENT [2], eValue [3] and ASSESS [4] are working on standardization of test programs.

The above mentioned ongoing and upcoming standardization processes will finally lead to an increased performance of the longitudinal and lateral guidance assistance systems and popularization of them throughout all segments of the vehicle types. However, the AEB systems have their functionality limitations and there are traffic situations in which the obstacle appears suddenly on the driving path and braking is not efficient enough to avoid a collision. These situations could happen either in the city traffic conditions e.g. pedestrian intruding a street or in the fast moving, inter-urban and motorway conditions e.g. sudden lane change maneuver or suddenly stopped traffic. In these cases a steering intervention becomes the only measure to prevent a collision [5]. It should be considered as additional functionality of the emergency evasive system in which the algorithm, based on the criticality of scenario conditions, decides about which evasive actions should be taken: braking; steering or both simultaneously. Up to now, there have been several technology research level demonstrator projects carried out successfully, showing the potential of steering assist systems [6], [7], [8]. These systems present different approaches towards the decision characteristics: acting either as a driver support in which the system only corrects the maneuver initiated by a driver [6], or fully autonomously vehicle control that applies appropriate steering patterns [7]. The fully autonomous evasive steering intervention that is being discoursed within the paper requires a widespread and detailed understanding of the road situation. The system needs to classify all the detected participants that are currently in the region of interest (ROI), predict all the possible actions of all ROI participants, including the host vehicle itself, and finally assess the severity of the consequences of the possible evasive actions. The described situation evaluation flow sequence determines the parameters that need to be monitored by the controller to undertake appropriate actions. As explained in the

[5], once the potential collision is detected, the system monitors the time to react (TTR) to determine the criticality of the situation. The TTR is the remaining time for a driver to avoid a collision by braking or steering, assuming the maximum performance (braking or lateral accelerations) of the vehicle resulting from each of the actions. Thus it can be computed as the maximum of time-to-brake (TTB) or time-to-steer (TTS) accordingly. This information is then being used by the controller to select the most suitable action to avoid the collision.

Though the accidentology studies justify the social need for developments of evasive systems and the research demonstrators proved their technological feasibility and effectiveness, product level implementations is not yet possible due to the potential product liability issues and lack of customer acceptance test results. It could be easily conceived that a driver needs to be capable to retain the control over the vehicle instantly after the autonomous maneuver is complete. This implicates that the yaw angle and yaw rate of the vehicle should be zeroed before the control is given back to the driver and that the lateral loadings resulting from autonomous maneuvering do not cause excessive misplacements of the occupants or/and contact interactions with the interior parts. This study is focusing on the latter, and tries to quantify the significance of the problem using simulation techniques and additionally depicts the potential out of position (OOP) problems in case of system failure and consecutive collision.

## METHODOLOGY

Previous studies have shown that autonomous systems, such as AEB or autonomous steering, can lead to a non-optimal occupant posture and position resulting in reduced performance of the occupant restraint systems in case of a collision [9]. Consequently, these active safety systems cannot be developed independently of the passive safety systems without risking suboptimal safety performance of the occupant restraint system (airbags, seatbelts). Instead, they need to be developed and assessed in an integral manner, considering it one complete integrated safety system. At the same time, the increasing presence of surround sensors allows for an improved performance of the passive safety systems by using information from before the crash. This information can be used to trigger restraint systems during the pre-crash phase e.g. pre-pretensioning of safety belts to reduce the occupant misalignments during pre-crash lateral or longitudinal loadings.

Currently, no experimental methods or simulation tools exist for evaluating the effects of pre-crash dynamics on the occupant injury risk during the crash phase. In the paper, the use of two software packages that together provide the potential to cover all critical aspects of the design of an integrated safety system is shown. One of the software packages (PreScan) focuses on the sensing and active control systems of a vehicle, and the other package (Madymo) predicts an occupant response and injury risk throughout the whole pre- and potential in-crash event. The methodology used in this study has been previously presented [10] when applied for the investigation into the frontal collision load case with pre-crash autonomous braking and the side collision load case with pre-crash triggered restrained systems [11]. In the current study, the methodology was appropriately adjusted to best represent the phenomena characteristic for the problem of low-g lateral loading during autonomous evasive steering (See Figure 1).

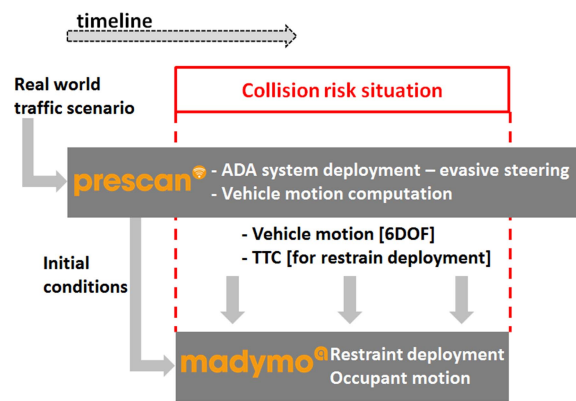


Figure 1. Methodology setup for integral analysis of autonomous steering maneuver.

The principles of the method remained the same as in case of frontal or side collision application. The real world traffic situation is represented in PreScan in which the vehicle model under investigation, equipped with the ADA system with evasive steering capabilities, is exposed to the collision risk situation. Once the evasive steering ADA system model detects and classifies the collision risk, Madymo simulation is initiated with the initial conditions imported from PreScan. The system actuation (applied evasive steering torque) is computed by PreScan and the resulting vehicle motion is being continuously sent to the Madymo simulation. Simultaneously, the estimated time to collision (TTC) information calculated from the surround sensor model outputs is used to timely deploy on-board restraint systems (e.g. belt pre-pretensioners) that accompany the evasive

steering maneuver. Madymo uses the above listed information to calculate the deployment of restraints (if present in the system) and computation of the occupant's motion as an effect of loadings created by autonomous vehicle control. The outputs from Madymo analysis is used to quantify the significance of occupant's misalignments and thus out of position postures for potentially following collision, and to evaluate the driver capabilities to take over the vehicle control instantly after the autonomous actions are finished.

The presented method is applied in the following paragraphs for the analysis of an autonomous evasive steering maneuver deployed due to collision risk situation with a suddenly cutting-in vehicle on a high speed road.

### Scenario Identification

80% of rear-end collisions happen on straight roads and one of the most common scenario is the one in which both vehicles drive at relatively high speed [12]. In 62% of the rear-end collisions the driver took an evasive action, this including braking or steering prior to impact, attempting to avoid the collision. Dedicated active safety systems [6] can assist the driver while attempting to avoid the rear-end collision by applying the necessary braking pressure or the necessary steering torque. More advanced systems can autonomously take actions on the vehicle, in order to minimize any risk of collision in case of driver distraction or inability to react/acknowledge a risky situation.

In this paper the effect of pre-braking (either autonomous or not) is neglected and the worst case scenario is selected, in which the driver would not react to the collision, and would be passively subject to a severe lateral loading caused by an autonomous steering maneuver.

A traffic scenario has been represented in PreScan software, in which a vehicle equipped with a radar sensor and an autonomous steering controller (host vehicle) drives at the velocity of 70 km/h (host vehicle). On the adjacent lane a second vehicle (target vehicle) drives at the speed of 50 km/h. Due to a road construction on its lane, it suddenly steers onto the left lane where the host vehicle is driving (See Figure 2). Behind the host vehicle and on its left lane no other vehicles are driving, thus leaving all the necessary space for a safe evasive steering maneuver. The velocities of both vehicles are kept constant during the maneuver and it is supposed that the vehicles keep driving at the same speed after the maneuver has been completed.

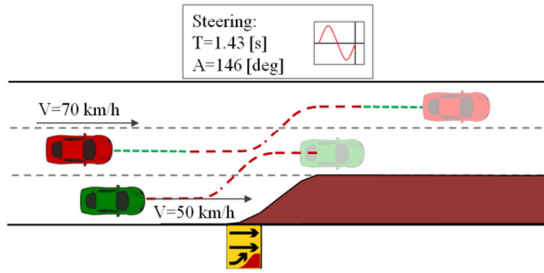


Figure 2. Traffic scenario setup.

### Maneuver Identification

As already mentioned in the introduction, the computation of TTb and TTS is used by the controller to select the most suitable action to avoid the collision. The severity of the maneuver increases when no prior actions are taken either by the vehicle (autonomous braking) or by the driver (attempt to brake and/or steer), as the magnitude of the steering angle has to ensure one lane change in a shorter time, thus becoming critical. As a result, the vehicle is heavily loaded laterally, thus increasing the risk of lateral slip and/or rollover, as well as occupants' injuries due to contact interactions with the passenger compartment. In addition, no risk of single-vehicle or vehicle-to-vehicle collision shall exist due to the application of such maneuver.

In conclusion, provided that no collisions with third parties (other vehicles or environment) would result from the execution of the evasive maneuver, four main factors shall be addressed when evaluating an autonomous evasive steering system:

1. Ability to assure the necessary lateral displacement of the host vehicle which would prevent the collision with the cutting-in vehicle.
2. Ensure vehicle's lateral stability.
3. Ensure that the occupants' misalignment does not result in injuries.
4. Ensure driver's capability of taking control over the vehicle after the maneuver.

The correct operation of the system (first two factors) has been represented using PreScan software; the modeling assumptions are discussed in the following paragraphs. Further on, the risk of occupants (driver and front-seat passenger) injuries is discussed.

**Vehicle Dynamics Model** A mid-class vehicle has been identified for this study and the simple vehicle dynamics model available in PreScan software [13] has been adopted to reproduce the vehicle loading resulting from the application of the

identified maneuver. The Bicycle Model representing the longitudinal and lateral vehicle motion is combined with a simplified model for the computation of the roll motion (See Figure 3). In the model it is assumed that:

1. The tires characteristic is linear, i.e. only small slip angles are applied.
2. The tires can always generate the maximum available lateral force.
3. Only small roll angles ( $\pm 5^\circ$ ) are applied.
4. The vehicle rolls with respect to the ground level.
5. An equivalent resistant rolling torque representing the reaction of the four suspensions is applied.
6. ESC system (Electronic Stability Control) is not represented.

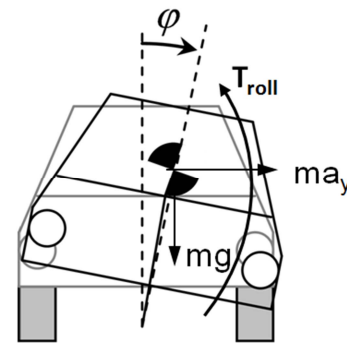


Figure 3. PreScan rolling vehicle model.

**Maneuver Dynamics** The adopted steering wheel angle profile is modeled as a single sine wave curve (Equation 1).

$$\delta = A \cdot \sin(\omega \cdot t) \quad (1).$$

In order to assess the severity of the evasive steering maneuver in terms of lateral loading, the NHTSA New Car Assessment Program (NCAP) Rollover resistance rating has been consulted [13], [14]. In order to evaluate the rollover risk of a vehicle for untripped rollovers (those in which tire/road interface friction is the only external force acting on a vehicle that rolls over), a dynamic test is carried out in order to evaluate whether and/or how much the resulting lateral loading causes a vehicle's inside tires to be lifted while performing a severe single-lane change maneuver (Fishhook maneuver).

The amplitude and angular frequency of the sine wave steering wheel angle profile have been identified by following the procedure defined by ECE-R13H and FMVSS126 [16,17] this being similar to the one defined by NHTSA. The amplitude

of the steering wheel angle profile has been increased until the single-lane change would let the car avoid the collision and require a lateral loading within the limits found in the NHTSA road tests (lateral accelerations of 0.8-0.9 [g]). Since the steering wheel angle profile here identified is intended to reproduce a single-lane change maneuver, it has been expressed as a simple sine wave profile, thus being simplified with respect to the Fishhook maneuver; however, the consequent lateral loading applied to the vehicle is comparable with the one measured on cars tested by NHTSA which have successfully passed the rollover test (i.e. no wheel lift or wheel lift below the required limit of 2 inches) with deactivated ESC system.

The capability of the host vehicle to successfully evade the collision with the cutting-in vehicle has been evaluated by means of simulation only, by monitoring the relative lateral displacement of the two vehicles. As a result, the amplitude of the sine wave was set to 146 [deg.], the angular frequency to 4.398 rad/s and the period to 1.43 s (See Figure 4).

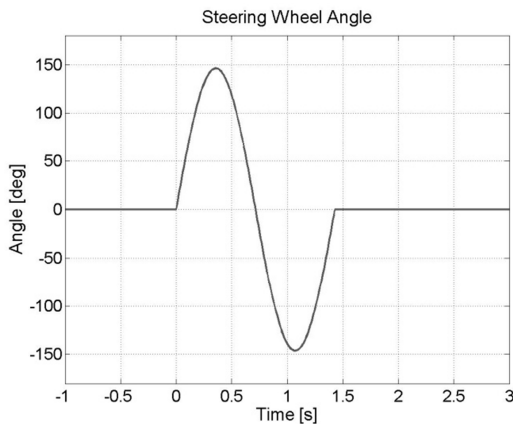


Figure 4. Steering wheel angle profile.

The above defined maneuver is optimized for this particular scenario and vehicles velocities, and is applied as soon as the emergency maneuver is triggered by the controller.

In order to prove the maneuver feasibility without the assistance of an ESC system, not available in the vehicle model, the vehicle loading subsequent to the identified evasive steering maneuver has been correlated to the CarSim base model's response, prior customization with the vehicle inertia properties of the PreScan model. The same steering wheel angle profile discussed before has been used as input to both models; the lateral loading at the vehicle velocity of 70 km/h has been simulated (See Figure 5).

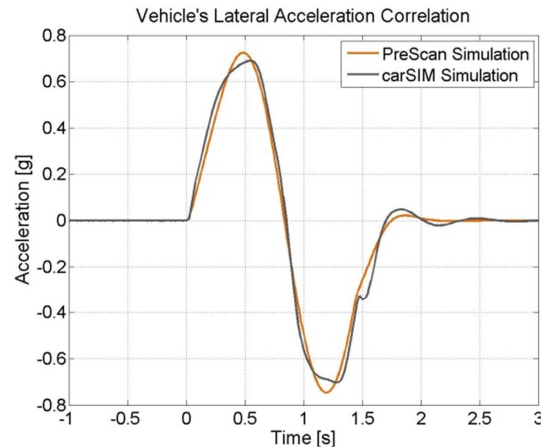


Figure 5. Vehicle's lateral acceleration correlated against CarSim model.

A good level of correlation has been observed (only the lateral acceleration is here commented) and neither lateral slip, nor rollover have been observed in CarSim. Therefore, it can be assumed that the limitation of not having any ESC system represented in the vehicle model does not compromise the occupant loading investigation.

The steering wheel angle profile was used as input to the PreScan vehicle dynamics model to produce the vehicle motion. Due to steering, at the velocity of 70 km/h, the vehicle is laterally loaded for two seconds and a maximum lateral acceleration of 0.72 [g] is observed (See Figure 6). A maximum roll angle of 2.3 [deg.] (See Figure 7) and a lateral displacement of 2.7 [m] (See Figure 8) are also observed.

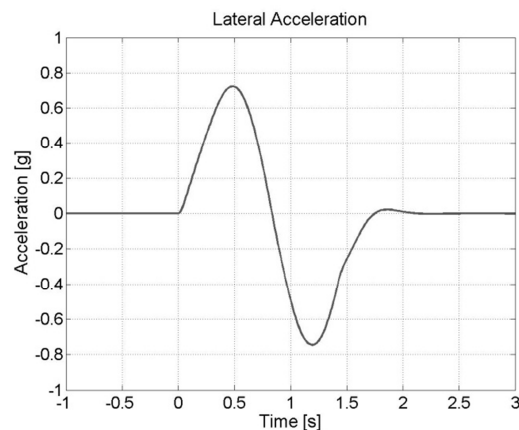


Figure 6. Vehicle's lateral acceleration.

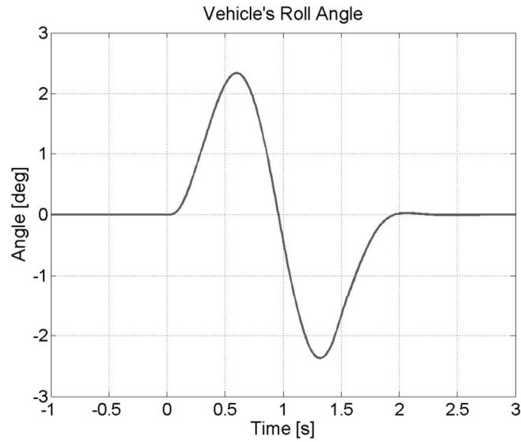


Figure 7. Vehicle's Roll Angle.

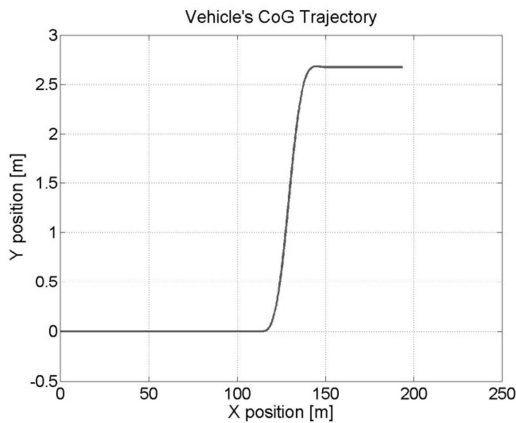


Figure 8. Vehicle's CoG (Centre of Gravity) trajectory.

The above mentioned maneuver dynamics characteristics have been used to load the occupants.

### Controller Principles and Sensor Model

A controller and a sensor have been modeled to reproduce the autonomous performance of the vehicle maneuver in case of risk of collision with the cutting-in vehicle. This study wants, however, to investigate the consequences of an emergency maneuver to the resulting occupants' motion, rather than the reasons why or the way the maneuver would be applied. Therefore, only a simplified triggering logic and an ideal sensor have been modeled in PreScan, using Matlab/Simulink as main platform for the sensor's readings processing by the logic. The actuator is represented by the steering module of the Simulink-based simple Vehicle Dynamics model. It is assumed that the host vehicle is equipped with one sensor only, placed in the middle of the vehicle, right on the front grid. The sensor model acts as a

ground-truth detector which monitors whether/when the CoG of an object comes into a predefined FoV (Field of View), a cone beam with an aperture of 50 [deg.] and a maximum range of 30 [m] (See Figure 9).



Figure 9. Vehicle's sensor model FoV.

The sensor model ideally reproduces a SRR (Short Range Radar) sensor and is scanning the area in front of the vehicle. No other sensors have been modeled, which would scan the areas on the sides and the rear of the vehicle, thus monitoring the whole area around the car. It is in fact assumed that there is only one potentially collidable vehicle and that no other vehicles are driving behind the host vehicle and/or overtaking it. With these assumptions, the controller could be further simplified and no traffic monitoring, nor object tracking had to be implemented.

Furthermore, since the cutting-in vehicle is not sensor-tracked before and during the maneuver, the steering wheel angle profile is built-in into the controller and applied as soon as the detected vehicle comes close to the host vehicle. No driver warnings are deployed.

The system acts in four main steps (See Figure 10). By means of the sensor model, the area in front of the vehicle is scanned and the relative lateral velocity of the detected object is continuously monitored; the control system identifies hazardous situation when the target vehicle cuts-in and triggers the emergency steering maneuver to avoid the collision.

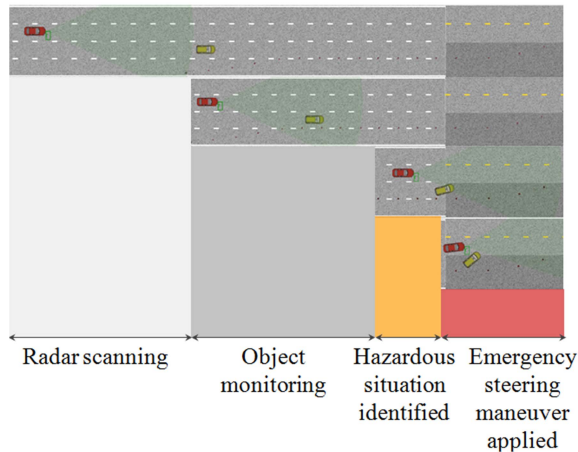


Figure 10. Logic overview.

### Internal compartment and restraint system models

The difference in the prediction of the occupants (driver and front-seat passenger) behavior resulting from the emergency maneuver when using two different models, the Madymo active human model 50<sup>th</sup> percentile and the Madymo ES-2 Q Dummy, has been investigated and is here discussed.

The ES-2 ellipsoid dummy is a well-established ATD (Anthropometric Test Device), typically used in all lateral crash test protocols. It is extensively validated in numerous component, full scale and full system tests and is best suited for all types of conceptual and development side crash analysis [18].

The active human model has an improved biofidelity and includes muscle activity and posture maintenance activation: the neck, spine, elbows and hips can be controlled in order to try to maintain the initial position under the influence of external loading. The active human model is validated for occupant pre-crash simulation with volunteer and PMHS (Post Mortem Human Subject) test data [19], [20].

In this study, for both the human occupant models, the neck and the spine are activated, while only the driver human model has active elbows, as he holds the steering wheel. The occupants' responsiveness (null in case of unaware occupant, maximum in case of full awareness) has been set to 70%, thus representing a normal driving conditions.

The model of the host car occupants, its environment and safety restraint systems have been built in Madymo software. The model of the vehicle interior compartment represents the interior of the generalized mid-size class passenger car and consists of: seats cushion and structure, knee bolster, dashboard, floor and foot rest, A-pillar and B-pillar covers and door-trims. The geometry of all vehicle

compartment elements is represented using ellipsoids technique and the compliance of the elements (seat cushions, knee bolster) is represented by means of force-penetration characteristics, representative of a generic vehicle. Furthermore, the door trims have rigid properties.

The belt model represents the functionality of a conventional belt system. The retractor is locked under a vehicle's lateral acceleration of 0.4 [g]. The pre-tensioning action, intended to reduce the misalignment of the occupants under low-g loading, has not been investigated within this study.

### Simulation Approach summary – Data Flow

By means of PreScan software, the traffic scenario is represented and the sensors readings are generated. In Matlab/Simulink software (running simultaneously with PreScan) the simple controller model processes the sensors inputs and initiates the evasive steering maneuver; the vehicle dynamics model reproduces the actuation of the steering wheel and the consequent vehicle motion (longitudinal and lateral position of the center of gravity, together with vehicles pitch, roll and yaw angle profiles).

The so generated vehicle motion data is imported into MADYMO software and applied to the compartment model, thus resulting in occupants loading. The occupants' kinematics and resulting contacts with the vehicle internal compartment (if any) are analyzed and commented in the paragraph below.

### RESULTS - OCCUPANTS KINEMATICS ANALYSIS

The simulation results of the occupants' behavior are here presented and discussed. The kinematic behavior during to the emergency maneuver is first analyzed with the Active Human models and then with the ES-2 dummy models. The head accelerations, together with head and chest displacements are reported and commented in order to evaluate injury risks on the occupants. In conclusion, the difference between the motion of the ES-2 dummy and the Active Human models is highlighted.

The evasive maneuver causes significant motion of both occupants and brings them out of position. Two main phases can be identified: vehicle steers to the left in order to evade the obstacle and then steers back to the original direction (See Figure 11). Both phases show a considerable motion of the upper torso of the AHMs, while the lower body is well restrained by the seat bolsters.

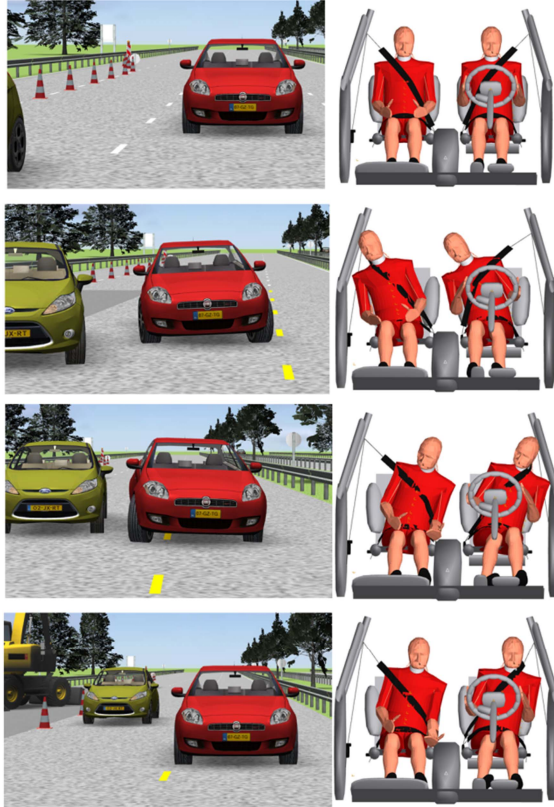


Figure 11. Sequence of events (AHM).

The restraining action of the passenger’s shoulder belt is predominant in phase 1, although it cannot prevent the head from coming into contact with the B-pillar (See Figure 12), thus producing a peak acceleration of 8.45[g] and a HIC value of 2.4. The driver is less restrained by the shoulder belt, as the relative slip with the torso in phase 1 brings him severely out of position, thus causing a higher head acceleration when impacting the B-pillar (phase 2), with a peak value of 24.50[g] and a HIC value of 62.6.

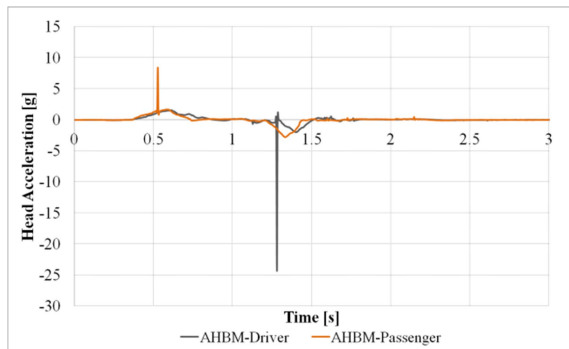


Figure 12. Driver and Passenger head accelerations (AHM).

The occupants’ absolute displacements differ in the two phases of the maneuver, with higher values when they move towards the center of the cockpit (See Table 1). The maximum head lateral displacement has been observed for the driver during phase 1, with the value of 0.311 [m], and for the passenger in phase 2, with the value of 0.299 [m]. The maximum chest lateral displacement of 0.228 [m] has been observed for the driver during phase 1, and of 0.176[m] for the passenger during phase 2. Therefore, phase 1 is the most critical in terms of driver’s lateral displacements, while the passenger undergoes the highest lateral displacements in phase 2 (See Figure 13 and Figure 14). The occupants do not come into contact with each other.

One second after the maneuver has been completed, the residual head lateral displacement is 0.121 [m] for the driver and 0.115 [m] for the passenger, and the residual chest lateral displacement is 0.111 [m] and 0.095 [m], respectively: neither of the occupants is back to the initial position.

**Table1.**  
**Occupants’ lateral displacements and head acceleration during the first and second phases of the maneuver (AHM)**

	AHBM Driver		AHBM Passenger	
	Phase 1	Phase 2	Phase 1	Phase 2
Head Displacement [m]	0.311	0.303	0.243	0.299
Chest Displacement [m]	0.228	0.195	0.165	0.176
Head Lat. Acceleration [g]	1.58	24.50	8.45	2.80

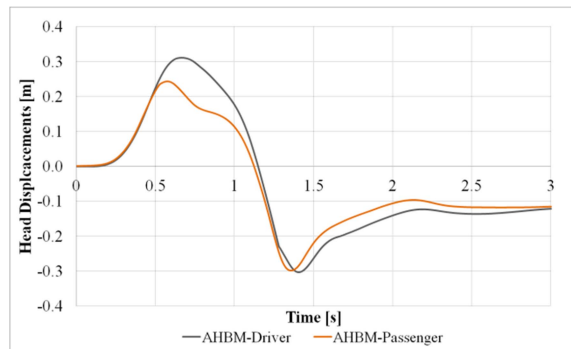


Figure 13. Head displacements (AHM).

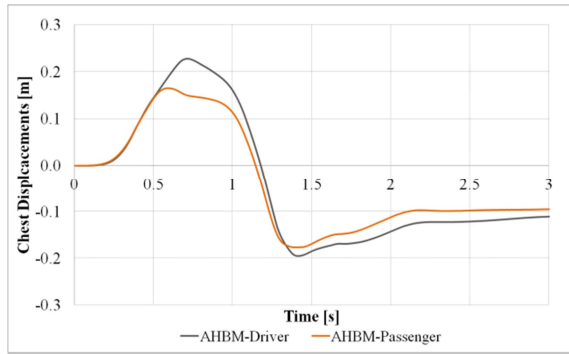


Figure 14. Chest displacements (AHM models).

When using the ES-2 dummy models less pronounced absolute displacements of both occupants has been observed, with the consequent avoidance of head impact with the B-pillar (See Figure 15). The shoulder belts restrained the occupants more effectively during the whole maneuver.

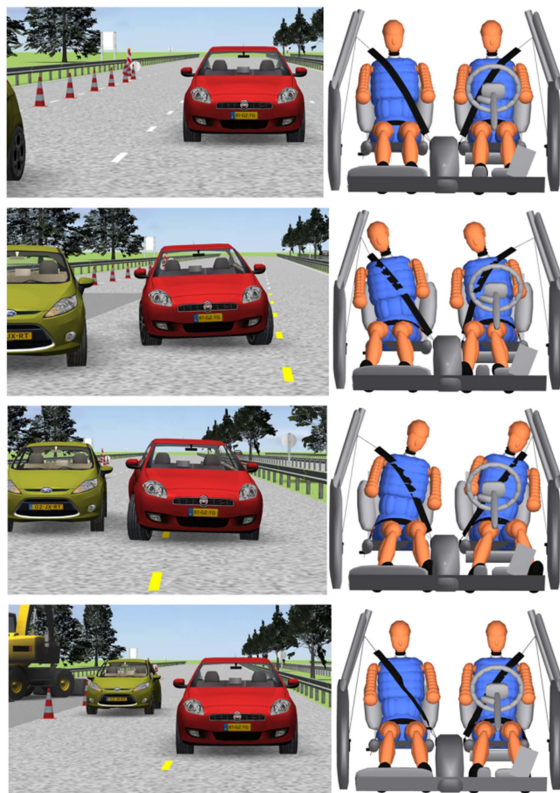


Figure 15. Sequence of events (ES-2 dummy model).

The maximum head lateral displacement has been observed for both the occupants during phase 2, with the value of 0.216 [m] and 0.218 [m], respectively (See Table 2). The same trend applies to the chest lateral displacements, with values of 0.084 [m] for

the driver and 0.086 [m] for the passenger. In contrast to what observed with the AHM models, phase 2 is the most critical in terms of head accelerations and occupants lateral displacements for both driver and passenger (See Figure 16 and Figure 17). The occupants do not come into contact with each other. One second after the maneuver has been completed, the residual head and chest lateral displacements are negligible, with the maximum value of 0.004 [m] for the driver's head: both the occupants are back to their initial position.

**Table 2.**  
**Occupants' lateral displacements and head acceleration during the first and second phases of the maneuver (ES-2 dummy model)**

	ES2 Driver		ES2 Passenger	
	Phase 1	Phase 2	Phase 1	Phase 2
Head Displacement [m]	0.146	0.216	0.144	0.218
Chest Displacement [m]	0.055	0.084	0.057	0.086
Head Lat. Acceleration [g]	1.67	2.15	1.32	2.09

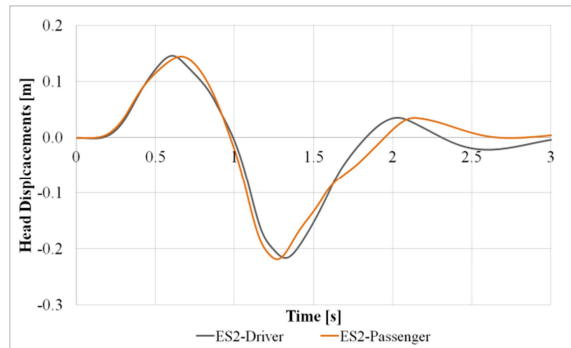


Figure 16. Head displacements (ES-2).

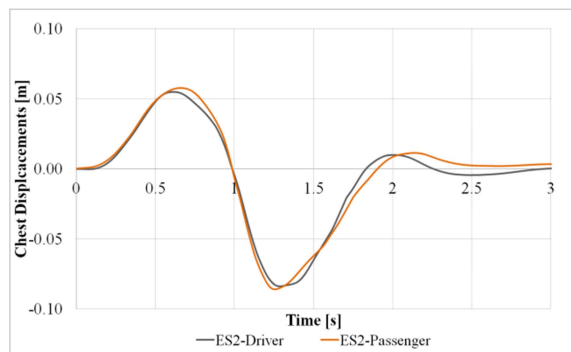


Figure 17. Chest displacements (ES-2).

The two selected occupant models show different behavior in the kinematics resulting from the applied lateral loading. By selecting the worst case phases, namely phase 1 for the driver and phase 2 for the passenger, the observed chest and head lateral displacements have been compared. Assuming the AHM response as reference (i.e. 100% displacement), the adoption of the ES-2 dummy model would result, for the driver, in a reduction of the estimated lateral displacements as big as 53% (head) and 76% (chest) (See Figure 18). Similarly, for the passenger, the observed reduction of the head lateral displacement is equal to 27%, the reduction of the chest lateral displacement to 51% (See Figure 19).

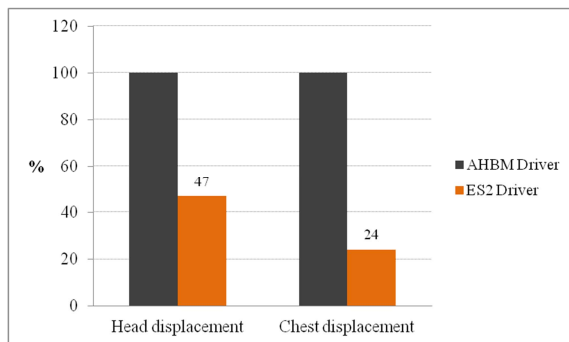


Figure 18. Phase 1\_Driver's head and chest lateral displacements comparison (ES-2 dummy model vs. AHM).

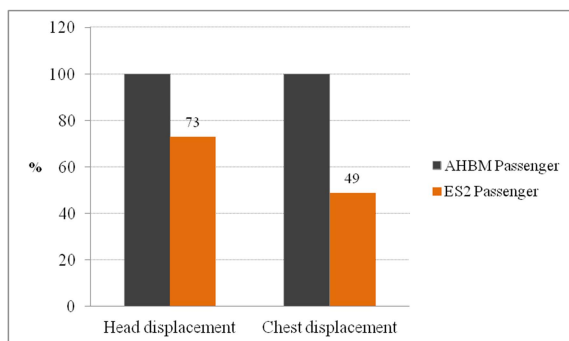


Figure 19. Phase 2\_Passenger's head and chest lateral displacements comparison (ES-2 dummy model vs. AHM).

Due to the different kinematics, the position of the occupants during and at the end of the maneuver show significant difference in the out of position. One second after the end of the maneuver, the AHM models are still out of position, while the ES-2 models are back to the upright position (See Figure 20).

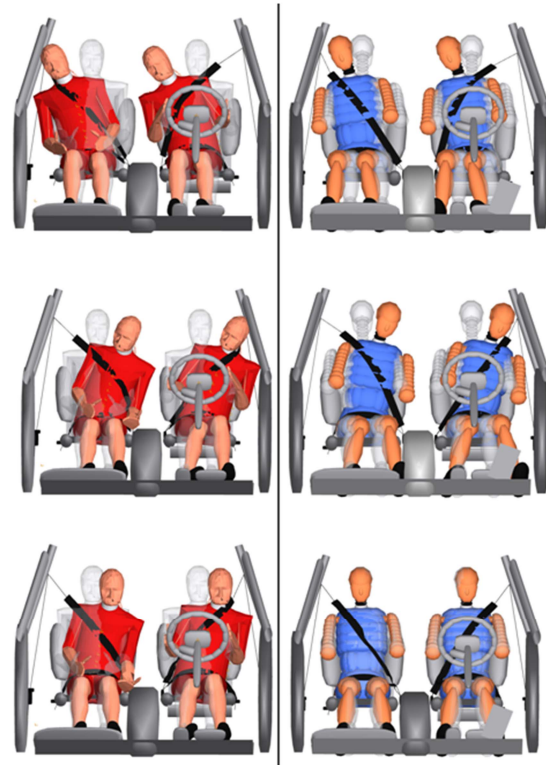


Figure 20. Occupants' OOP comparison (AHM vs. ES-2 dummy model).

## CONCLUSIONS

The simulation results of the passenger head and chest lateral displacements, presented in the Table 1, correlate well with the experimental test results obtained in the previous studies [9] in which comparable loading conditions were applied (double lane change maneuver defined by ISO 3888-2). The maximum averaged values obtained in the road experiments amount to 275mm and 165mm for the head and chest lateral displacement respectively, which should be compared to the maximum 299mm and 174mm obtained in the simulated tests with active human model (AHM). Assuming the modeling limitations, and the possible boundary conditions differences (differences in the seat shape, occupant anthropometry, clothing, seat belt response), it can be concluded that the overestimations of 5-8% for the simulation model are of a good representation. The results of the head accelerations and consequently HIC values resulting from the contact interaction with the B-pillar during maneuvering should not be treated quantitatively due to the simplified representation of the vehicle interior model and b-pillar contact characteristics. It should be perceived as an incidental parameter, indicating

that the head contact with B-pillar or roof rail is possible and should be considered for further testing on the customer acceptance and driving capabilities. However, the obtained results of HIC=62 would correspond to the abbreviated injury scale value (AIS) below AIS=1, that potentially can create headache or/and dizziness. This would further imply that the driver capabilities of taking over the control of the vehicle after the maneuver may be impaired. The analysis of a passenger and a driver motion shows, that the total lateral displacement of a driver is more pronounced than the one of a passenger. This is characteristic for a type of a maneuver (evasion to the left) and the fact that a driver is first misplaced towards the center of a vehicle (Phase 1- to his or her right hand side) and then to the B-pillar direction (Phase 2). The differences are more significant in Phase 1 of the maneuver (over 20%) and less pronounced for the Phase 2. This indicates that the potential predictive countermeasure systems for restraining the occupant motion during autonomous maneuvering should take into account the direction of intended steering and apply countermeasures accordingly per occupant and a driver. Within the conclusive analysis of the results presented above, it should be noted that the limitations of the models and the approach used in the investigation may affect the results and thus conclusions. The quantitative assessment of the lateral occupants' displacements can be affected by modifying the executed maneuver and the critical model components: seat geometry and characteristics, interior part contact characteristic, interior geometry, occupant activation level and the occupant model itself. The components used in the study were generalized to observe the significance of the hypothesized problems globally; however they become a limitation in case the phenomena under investigation are required to be studied in a greater detail. Though the simulation results show very good correlation with the real experimenting [9], the selection of AHM activation settings (awareness, neck co-contraction, delay time, head-neck alignment) may not be representative enough for determining the problems globally and thus the aforementioned conclusions may have limited transferability. To address this, further studies into the sensitivity of the displacements results to the human activation level are needed.

The original hypothesis that the emergency autonomous evasive steering may result in significant occupants' misplacements during the maneuver has been confirmed in the above presented simulation results. This can pose a potential problem for customer acceptance of such systems due to the

discomforting experience and/or potential risk of impaired driving capabilities instant after the maneuver. Implementation of autonomous evasive steering systems would then require application of additional measures to reduce the occupant motion during the highly dynamic maneuvering e.g. belt pretensioners or inflatable side bolsters, deployed prior to the steering execution. Those should partially reduce the misplacements to an adequate level. The other problem is the potential risk of impaired driver capabilities to continue driving due to the excessive misplacement or interaction with the B-pillar or roof rail. This requires a dedicated investigation that includes volunteer testing to validate and quantify the observed incidents.

As concluded in the previous studies [9], the dynamic loadings resulting from autonomous operations of a vehicle (braking or steering) may lead to out of position (and thus reduced protection of restraint systems in case of a collision. In case of a lateral displacement of such magnitude as presented in the study and depicted in the results paragraph, the problem can be easily conceivable as significant for potential frontal, lateral or rear collision. The displacements of occupants misalign their position with respect to the frontal airbags, and back- and head-rests. Additionally, the belt routing geometry is also altered from intended placement. As a result the effectiveness of the complete passive restraint system in case of a frontal collision can be significantly reduced due to altered injury mechanisms or/and potential contact with the instrument panel resulting from misaligned interaction with an airbag. Similarly for the other direction collisions, the misplaced position of occupants can reduce effectiveness of head rests in case of a rear impact, or impair the intended operation of the side protection systems (door trim or side/curtain airbags). Further studies are needed to quantify the problem and determine acceptable levels of displacements with respect to the intended position that are necessary to ensure optimal protection from the passive safety systems perspective. Definition of acceptance corridors will enable to define requirements for potential preventive systems meant to reduce the occupant misplacement due to autonomous vehicle control and thus addressing both problems: capability to take over vehicle control after the maneuver and sub-optimal protection in case of a collision. This can be only ensured when both active safety systems and passive safety systems are developed in an integrated manner.

The objective of the analysis performed with the ES-2 dummy model was to illustrate the potential

differences between the human and anthropometric test device (ATD) models in capturing occupant response to the low-g loading conditions. Both models, used as tools in the same analysis process, exposed to the same loading conditions, show significantly different responses. The differences in lateral head and chest displacements vary between 23% and 76%, and can be considered as highly significant and are of paramount importance for any subsequent studies and conclusions. The significant differences can be explained by the fact that ATDs were designed and built to replicate human behavior under high-g, crash level loadings and cannot represent well the flexibility of a human body under lower loadings. These observations impose the requirements on the methodologies for integrated safety developments to use either human model simulations or volunteer tests for determining pre-crash occupant motion. Additionally it is expected that ATDs may not be suitable to represent human behavior accurately enough in the in-crash phase if initially set to out of position resulting from pre-crash loading (due to their limitations in representing human kinematics for other than standardized initial settings). However this hypothesis requires further investigation and verifications.

The increasing presence of autonomously operating vehicle control systems exposes the occupants of these vehicles to the highly dynamic loadings during the traffic situations with high risk of collision when these ADA systems are operating. This generates the need to develop the countermeasure systems that can control occupants' unfavorable motion and thus reduce the misplacements of the occupants with respect to their intended positions at which the passive systems are the most effective. The work presented within this paper shows the importance of including the effect of ADA system operation on the occupants' misplacements into the system integration development processes and presents the complete simulation methodology that enables conceptual investigations into the required functionalities of current and future integrated safety system.

## REFERENCES

[1] EC/No 661/2009. "Type-approval requirements for the general safety of motor vehicles, their trailers and systems, components and separate technical units intended therefor" (July, 13)

[2] EC project PReVENT website:  
<http://www.prevent-ip.org>

[3] EC project eVALUE website: <http://www.evaluate-project.eu>

[4] EC project ASSESS website: <http://www.assess-project.eu>

[5] Eskandarian, A. (ed.). "Handbook of Intelligent Vehicles", ISBN 978-0-85729-084-7, Springer-Verlag London Ltd. 2012

[6] Fausten, M. 2010. "Accident Avoidance by Evasive Manoeuvres." In Proceedings of the 4th Tagung Sicherheit durch Fahrerassistenz (TVSD, Munich, April 15–16)

[7] Keller, C. G., Thao, D., Fritz, H., Joos, A., Rabe, C. and Gavrila, D. M. 2011. "Active Pedestrian Safety by Automatic Braking and Evasive Steering." IEEE Trans. Intell. Transp. Syst 12, No. 4, Dec: 1292–1304

[8] Isermann, R.; Schorn, M. and Staehlin, U. 2008. "Anticollision System PRORETA with Automatic Braking and Steering." Vehicle Syst Dyn 46, No. 1:683–694

[9] Mages, M.; Seyffert, M. and Class, U. 2011. "Analysis of the Pre-Crash Benefit of Reversible Belt Pre-Tensioning in Different Accident Scenarios." In Proceedings of the 22<sup>nd</sup> International Technical Conference on the Enhanced Safety of Vehicles (ESV) (Washington, D.C., June 13-16)

[10] Bours, R.; Verhoeve, R.; Kietlinski, K. and Tideman, M. 2012. "Enhancing Real-Life Safety by Integration of Active and Passive Safety System Simulation," In Proceedings of the 2012 Annual Congress of the Society of Automotive Engineers of Japan (Pacifico Yokohama, Japan, May 23–25). JSAE

[11] Velardocchia M., Unger M., Vigliani A., Leone N., Kietlinski K. and Galvagno E. "Integrated Active and Passive Systems for a Side Impact Scenario." 2013 SAE International

[12] Lenard J., Danton R. 2010 "Accident data study in support of development of Autonomous Emergency Braking (AEB) test procedures" Project Reference: LUEL 5989/6175, Loughborough University

[13] PreScan R6.3.0 Theory Manual

[14] National Highway Traffic Safety Administration, 2001. "Docket No.NHTSA-2001-9663; Notice 2." Notice of Proposed Rulemaking

[15] National Highway Traffic Safety Administration, 2001. "Docket No.NHTSA-2001-9663; Notice 3." Final Policy Statement

[16] E/ECE/324/Rev.2/Add.12H/Rev.2, 2001. "Uniform provisions concerning the approval of passenger cars with regard to braking." Annex 9, pp.72-82

[17] FMVSS No. 126, 2007. "Electronic Stability Control Systems."

[18] Madymo Quality Report Release Update, 2012. "ES-2(re) ellipsoid Q model version 1.2 (R7.4.2)." Report No. QES2-121130

[19] Madymo Active Human Model Manual, 2012

[20] Meijer, R., van Hassel E., Broos J., Hala W., van Rooij L. and van Hooijdonk P. 2012. "Development of a Multi-Body Human Model that Predicts Active and Passive Human Behaviour.0" In Proceedings of the IRCOBI Conference (Dublin, Ireland, September 12-14)

# Study of Neck injury evaluation and improvement method for US NCAP 5% Dummy

**Raeick, Jang (Author)**  
**Myeongkill, Lee**  
**Hyobae, Lee**  
 R&D / Hyundai MOBIS  
 KOREA  
 Paper Number 13-0364

## ABSTRACT

NHTSA has carried out a lot of New US-NCAP tests became effective from MY2011. Injury probability of New US NCAP test is more severe than previous NCAP test. The Hybrid III 5<sup>th</sup> %ile dummy in front passenger position is used instead of 50<sup>th</sup> %ile dummy. 5<sup>th</sup> %ile dummy gets lower points than 50<sup>th</sup> %ile dummy in many tests. One of the main cause is Nij. Especially neck extension moment value is main factor to improve Nij.

US NCAP frontal test data was reviewed to know tendency of neck extension moment value. The object of the study is to find out how neck moves and neck extension moment occur. Furthermore, CAE test with new concept of passenger airbag is conducted to improve extension moment based on analysis result.. New concept of passenger airbag has two main vent holes that can be closed to retain inner pressure of airbag. Retaining inner pressure of airbag can decrease relative motion between head and neck to improve Nij.

## INTRODUCTION

It's not easy to get high point for US-NCAP for passenger because New assessment method is more severe than previous one. New US-NCAP adopted HIC 15, Nij, Chest Deflection, Femur for 5%ile dummy on passenger. Especially Nij(Neck injury) is of great importance from other injury. An effort is being made to improve neck injury in many method.

This paper analyse neck injury characteristic of MY2012 ~ MY2013 test car and suggests neck injury improvement with concept keeping inner PAB pressure.

## Neck Injury Analysis

50 crash test car of model year 2012 ~ 2013 were analyzed for data collection. Passenger overall rating is lower than driver. Passenger gets 5star rating less than about 25% comparing to driver getting 5star more than about 50%. Main cause of lower rating of passenger is neck injury. Neck injury is calculated as equation 1.

$$\text{Equation 1. } N_{ij} = \frac{F_z}{F_{zc}} + \frac{M_{ocy}}{M_{yc}}$$

If driver and passenger get the same moment and force value, each Nij value is different because of different Myc (Moment Y Constant) as table 1.

**Table 1.**  
**Neck Injury Critical Value**

Dummy	Fzc(N) Tension	Fzc(N) Compression	Moment Yc(Nm) Flexion	Moment Yc(Nm) Extension
HIII 50%	6806	-6160	310	-135
HIII5%	4287	-3880	155	<b>-67</b>

The most extension moment y(-My) have great effect on Nij. Nij has 4 type of injury as NTE, NCE, NTF, NCF. But only Nte and NCE occurred among almost 50 cars. This simply means that the bigger the extension moment Y, the worse neck injury as table 2. So improving extension moment y is the most important work for getting good overall point.

**Table 2.**  
**Passenger Result According to Neck Injury**

Passenger Rating	Nij	Extension Moment Y (-My)
★★	0.79	47.1
★★★	0.53	30.9
★★★★	0.46	25.3
★★★★★	0.33	17.9

**Neck Motion Analysis by Using Other Sensors**

Generally moment y pulse is as figure.1 In part 1, belt pretention is working before dummy contact on PAB. Dummy head is going upward and forward. - force x, - moment y, + force z are occurred. In part 2, after head contact on PAB, dummy head reaction is occurred to rearward. + force x, + moment y occurred. In part 3, before head rebounding, force x and moment y are steady downward curve. In this part, the most important work is how to decrease downward curve.

In all part, force x and moment y curves are similar at the same time as figure 1. This means dummy neck force and moment y are associated.

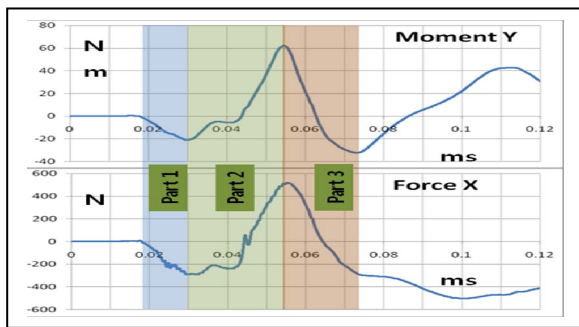


**Figure 1. Neck Moment Y and Force X Curves**

Neck sensor is located on top of neck. So neck itself motion cannot be analyzed through the video. To know neck sensor how to work, two angle sensors are used. One is attached on top of neck and the other one is attached on head C.G. Relative angle between head and neck can be known comparing moment y as figure 2.

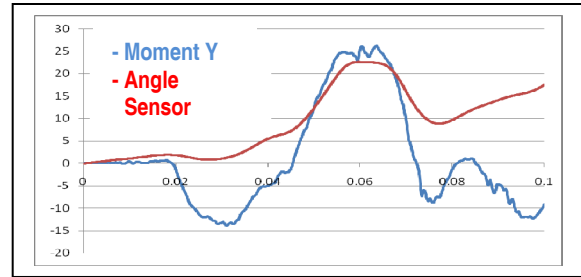


**Figure 2. Relative Angle Between Neck and Head.**

This means that neck motion can be known by two curves. When force x and moment y are minus sign, head moves toward from the top of neck(joint) and head is extension motion as figure 3. When force x and moment y are plus sign, head moves reward from the top of the neck(joint) and head is flexion motion as figure 4.

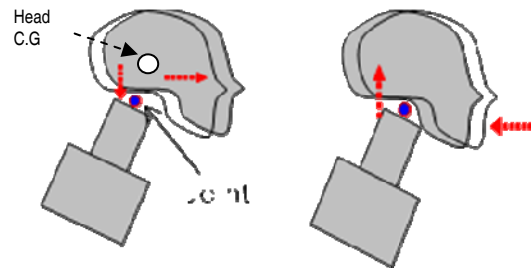


**Figure 3. Neck Motion #1**

**Figure 4. Neck Motion #2**

In conclusion, relative motion between top of neck and head C.G should be decreased to improve moment y and force x. Especially, head moving toward from top of neck should be decreased.

**PAB Vent Position**

Vent hole size should be optimized for passenger injury because vent hole can control inner pressure of airbag. If vent hole is too big, head injury can be better. But neck injury can be worse because of relative motion between neck and head. If vent hole is too small, relative motion between neck and head can be decreased. But head injury can be worse. Here is a car shows how to control inner pressure of PAB.

Vent hole is much the same as other one before 60ms. But after 60ms, vent hole is blocked partially by a pillar, instrument panel and wind shield. This means that relative motion between head and neck can be decreased by controlling pressure of PAB. Refer to figure 5.

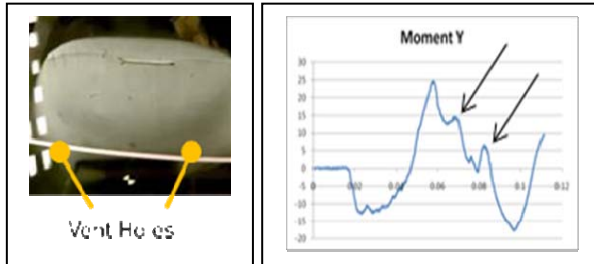


**Figure 5. PAB Vent Holes Position and Moment Y Curve**

**Belt Load Characteristic**

Belt load limiter can control relative motion between head and neck. High belt load made much relative motion and low belt load made small relative motion. Belt result of ★5, ★4 star cars are as table 3. Max belt load of good rating cars is lower than other cars. Belt Load area of good Nij cars before nij occurred lower than other cars. The smallest Nij of a car is 0.25 and belt load is the smallest.1.9kN.

**Table 3. Shoulder Belt Load Characteristic**

	Nij	Max Load	Area just before Nij Time	Load at Nij Time
5star	0.33	3.1kN	570	1.3kN
4star	0.51	4.5kN	750	3.2kN

**Time Gap Between Head and Neck Moment Y**

This paper gives new concept of PAB. For this, time gap between head and neck moment y should be known. By controlling PAB pressure, neck moment y can be controlled. But head injury is also affected. If neck injury is getting better, head injury can be worse. This paper suggests to improve neck injury without making head injury worse.

The Head Injury, Hic15, is calculated with head resultant value. Normally, head resultant peak is occurred earlier than extension moment y peak. Refer to table 4.(40cars of 50cars are collected - some car's neck injury are so early as 30ms before head contacts on PAB, some car's neck injury cannot be collected because it's impossible to know when is the peak) After head peak, if PAB pressure is kept, neck extension moment y can be improved.

**Table 4. Head and Moment Y Peak Time Difference**

	Head Peak	Extension Moment Y Peak
Time	64ms	87ms

**Improvement Method for Neck Injury**

**Airbag – Main Vent Close Concept**

To improve Nij(NCE, NTE), the most important work is to decrease extension moment y peak occurred after head resultant peak. The first suggestion is PAB inner pressure controller. Excessive PAB pressure can cause poor head injury and insufficiency PAB pressure can cause poor Nij injury. If these two factors are in harmony, head and neck injury can be improved at the same time.

The main concept is to close the vent hole that is main factor can control PAB pressure. Before head resultant peak time, main vent is open so that head injury can be improved. After head resultant peak, main vent is close so that extension moment y and force x down ward curves are decreased by decreasing head movement forward. Test is conducted by MADYMO sled test to know effectiveness of vent close concept as figure 6.

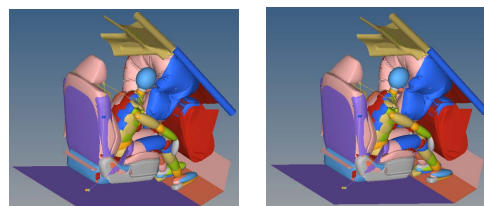


**Figure 6. MADYMO Test (Left : Vent Open / Right : Vent Close)**

There are two 45mm main vents in the base test. Hic15 is 233 at 60ms and Nij is 0.46 at 80ms. Nij is not so good for good overall rating. Improvement test is conducted by closing two main vents by controlling vent close time. Closing only one vent test is also conducted as table 4.

**Table 4.**  
**Test Matrix and Result**

	Vent Size (mm)	Vent Close Time(ms)	HIC 15	Nij	Rating
1	45mmX2	N/A	233	0.46	4.76★
2	45mmX2	65ms	318	0.31	5.03★
3	45mmX2	75ms	244	0.41	4.90★
4	45mmX2	75ms(one vent close only)	244	0.46	4.76★
5	45mmX2	80ms	233	0.43	4.88★

Head g value is going up when vents close. The earlier vent close, HIC15 value gets higher. When vents at close at 65ms, Hic15 became 318 from 233. Although Hic15 becomes worse, extension moment y is improved greatly. Force x and moment y tend to move upward. This means that relative motion between head and neck is decreased as a result, Nij is 0.31.

When vents close at 75ms, Hic15 is almost not changed. Hic15 is increased from 233 to 244. Nij is improved from 0.46 to 0.41. HIC gets little bit worse and Nij gets better.

HIC15 and Nij injury are changed differently by vent close time. This means closing time of vents should be considered.

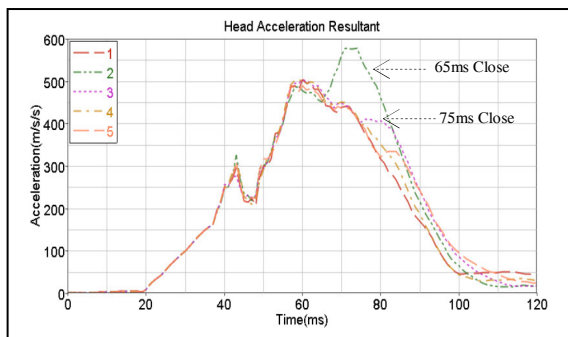


**Figure 7. Head Acceleration**

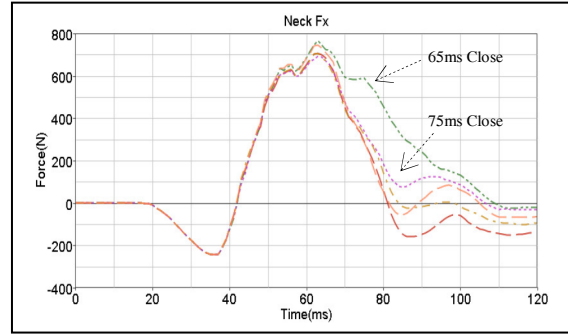


**Figure 7. Neck Force X**

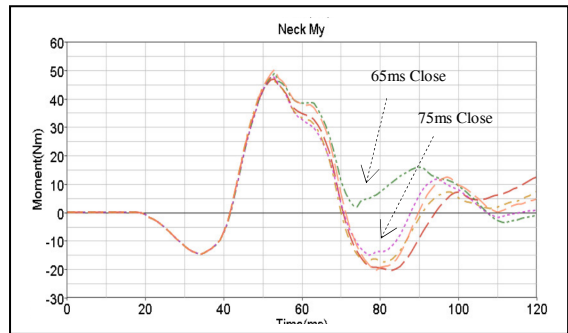


**Figure 8. Neck Moment Y**

When vent is close, head, neck force x, neck force y are going up at the same time. But if vent close time is optimized, only neck injury value can be improved only.

### Belt Characteristic

For good result of head, neck, chest and femur as well, belt characteristic is one of main factor. As mentioned above, each car has different belt load characteristic. Belt can effect on head and neck injury. High belt load makes big motion and low belt load makes low motion. For improving neck injury, belt and airbag should be considered at the same time.

### **CONCLUSIONS**

Neck injury should be improved for good overall rating in passenger 5%ile dummy. For this, understanding cause why and how neck injury occurred by the time should be done. A factor is suggested to improve neck injury by closing main vent holes.

1) Neck motion through the video analysis is not exact. In other word, neck sensor is not located on middle of neck. Neck sensor is on top of neck. So relative motion between neck and head to should be analyzed to know how sensor works. Force X and angle sensor are used to analyze neck motion. When head moves toward from the top of neck, force x and moment y are negative curves. At this time, relative angle between head and top of neck is worked as force x and moment y. To improve extension moment y, head movement forward should be decreased.

2) This paper suggests vent close concept. After head resultant peak passed, main vent holes are close to keep inner pressure of PAB. It can prevent that relative motion increasing between head and neck. The time when vent close is main factor to improve  $N_{ij}$ . It can be one factor to improve dummy injury.

※ By using this concept, main vent holes can be larger to improve HIC in full frontal test, LRD regulation test, unbelt regulation test before vent close. After vent close,  $N_{ij}$  in full frontal test, head bottom out in unbelt regulation test can be improved.

3) Belt characteristic, PAB shape, car characteristic and such should be considered at the same time to improve dummy injury, especially neck injury.

4) The plan with actual sled test would be come to action

## REFERENCES

- [1] NHTSA, NCAP Final Decision Notice, NHTSA-2006-26555, 2008.
- [2] H.K. Beom “Statical Review for USNCAP Front Crash Result in MOMENT Y2011, KSAE, Conference Proceedings
- [3] Matthew R. Maltese “Neck Pendulum Test Modifications for Simulation of Frontal Crashed”, SAE World Congress, 2008